JAN 2 2 1946

THE JOURNAL OF CHEMICAL PHYSICS

VOLUME 14 NUMBER 1

JANUARY, 1946

Published by the

AMERICAN INSTITUTE OF PHYSICS

LANCASTER, PA. AND NEW YORK, N. Y.

CHEMICA[illegible]CS

[illegible]ITORS

[illegible]

[illegible]

[illegible] *December 31, 1947* [illegible] *December 31, 1948*

[illegible] Cross — Charles D. Cornell

[illegible] Fuoss — F. [illegible]

[illegible]rewood — L. [illegible]homas

[illegible] — G. [illegible]Wetherill

[illegible] — E. Brig[illegible]lson, Jr.

[illegible]

[illegible] exponents. The solidus (/) should be used wherever [illegible] for fractions.

[illegible] illustrations should accompany manuscript and [illegible] always be referred to in the text. Line drawings [illegible] must be made with India ink on white paper or on [illegible] tracing cloth. Coordinate paper is not desirable, but if [illegible] used must be blue-lined with the coordinates to be repro[illegible]duced drawn with India ink. Lettering should be of [illegible] sufficient size to be legible after reduction.

[illegible] and all correspondence concerning papers in the [illegible] of publication should be addressed to the Publica[illegible] Manager, American Institute of Physics, 57 East [illegible] Street, New York 22, New York.

Subscription Price

The United States and Possessions, Canada and Mexico $10.00

Elsewhere 11.00

Back Numbers

Complete set: Vol. 1, 1933—Vol. [illegible] 1948 ..... $130.00

Single rate: $11.00.

Single copies: $1.00 each.

Subscriptions and orders for single copies should be addressed to Prince and Lemon Streets, Lancaster, Pennsylvania, or to the American Institute of Physics, 57 East [illegible] Street, New York 22, New York.

Changes of address should be sent to the Business Manager, American Institute of Physics.

[illegible] is published monthly at Prince and Lemon Streets, Lancaster, Pennsylvania.

[illegible] December 20, 1[illegible] at the Post Office at Lancaster, Pa., under the Act of August [illegible], 1912. Acceptance for [illegible] Act of February 28, 1925, embodied in paragraph 4, Section [illegible] P. L. R.: authorized

THE JOURNAL
OF
CHEMICAL PHYSICS

VOLUME 14, NUMBER 1 JANUARY, 1946

Thermal and Photochemical Decomposition of Gaseous Aluminum Trimethyl

LOURDU M. YEDDANAPALLI AND CLARENCE C. SCHUBERT*
Canisius College, Buffalo, New York

(Received September 22, 1945)

The thermal decomposition of gaseous aluminum trimethyl, in the absence of hydrogen, is nearly 94 percent homogeneous and of kinetic order three-halves over the pressure range 10 to 85 mm measured at room temperature. The reaction products consist largely of methane and to a lesser extent ethane, ethylene, and hydrogen and a solid deposit on the walls of the reaction vessel. A reaction mechanism involving methyl radicals is proposed. The apparent energy of activation, calculated on this basis, is found to be 45 kcal., in agreement with the experimentally determined figure. The high ratio of methane produced to alkyl decomposed suggests that aluminum trimethyl in the vapor state at room temperatures must consist at least of tetrameric molecular complexes. In the presence of hydrogen, both the decomposition rate and the energy of activation are reduced as compared to the decomposition of the pure alkyl, a puzzling effect for which no satisfactory explanation can at present be offered. Photochemically, the presence of hydrogen seems to have little effect on the over-all decomposition but enhances the relative amount of methane slightly. In this, aluminum trimethyl appears to differ from mercury dimethyl which is known to decompose faster thermally and photochemically in the presence of hydrogen than in its absence.

SINCE the recent[1] publication of more precise data on the physical properties of aluminum trimethyl, such as vapor pressure, molecular weight, and molecular association, attention of research workers has been drawn to the study of the compound, particularly with regard to the structure of its fairly stable dimeric molecules.[2] No kinetic study, however, of gaseous aluminum trimethyl, has, up to date, been published. It was thought to be of interest to investigate the kinetics of its decomposition and compare the behavior of this trivalent metal alkyl with that of divalent mercury dimethyl[3] and tetravalent alkyls like silicon tetramethyl[4] and tin tetramethyl,[5] and obtain at the same time some information which would throw light on the molecular structure of polymeric aluminum trimethyl, which is still in question. Investigation has, therefore, been made of the thermal and photochemical decomposition of the compound in the gas phase in absence and in presence of hydrogen. The kinetic behavior of aluminum alkyl appears to be, in many respects, dissimilar to that of the corresponding divalent and tetravalent alkyls.

* Abstract from the thesis presented by C. C. Schubert in partial fulfillment of the requirements for the Master's degree.

[1] A. W. Laubengayer and W. F. Gilliam, J. Am. Chem. Soc. **63**, 477 (1941).

[2] N. R. Davidson, J. A. C. Hugill, H. A. Skinner, and L. E. Sutton, Trans. Faraday Soc. **36**, 1212 (1940); L. O. Brockway and N. R. Davidson, J. Am. Chem. Soc. **63**, 3287 (1941); R. S. Wiswall, Jr., and C. P. Smyth, J. Chem. Phys. **9**, 352 (1941); Kohlrausch and Wagner, Zeits. f. physik. Chemie **B52**, 185 (1942).

[3] John P. Cunningham and H. S. Taylor, J. Chem. Phys. **6**, 357 (1938).

[4] Helm and Mack, J. Am. Chem. Soc. **59**, 60 (1937).

[5] Chas. E. Waring and William S. Horton, J. Am. Chem. Soc. **67**, 540 (1945).

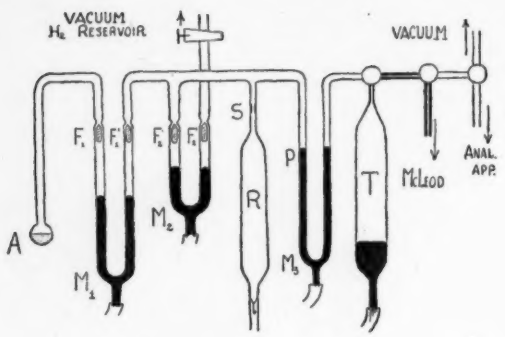

FIG. 1.

EXPERIMENTAL

Materials

Aluminum trimethyl was prepared[6] by heating together aluminum metal foil and mercury dimethyl in a sealed tube on a boiling water bath, the mercury alkyl having been obtained according to the method indicated by Marvel and Gould.[7] Since the aluminum alkyl is highly and spontaneously inflammable in air, decomposing even in traces of oxygen, it was distilled in an oxygen-free nitrogen atmosphere in an all-glass set-up. The aluminum alkyl fraction collected boiled at 126–127°C at atmospheric pressure. It was further purified by distillation in vacuum *in situ* in the gas kinetic apparatus and stored in a bulb coated with carbon black and kept in a bath of acetone and dry-ice mixture.[8]

Hydrogen from commercial cylinders was purified by passage over platinized asbestos, then through a phosphorus pentoxide tube, and finally through a trap cooled in liquid air. A quartz mercy lamp of the Uviarc type, run hot so as completely to reverse the mercury resonance lines, served as the source of illumination in photochemical experiments. An electrical furnace of block aluminum core provided with a quartz window for illumination was used for maintaining temperature. In the thermal runs, various constant boiling baths of organic compounds were employed.

[6] Buckton and Odling, Ann. Chim. Phys. **4**, 492 (1865).
[7] Marvel and Gould, J. Am. Chem. Soc. **44**, 153 (1922).
[8] Mention may be made of a new alkyl of aluminum and mercury which was by accident prepared in this connection. When the sealed tube containing aluminum foil and mercury dimethyl was heated in the water bath for several hours beyond the stage at which most of the mercury in the alkyl was displaced by aluminum, most of the resulting liquid, on fractionation, distilled off at 49–51°C at atmospheric pressure, This liquid, from preliminary tests, appears to be, not a molecular mixture, but a true molecular compound of aluminum-mercury alkyl and is more highly and spontaneously inflammable than the pure aluminum trimethyl. Further study of it is in progress.

Apparatus and Procedure

The essential features of the apparatus for the handling of aluminum alkyl vapor are indicated in Fig. 1. The *F*'s are ground-glass float valves by means of which not only could the compound be stored in the bulb *A* out of contact with mercury of manometer M_1 but also prevented from contamination by the grease of the stopcocks of the vacuum system.

The reaction vessel for the thermal runs consisted of a cylindrical Pyrex tube of 1.9 cm inner diameter and 22 cm in length, with a surface to volume ratio of about 2. When initially sealed at one end to the manometric system, the reaction vessel carried at its free extremity a capillary inner seal, as shown in Fig. 1. The volume of the reaction vessel, and that of any portion of the dead space of the manometric system whose value was required to be known in order to calculate the absolute amount of the alkyl in the reaction chamber, could be evaluated by admitting air or nitrogen into the system and measuring the pressures with the help of the calibrated McLeod gauge.

To fill the reaction tube with the desired amount of the aluminum alkyl, the storage bulb *A* was maintained at a temperature below room temperature so as to avoid condensation of the vapors during the subsequent pressure measurements, and the vapor admitted into the space confined between F_1, F_2, *P*, and the reaction vessel *R*, and its pressure was read on the manommeter M_3. It was then condensed completely into *R* with the help of an ether-dry-ice mixture, and the reaction vessel was sealed off from the system at *S*. Knowing the volume of the alkyl vapor whose pressure was read on the manometer and that of the reaction vessel, the pressure of the vapor in the vessel could be calculated. When hydrogen was to be added initially to the alkyl, the reaction tube was filled first with the latter and then with the required amount of hydrogen. Similar procedure was adopted in the case of the quartz reaction tube

which was provided at its two ends with graded seals. After the completion of the decomposition, the reaction tube was re-sealed to the manometric system, at the end carrying the inner capillary seal which could be broken by an iron-in-glass plunger propelled by an electromagnet, in order to study the nature of the reaction products.

It may be noted that before breaking the capillary seal as well as before initially filling the reaction vessel with the alkyl, the whole manometric system was flushed with some aluminum trimethyl vapor and then completely evacuated. This precaution was found necessary in the light of preliminary experiments which revealed decomposition, to varying degree, of the alkyl vapor at first contact with clean glass walls. The reaction tubes before use were cleaned, always in a uniform manner, with warm chromic acid solution, followed by distilled water.

Analysis

The reaction vessel containing the products of the thermal or photochemical decomposition was first surrounded with a liquid-air bath; the mixture of non-condensable methane and hydrogen was transferred by means of the Toepler T into the McLeod gauge and its absolute total amount measured. The liquid-air bath was then replaced by an ether-dry-ice mixture in order to remove the two-carbon hydrocarbons and measure their amount after transference into the McLeod gauge. Since the amounts of the gases were extremely small, particularly in the case of the two-carbon hydrocarbons at low percentage decompositions, their analyses were conducted in the microchemical gas analysis apparatus of Blacet and Leighton.[9] In the hydrogen-methane mixture, hydrogen was determined by oxidation over an alkaline copper oxide bead and the methane calculated by difference. In the hydrocarbon mixture, ethylene was estimated by absorption by fuming sulfuric acid in a porous glass bead and the ethane evaluated by difference. Tests in this mixture for acetylene by means of an alkaline cuprous chloride bead did not give positive results.

[9] F. E. Blacet, P. A. Leighton, and G. D. MacDonald, Ind. Eng. Chem. Anal. Ed. **3**, 266 (1931); **5**, 272 (1933); **6**, 334 (1934).

Experimental Results

The analytical data on the thermal and photochemical decomposition of aluminum trimethyl both in absence and in presence of hydrogen are presented in Table I. The pressures of gases are given in mm Hg at room temperature. The reaction time in all cases was 60 min., except in a few instances as indicated in the footnotes to the table. The last column gives the amount of methane produced per unit of alkyl decomposed. The zero values represent in some cases traces of the particular component. The bracketed experiments are meant to show the reproducible character of a run, which from other data, not given in the present table, was quite satisfactory. Average values of these experiments will later be utilized for calculating specific reaction constants. Experiments 40 and 39 give the data for the decomposition in packed reaction vessels with increased surface to volume ratios. The unpacked vessels used in all the other experiments had a ratio of about 2.

In every run, besides the gaseous reaction products recorded in the table, there was a solid deposit on the walls of the reaction vessel which was in some cases a thin film with a bluish metallic sheen, soluble in dilute acid and alkali,

TABLE I.

Expt.	T°C	Init. alkyl mm	Init. H_2 mm	Final alkyl mm	CH_4 mm	C_2H_6 mm	C_2H_4 mm	H_2 mm	$\frac{CH_4}{Alkyl}$
				Thermal					
40[a]	298	14.7		12.7	9.16	0.69	0.06	0.34	4.6
39[b]	298	14.9		12.6	12.55	0.92	0.10	0.40	5.4
38	298	9.1		8.4	3.60	0.49	0.01	——	5.1
32	298	15.4		13.5	6.72	0.57	0.02	0.19	3.6
34	298	14.8		13.1	6.85	0.51	——	0.21	4.0
66[c]	298	15.7		14.4	4.93	0.49	0.02	0.03	3.8
67[d]	298	15.2		0.0	61.70	0.55	0.00	0.00	4.1
37	298	29.2		24.6	16.60	——	——	0.20	3.6
45	298	29.8		25.0	17.36	0.39	0.02	0.54	3.6
47	298	48.0		37.8	40.30	0.27	0.00	——	4.0
48	298	50.9		39.8	43.50	0.43	0.00	0.52	3.9
49	298	85.5		63.1	205.20	0.60	0.00	0.00	9.2
70	313	15.1		10.9	17.40	0.52	0.02	0.90	4.3
65[e]	334	15.1		9.1	27.20	0.58	0.02	——	4.5
51	334	15.1		4.8	46.20	0.44	0.01	1.10	4.5
57	298	15.2	14.8	13.8	8.13	0.32	0.01	15.2	5.8
62	298	15.1	15.5	13.9	8.90	0.33	0.01	15.0	7.4
71	313	14.7	15.5	12.6	10.70	0.51	0.01	16.4	5.1
58	334	14.7	15.1	9.8	28.00	0.38	0.01	13.9	5.7
59	334	14.8	26.6	9.6	29.40	0.40	0.02	26.4	5.7
				Photochemical					
68[e]	29	13.8		13.1	0.52	1.47	0.00	0.03	
61[f]	120	13.6		13.1	0.76	0.98	0.00	0.03	
60[f]	120	13.7	15.7	13.1	1.26	1.06	0.00	15.00	

[a] In a packed vessel with surface to volume ratio 5.3; [b] 10.8.
[c] Decomposition time—40 minutes.
[d] Complete decomposition—several hours.
[e] Decomposition time—180 minutes; [f] 90 minutes, current being 4 amp.

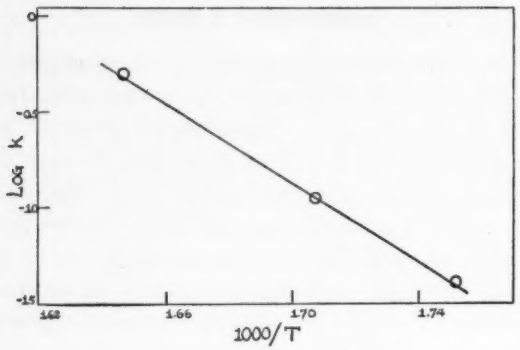

FIG. 2.

and in cases of higher temperature and pressure and longer reaction period, a complex of metallic and brownish polymeric material. At the highest pressure investigated, 85.5 mm, a heavy yellowish deposit was formed at the two ends of the reaction vessel; it reacted vigorously with water yielding gases which seemed to contain, as judged by the smell, some ethylene; the main component of these gases might be methane, since aluminum carbide, yellowish in color, is known to decompose with water into methane and aluminum oxide.

It may be remarked that the chief source of error in the data was the measurement of the alkyl pressure manometrically, which could not be accurate to more than 0.5 mm, so that in cases of low percentage decompositions, as in Experiment 38, a large error could creep into the value of alkyl decomposed, obtained as the difference between initial and final pressures recorded in the table. It may be well also to add that the tediously long procedure involved in the completion of a run is partly responsible for the lack of more abundant data at different initial pressures of alkyl at 334°C and in the presence of hydrogen.

DISCUSSION OF RESULTS

Thermal Decomposition in Absence of Hydrogen

Surface Effect

From the amounts of alkyl decomposed, Experiments 39 and 40, in packed vessels with a surface to volume ratio of 5.3 and 10.8, respectively, calculation, according to the method indicated by Geddes and Mack,[10] leads to about 6 percent heterogeneity for the reactions conducted in unpacked vessels employed in our experiments whose surface to volume ratio was about 2. Consequently the thermal decomposition of aluminum alkyl is mainly a homogeneous reaction.

Order of Reaction

Preliminary calculations for the order of the alkyl decomposition at varying initial pressures, employing the expression

$$\Delta x_1/\Delta x_2=(p_1/p_2)^n,$$

where Δx_1 and Δx_2 are the decrease in pressure per unit time and p_1 and p_2 are the average of initial and final pressures in the two cases, gave an average value of about 1.5 for n, the order of the reaction. On the basis of three-halves kinetic order, the specific reaction rate constants for various initial pressures at 298°C were calculated using the rate expression in its integrated form,

$$k=\frac{2}{t}\left[\frac{1}{(a-x)^{\frac{1}{2}}}-\frac{1}{a^{\frac{1}{2}}}\right],$$

where a and $(a-x)$ are the initial and final concentration, after time t sec., concentration being expressed in moles per cc, so that k has the dimensions of $cc^{\frac{1}{2}}$ $mole^{-\frac{1}{2}}$ $sec.^{-1}$. The constants are presented in Table II at three temperatures. The slope of the plot of log k *versus* reciprocal of absolute temperature T, in Fig. 2, yields, for the apparent activation energy E of the process, a value of about 45 kcal. The frequency factor A, in the rate expression,

$$k=A\times e^{-45000/RT}$$

has a value of 8.1×10^{15}, quite comparable as to

TABLE II. Percentage composition of gaseous products at 334°C with an initial alkyl pressure of 15 mm.

Expt.	Time in min.	CH_4	C_2H_6	C_2H_4	H_2
53	5	91.34	8.03	0.63	Traces
54	10	93.36	6.16	0.48	Traces
52	15	95.07	4.80	0.12	Traces
65	40	97.84	2.09	0.07	Traces
51	60	97.00	0.90	0.04	1.9
9	180	98.00	0.50	0.00	1.5

[10] Geddes and Mack, J. Am. Chem. Soc. **52**, 4372 (1930).

the order of magnitude with the values of frequency factors for other three-halves order reactions.[11] The slight increase over the normal value of 10^{15} is not unexpected in view of the probably high entropy of activation which can be accounted for by the polymeric nature of the reactant in its initial state, as will be presently indicated. The three-halves order might, at first sight, appear to hold only within the pressure range recorded in Table I, namely 10 to 85.5 mm. Actually, however, since aluminum trimethyl is known to exist completely in the dimeric form even at 70°C,[1] and since the experimental pressures were measured at room temperature at which the alkyl might be in a higher polymeric state, the effective pressure range, in reference to the decomposition temperatures at which the polymer molecules would be completely dissociated into simple monomeric molecules, would be about 20 to 170 mm. Over this whole range, therefore, the kinetic order of the reaction would seem to be three-halves.

Reaction Products

The predominant component of gaseous reaction products is methane, with smaller amounts of hydrogen, ethane, and ethylene, besides a complex solid deposit on the walls of reaction vessel, which might be composed of metallic aluminum, aluminum carbide, and some polymer material. The variation of the percentage composition of gaseous products with time at 334°C is expressed by the data in Table III. Impossibility of obtaining measurable and analyzable amounts of products prevented the performance of runs with shorter periods than 5 min., and at temperatures below 334°C. The general trend of the results obtained is nevertheless quite clear. Methane percentage, and in a smaller degree that of hydrogen, increase with time, whereas the percentages of ethane and ethylene suffer a regular decrease. This may be attributed to progressive pyrolysis with time of ethane to give methane, thus increasing total methane percentage. The gradual decrease of ethylene and its final disappearance in three hours, Experiment 9, might be due, partly, to its hydrogenation, and partly to pyrolysis and subsequent polymerization.

TABLE III.

T°C	298	298	298	298	313	334
Init. alkyl mm	15.1	29.5	49.5	85.5	15.1	15.1
$k_{1.5}$	0.042	0.040	0.044	0.042	0.110	0.476

It is of interest to note the high ratio of methane to alkyl, about 9, in the last column of Table I, at the highest initial pressure of alkyl employed, namely 85.5 mm. The repetition of another high initial pressure run gave also a similar high methane to alkyl ratio. This presupposes at least a tetrameric form of the aluminum alkyl in the vapor at room temperature, as will be evident from the following stoichiometric relation,

$$[Al(CH_3)_3]_4 \rightarrow Al_4C_3 + 9CH_4.$$

The possibility of such a relatively high polymeric form of aluminum trimethyl is suggested by the nature of the molecular weight *versus* temperature curve of Laubengayer and Gilliam,[1] and also by the ability of this alkyl to form associated complexes with other compounds.[12] Hence aluminum trimethyl seems to exist in the vapor phase at room temperatures in a more complex molecular state than dimeric, probably in a tetrameric form.

Reaction Mechanism

To account for the above facts, the following mechanism is suggested. The thermal decomposition of aluminum trimethyl being of three-halves order, must, by analogy with other similar reactions, involve a chain mechanism, the initial step being the splitting of a methyl radical according to the equation,

$$Al(CH_3)_3 \rightarrow Al(CH_3)_2 + CH_3. \qquad (1)$$

The complex radical $Al(CH_3)_2$ might break down further into methyl radicals or alternately could be the source of ethane which appears in relatively high percentages in the early stages of the reaction, before it has time to decompose as in the long period runs in which it is present in smaller percentages. This would also account for

[11] See R. N. Pease, *Equilibrium and Kinetics of Gas Reactions* (Princeton University Press, Princeton, 1942), p. 133.

[12] Norman Davidson and Herbert C. Brown, J. Am. Chem. Soc. **64**, 316 (1942).

the metallic deposit observed on the walls of the reaction vessel.

The formation of methane probably occurs by the reaction,

$$Al(CH_3)_3+CH_3\rightarrow CH_4+Al(CH_3)_2\cdot CH_2. \quad (2a)$$

The latter radical, by analogy with other complex radicals, like propyl, etc., may tend to lose a methyl radical and revert to a stable molecule.

$$Al(CH_3)_2\cdot CH_2\rightarrow CH_3+Al(CH_3)\cdot CH_2. \quad (2b)$$

Actually compounds of the type $BrAl:CH_2$ have been prepared from aluminum and CH_2Br_2. It seems probable therefore that $Al(CH_3)\cdot CH_2$ could be stable and could deposit out in this or in a polymerized form on the walls of the reaction vessel, thus accounting for some of the solid deposit which has been remarked earlier.

Steps (2*a*) and (2*b*) would together constitute a chain. The chain breaking step must be the recombination of the radicals into ethane,

$$CH_3+CH_3\rightarrow C_2H_6, \quad (3)$$

in order to account for three-halves order. Further reactions of the type (2a) and (2b) with the eventual production of aluminum carbide, the presence of which in the deposit was indicated by its vigorous reaction with water, as has already been remarked, would kinetically be similar. The molecule in step (2*b*) in its simple or polymeric form would probably also react with water to yield some methane and plausibly also unsaturated hydrocarbons. For all these reactions a constant k_2 may be assigned, which would evidently be a complex of the rates of several reactions of the type (2*a*).

The steady-state concentration of methyl radicals, on this basis, is given by steps (1) and (3), as the steps (2*a*) and (2*b*) mutually cancel.

$$[CH_3]=\left(\frac{k_1}{k_3}[A]\right)^{\frac{1}{2}}$$

[A] standing for aluminum alkyl concentration. The over-all rate of disappearance of the alkyl is given by

$$-\frac{d[A]}{dt}=k_1[A]+k_2[A][CH_3].$$

Substitution for concentration of methyl radicals yields

$$-\frac{d[A]}{dt}=k_1[A]+k_2\left(\frac{k_1}{k_3}\right)^{\frac{1}{2}}[A]^{\frac{1}{2}}.$$

The initial rate $k_1[A]$ will be negligible in comparison with the rate of chain reactions, and therefore the observed three-halves order for the over-all decomposition is accounted for.

On this basis, the apparent energy of activation E observed will be

$$E=E_2+\tfrac{1}{2}(E_1-E_3).$$

E_2 the energy of activation of reaction (2*a*) is that of a radical-molecule reaction, which seems to have in general a value of 15 kcal. or less. E_3, the energy of activation of recombination of two methyl radicals is very small and may be neglected. E_1, essentially the strength of the Al−C bond in the alkyl is not known. A probable estimation can be made from a knowledge of related alkyl compounds. For the Hg−C bond in mercury dimethyl, Terenin[13] gives a value of 40–50 kcal. Sodium methyl decomposes rapidly at 100°C, and mercury dimethyl would decompose rapidly around 400°C.[3] This would mean a value of 20 to 25 kcal. for the Na−C bond. The C−C bond energy is about 85 kcal. A value of about 60 kcal. for the bond between C and an element like Al in group III of the Periodic Table seems reasonable. Substitution of this value for E_1 in the expression will give for E of the over-all decomposition

$$E=15+\tfrac{1}{2}(60)=45 \text{ kcal.}$$

a value in agreement with the experimental value of ~45 kcal.

Compared to tin and silicon tetramethyls, aluminum trimethyl appears to be different as regards both kinetic order and apparent energy of activation. Waring and Horton[5] report for thermal decomposition of tin tetramethyl a first-order constant above 80 mm of initial alkyl pressure and below this pressure an order approaching 2, and an energy of activation for the first-order reaction of 82 kcal., which high value is interpreted as evidence of a decomposition mechanism through molecular rearrangement. Silicon tetramethyl[4] too decomposes according to first order, with an energy of activation of 79 kcal. For dimethyl mercury,[3] similar data are not available; but it is known that it decomposes readily only at a higher temperature than

[13] A. Terenin and N. Prilezhaeva, Acta Physicochimica 1, 759 (1934).

does aluminum trimethyl. An adequate explanation of these differences would require further research and examination

Thermal Decomposition in Presence of Hydrogen

The effect of hydrogen, as is seen from the last section of the data in Table I, is to decrease the over-all rate of decomposition of the alkyl and to increase the ratio of methane to alkyl decomposed. An approximate doubling of hydrogen pressure for the same initial alkyl pressure of about 14.7 mm, cf. Experiment 59, produces little change over the value of Experiment 58. With this piece of evidence, in spite of the absence of data on the effect of varying initial pressure of alkyl in presence of a constant pressure of hydrogen, it might tentatively be assumed that the kinetic order of alkyl decomposition is three-halves as in the case of the pure alkyl. The specific reaction rate constants calculated on this basis are presented in Table IV at three temperatures, and the plot of log *k versus* reciprocal of absolute temperature is given in Fig. 3. The slope of this straight line yields for the apparent energy of activation E a value of 30.5 kcal. Calculation of E on the basis of a first-order reaction, just as a check, gave a value of 29 kcal., not materially different from the previous one. This is rather puzzling in that the presence of hydrogen should reduce both the rate of decomposition and the apparent energy of activation. At present we are not able to offer any satisfactory explanation. The fact that the presence of hydrogen increases the ratio of methane to alkyl decomposed from about 4 to 5, does not throw much light on the above mentioned problem. It might well be that the kinetics in the two cases are quite different and can be elucidated only by further investigation of the problem.

It must be noted that the behavior of aluminum alkyl in presence of hydrogen is markedly

TABLE IV.

T°C	298	313	334
Init. alkyl mm	15.1	14.7	14.7
$k_{1.5}$	0.028	0.050	0.140

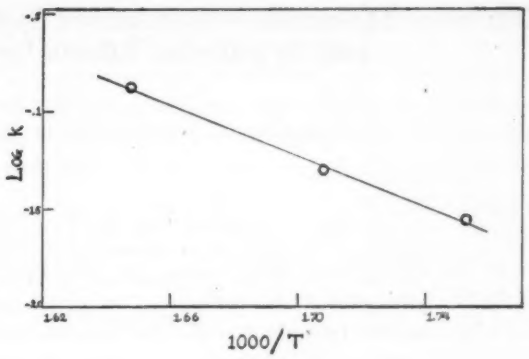

FIG. 3.

different from that of mercury dimethyl[3] which decomposes faster in presence of hydrogen than in its absence, the accelerated rate increasing with increase in hydrogen pressure and consuming hydrogen in the process. In the case of aluminum, the adverse effect of hydrogen becomes constant after a pressure value of 15 mm, further increase of hydrogen making little difference, as can be seen from Experiments 58 and 59, though no hydrogen is used up.

Photochemical Decomposition

The few photochemical experiments whose results are presented in Table I were performed primarily to verify whether the difference which was observed in the thermal decomposition of aluminum and mercury alkyls would hold also in the photodecomposition. The effect of hydrogen in Experiment 60 as compared with its absence in Experiment 61, is not appreciable at all, whereas in the case of dimethyl mercury, hydrogen noticeably accelerated the rate of decomposition of the alkyl. No definite conclusions can now be drawn regarding the nature of the photochemical decomposition of aluminum alkyl in absence of exhaustive data. Still the difference in behavior of aluminum and mercury alkyls is evident. Further photochemical study of aluminum trimethyl will soon be undertaken in this laboratory.

ACKNOWLEDGMENT

The authors wish to thank Father Brown for his interest in the research and Professor H. A. Taylor for his helpful discussion and suggestions and Professor H. S. Taylor for reading the manuscript.

THE JOURNAL OF CHEMICAL PHYSICS VOLUME 14, NUMBER 1 JANUARY, 1946

Motions of Molecules in Condensed Systems: I. Selection Rules, Relative Intensities, and Orientation Effects for Raman and Infra-Red Spectra

RALPH S. HALFORD
Mallinckrodt Chemical Laboratory, Harvard University, Cambridge, Massachusetts
(Received August 30, 1945)

A method is described that permits deduction of selection rules for Raman and infra-red spectra of crystals from a knowledge of just the space group designation and the population of the unit cell. When implemented by an appendix to this article showing, in a convenient arrangement, the distribution of point symmetries within space groups the method can be applied by a user familiar with point group manipulation but having no special knowledge of space groups. There are no selection rules operating in the liquid state. Some tentative qualitative conclusions are drawn concerning the relative intensities of certain kinds of components appearing in spectra of condensed systems. Sharpened selection rules are expected, and have been observed by others, to operate for single crystals containing non-rotating molecules when these are given special orientations in the light path. These special orientations and the appropriate selection rules can be predicted from information mentioned above along with inspection of the external form of a crystal. All procedures have a desirable advantage of simplicity over prior ones directed toward the same ends.

INTRODUCTION

DETAILED studies, both experimental and theoretical, of the motions of isolated molecules have yielded a vast dividend of valuable accurate information about gaseous substances. This information not only has immediate physical significance but also, when combined with powerful tools of statistical mechanics, contains many chemical implications. The store of substances which may be regarded conveniently as vapors is becoming rapidly exhausted while generally reliable procedures for dealing similarly with substances in condensed states remain to be developed. Theoretical problems which must be overcome in this connection are severely complicated and are not likely to be solved without the aid of simplifying idealizations. The possibilities in this direction are numerous while an intelligent assessment of their merits is hampered by an insufficiency of experimental information in several categories, especially concerning the details of molecular motions in condensed systems.

The most direct experimental route to knowledge of molecular motions in any situation is through the spectra they produce. The interpretation of spectra demands certain concomitant theoretical machinery. This communication will be devoted to the development of some principles appropriate for condensed phases, that will be applied subsequently in separate reports to the interpretation of experimental investigations.

SELECTION RULES FOR CRYSTALS

Well-known procedures[1] permit the deduction of selection rules for vibration-rotation spectra of isolated symmetric molecules. To review them briefly, the mutual potential energy of a collection of interacting atoms will reflect the symmetry of their equilibrium configuration. This symmetry can be described by means of a *group* of physical operations. The term *group* is used here in a specialized mathematical sense and implies many consequences that follow logically from the restrictive definition. For instance, associated with the group is a set of irreducible representations which may be visualized as non-equivalent examples of the given symmetry. These are limited in number and have the property that all other examples of the same symmetry can be constructed from combinations of the irreducible ones. Thus, the potential energy of a distribution of interacting points can be analyzed into a sum of independent contributions. Each contribution is associated with some one of the irreducible representations of the group describing the symmetry of the equilibrium con-

[1] For details see J. E. Rosenthal and G. M. Murphy, Rev. Mod. Phys. 8, 317 (1936); L. Tisza, Zeits. f. Physik 82, 48 (1933).

figuration. Each contribution to the analyzed potential energy determines a set of fundamental modes of motion. The totality of fundamental modes is the composite sum extended over all irreducible representations. Finally, the collection of points in motion will possess a transitory electric moment and a transitory polarizability. These properties furnish two mechanisms for exchange of energy with a radiation field and so give rise to infra-red and Raman spectra, respectively. These properties also reflect the symmetry of the equilibrium configuration and therefore can be analyzed into components associated with the irreducible representations. Only those modes of motion will be concerned in the corresponding spectra that appear in irreducible representations along with components of the transitory electric moment or transitory polarizability. Selection rules deduced in this way from the symmetry of an isolated molecular configuration find application in the analysis of spectra of dilute vapors where the condition of isolation is achieved. However, they are inappropriate for the analysis of spectra of condensed phases.

It is evident from the foregoing discussion that selection rules can be deduced in the same way for any situation where it is possible to specify and analyze the symmetry of a suitable configuration of interacting points. Recognizing this opportunity, Bhagavantam and Venkatarayudu[2] have taken the lead in developing methods to permit deduction of selection rules for molecular crystals. They propose that all of the spectroscopically important *frequencies* can be discovered and classified by examination of the isolated crystallographic unit cell. This proposal is almost certainly correct, not only for the reasons advanced by its authors but also in the light of experimental findings. The unit cell is then regarded as an example of the **space group** appropriate for the crystal lattice; a point is deemed invariant under any operation that carries it either into itself or into the identical point in another unit cell but not so under an operation that carries it into an equivalent point in its own or another unit cell. The logic of this last convention, considered in relation to the potential energy of the complete crystal, is not altogether satisfactory under close scrutiny.

This theoretical machinery for crystals has been tested against a number of experimental cases.[2,3] In practice it is found that the method introduces and emphasizes distinctions that are without meaning in relation to available experimental techniques. The results require further assessment and interpretation on this account so that the method is often cumbersome and sometimes even tedious to apply. The rhombic modification of crystalline sulfur furnishes an extreme example. The unit cell contains 16 molecules of S_8 and exhibits 384 distinct modes of motion whereas the Raman spectrum consists of only 10 lines.[4] This discrepancy is not the result of exceedingly strict selection rules but instead is caused by the circumstance that the 384 modes can be collected into sets such that the theoretically distinguishable frequencies in any one set are indistinguishable in practice. In a molecular crystal it is convenient to consider separately two types of motions: (1) lattice modes, which are approximately the motions of rigid molecules and (2) molecular modes, which are approximately the distortions of molecules whose centers of mass and principal axes of inertia are at rest. For sulfur, 288 molecular modes are distributed among 14 sets, each set having a representative frequency not sensibly different from one of the 14 fundamental frequencies of an isolated S_8 molecule. The members of a given set correspond to different ways of coupling the motions of 16 molecules when all are moving with the same frequency. In principle the coupling will yield 16 new frequencies but in practice the distinctions are not apparent. Similar considerations apply to lattice modes although in this category the opportunities should be better for practical resolution of the distinctions. Even so, in the example under discussion, only 2 somewhat broadened lines can be attributed to 48 modes arising out of restricted rotation of molecules contained in the unit cell. The lattice modes of translatory origin have low frequencies along with low intensities and so are not likely to be observed. In general the organization of modes

[2] S. Bhagavantam and T. Venkatarayudu, Proc. Ind. Acad. Sci. **9A**, 224 (1939); S. Bhagavantam, Proc. Ind. Acad. Sci. **13A**, 543 (1941).

[3] See review by G. Glockler: Rev. Mod. Phys. **15**, 111 (1943).

[4] R. Norris, Proc. Ind. Acad. Sci. **13A**, 291 (1941).

into sets can be accomplished more or less readily; when this has been done it still remains to examine the different selection rules for the members of a set in order to arrive at a representative selection rule for the common frequency. In summary it may be said that this ingenious procedure leaves something to be desired, both logically and practically speaking.

This writer prefers to employ another plan of attack. The idealization adopted is the one so strongly implied in experimental findings; i.e., to treat the motions of one molecule moving in a potential field reflecting the symmetry of the surrounding crystal. This permits the use of *point* symmetry rather than **space** symmetry and attributes a more logical quality of invariance to the potential energy of the complete crystal under the appropriate symmetry operations. The treatment yields at once a suitable number of *frequencies* with appropriate selection rules. Of course, the corresponding motions are fictitious in principle but so are those attributed by the other procedure to an isolated unit cell. If one is forced to adopt an idealization there is little to be gained by making it unduly elaborate. Furthermore, there is good reason to believe that the picture of molecular modes derived from examination of one molecule may be more accurate than the one derived from examination of the unit cell; coupling between molecular motions in different molecules is extremely weak, *ex post facto*.

A prerequisite to the treatment of any molecular crystal is a suitable knowledge of the crystal structure. This is provided by a detailed pattern of the unit cell, when one is available, but most often when found in convenient summaries consists merely of the **space group** designation along with the number of molecules per unit cell. It is highly expedient to have theoretical machinery designed to manufacture the desired results from the latter form of raw materials since these are so comparatively easy to procure. Such a formalism can be developed to operate in the great majority, if not all cases. If it is found to fail occasionally, the shortcoming will be apparent at once and resort can then be had to the information contained in a detailed pattern of the unit cell.

In order to make clear the basis for the formalism it is convenient to recall at this time a few well-founded principles of crystallography.[5] Crystals can be assigned, on the basis of their external symmetries, among 32 classes, each class being identified with a collection of symmetry elements and a unique *point group* of operations concerned with them. Each *point group* generates a characteristic number of **space groups**, descriptive of the internal crystal structure, when its operations are combined in various numbers and various ways with the primitive translations that carry one lattice point into another. An arbitrarily chosen point in the crystal is a member of a set of equivalent points, all contained within the same unit cell. The set can be generated by applying in turn the operations of the **space group** to the chosen point. In general, the number of equivalent points per set is equal to the number of operations in the **space group**. However, if a point is situated on one of the symmetry elements and if the operations of the **space group** concerned with that element are not composite translations, then the point remains invariant under these operations. Consequently, such a point belongs to a set having population less than the number of operations in the **space group**. Although usually called otherwise, such a point will be designated henceforth as a *site*. In general, a unit cell exhibits several different kinds of sites and sometimes several distinct sets of the same kind. As a further consequence of its definition a site is necessarily the affix for a point group, the *site group*, which is a sub-group of the **space group**. Thus, an infinite crystal (the limit is always appropriate in practice) has the point symmetry of a *site group* about each and every site.

The center of mass of a molecule is invariant under the operations of the associated *molecular group* and its equilibrium position in the crystal will be called the *affix* of this group. It is a well-substantiated rule[5] of crystallography that the affixes of symmetrical molecules are usually situated on sites. In order that this be so it is necessary that the *site group* be a sub-group of the *molecular group*. Thus, the complete potential energy of a crystal when considered from the affix

[5] For detailed development see R. W. G. Wyckoff, *The Analytical Expression of the Results of the Theory of Space Groups* (Carnegie Institution of Washington, 1930), second edition.

of any of its constituent molecules always has the symmetry of the appropriate *site group*. When the site group has been identified the selection rules can be deduced in the usual way for its irreducible representations. Furthermore, since the occupant of the site is a valid example of its symmetry the motions of one molecule can be assigned to the irreducible representations without regard for the motions of the rest of the crystal. Since this procedure accounts for a suitable number of *frequencies* no further elaboration is required. Of course, one retains the reservation that each motion of the one molecule is coupled to some degree with the motions of the rest of the crystal that are associated with the same irreducible representation of the *site group*. The relation between motions of an isolated molecule and those of one in the crystal can be established readily by comparing character tables for the *molecular group* and the *site group*.

The deduction of selection rules for a molecular crystal can be accomplished as outlined above, whenever the *site groups* have been identified. An acceptable *site group* must be a sub-group of both the **space group** and the *molecular group*. When the latter two groups are compared only a few common sub-groups will emerge and sometimes only one. In the latter case the choice is unequivocal and the *site group* is unambiguously identified. When more than one acceptable *site group* emerges, a further elimination is possible on the basis of the number of molecules contained in the unit cell. The molecular affixes must occupy a complete set of sites and the number per set varies with the order of the *site group*. When applying this criterion it is necessary to take into account the possible multiplicity of identical sets of sites, for several such sets may be in use. In most cases the foregoing considerations will suffice, but ambiguous situations are possible. These arise infrequently; when they do it is perhaps safest to refer to a map of the unit cell. In order to employ the easy procedure indicated in this paragraph it is necessary to have at hand a tabulation of the *site groups* contained in each **space group**, the numbers of equivalent sites per set, and the multiplicities of sets. This information can always be found in works on crystallography, but not arranged conveniently for the present purpose. Therefore, in order to implement the procedure to the fullest possible extent, the requisite material has been compiled in a convenient form and appears as an appendix to this article.

An analysis of the spectra of calcite and aragonite will be undertaken now as an illustration of the procedure. Calcite is a representation of the **space group** $\mathbf{D_{3d}^6}$ with two molecules per unit cell. Consultation of the appendix shows that this population can be accommodated only on *site groups* D_3 and C_{3i}. The first is a sub-group of the *molecular group* D_{3h} for carbonate ion whereas the second is not. On the other hand the second is suited to the point symmetry of calcium ion. Hence carbonate ion is surely on site D_3 and calcium ion on site C_{3i}. Resorting next to the usual analysis of group characters[1] one finds that the three lattice modes of translatory origin associated with calcium ion are forbidden in the Raman spectrum but permitted in the infra-red spectrum. Similarly one finds that carbonate ion yields four molecular frequencies, one permitted only in the Raman spectrum, another permitted only in the infra-red spectrum, and two others permitted in both spectra. In addition it yields one lattice frequency of translatory origin and one of rotatory origin active in both spectra along with one frequency of each type active only in the infra-red spectrum. The conclusions concerning molecular frequencies are in complete harmony with experimental observations while the ones concerning lattice frequencies are not violated although fewer than the expected number of frequencies are observed.[2a] The contrasting conclusions for aragonite follow readily from the knowledge that this crystal is a representation of the **space group** $\mathbf{V_h^{16}}$ with four molecules per unit cell. Reference to the appendix places calcium ion on site C_i and carbonate ion on site C_s. The lattice modes attributable to calcium ion are once again forbidden in the Raman spectrum but permitted in the infra-red spectrum. However, six molecular frequencies are now permitted to appear in both spectra. The two extra frequencies arise from removal of a degeneracy prevailing in both the free carbonate ion and calcite; if the splitting is not resolved only four frequencies will be observed. The lattice modes attributable to carbonate ion are now six in number and are permitted to appear in both spectra. Once more,

these conclusions are in harmony with experimental data.[2] Essentially the same predictions can be made, but less conveniently, by the method employing **space groups**.

The only failure of the easy procedure, encountered thus far by the writer in the course of examination of a substantial number of crystals, occurs with rhombic sulfur. A representation of the **space group** V_h^{24}, the unit cell, contains sixteen molecules. Referring to the appendix one finds that this population can be accommodated equally well on two sets of eight sites each with symmetry V or on one set of sites with symmetry C_2. Further discussion will be omitted except to mention that the analysis now involves only 24 instead of 384 modes.

In general, the *site group* will be of lower order than the *molecular group* although this is not necessarily the case. When true, the selection rules for the crystal will be less strict than those for the isolated molecule with the result that the crystal will possess a richer spectrum than the vapor. For *site groups* C_2, C_s, and C_3, it can be said without further examination that no selection rules will operate.

An interesting aberration develops in the case of ammonium chloride. The ammonium ion occupies a site having point symmetry O_h which is of higher order than the *molecular group* T_d. From this circumstance one must infer that the ion interacts with the rest of the crystal as though it were a point, a view which is entirely consistent with the prevalent conception that the ion is able to rotate freely in this crystal. Special selection rules will apply.

LIQUIDS

Turning now to the other common condensed state, *there will be no selection rules operating in the liquid phase.* This conclusion follows at once from the conception of the liquid state as one of disorder. The short range order in a liquid does not connote symmetry. Convincing proof will be presented in a separate communication describing an experimental study of liquid and solid benzene. For the present, attention is directed toward the observation[6] that the infra-red spectrum of pentaerythritol, $C(CH_2OH)_4$, in solution exhibits a characteristic absorption band in a certain neighborhood whereas a comparable amount of solid in the light path is transparent at the same place while exhibiting other regions of absorption in common with the solution. Molecules of pentaerythritol[7] occupy sites S_4 in the crystal. This group has four irreducible representations and one of them, totally symmetric, containing six frequencies is forbidden to contribute to the infra-red spectrum. The case does not afford unequivocal proof of the general absence of selection rules for liquids. It can be argued that hydrogen bonds stabilize a symmetrical form in the crystal whereas the molecule, isolated from others of its own kind, might exhibit several configurations of approximately equivalent energy and no net symmetry. This alternative seems unlikely when attention is given to the observation[8] that pentaerythritol halogenohydrins have point symmetry S_4 in the vapor phase.

RELATIVE INTENSITIES

Although selection rules forbid certain modes of motion from contributing to a given spectrum they do not guarantee that contributions from the others will always be observed. It is outside the scope of currently workable theory to predict quantitatively the relative intensities in different regions of a spectrum. Nevertheless, cogent arguments can be directed at some aspects of this problem for a substance which follows the dominant pattern of behavior. Certain modes of motion develop spectroscopic activity in a condensed phase but do not contribute to the spectrum of the vapor. The intensity of this newly acquired activity depends upon the degree of interaction between the molecule and its surroundings. In a similar manner, for those modes of motion that are permitted to contribute to both spectra, the intensities depend as well upon the interactions residing within the molecule. In any condensed system where it is legitimate to speak of a collection of molecules the latter class of interactions must be considerably stronger than the former one. Hence, the contribution to the spectrum of a condensed phase, by a mode that

[6] Private communication from Dr. Daniel Norman, New England Spectrochemical Laboratories, Medway, Massachusetts.

[7] F. J. Llewellyn, E. G. Cox, and T. H. Goodwin, J. Chem. Soc. 882 (1937).

[8] H. de Laszlo, Comptes rendus **198**, 2235 (1934).

is active in the spectrum of the isolated molecule, will certainly be more intense than the contribution from a mode that becomes active only after condensation. Thus, the customary practice seems quite legitimate whereby the most intense frequencies are selected from the spectrum of a liquid for assignment to fundamentals permitted by the selection rules for the isolated molecule. At the same time, the interactions causing condensation are substantial, and it is an established fact that new contributions of appreciable intensity do appear in the spectrum of the condensed phase. Furthermore, the interactions become more powerful in a crystal than in a liquid so that some general increase of intensity might be expected to accompany solidification. This increase, when observed, will be most noticeable for fundamentals that develop activity only after entering the condensed phase. Components of the spectrum permitted also in the vapor will exhibit merely a small increment in a basic level of intensity; combinations that develop only after entering the condensed phase will be comparatively weak so that the increase of intensity will not be striking; the newly developed fundamentals will have medium intensity and their growth will seem more spectacular. Lattice modes of rotatory origin can develop high intensities,[3,4] whereas those of translatory origin may be strong in the infra-red spectra of ionic crystals but are probably weak otherwise.

ORIENTATION EFFECTS

The selection rules deduced for crystals by procedures described here are sometimes susceptible to further refinement for special conditions of observation. In addition to the usual alterations of a Raman spectrum resulting from the use of polarized light there are entirely new possibilities that have no counterpart in spectra of fluids. When a fluid is irradiated, its randomly oriented molecules present all possible aspects to the radiation. Consequently, the electric vector of the light can enter all suitable irreducible representations of the molecules in the course of a sufficiently large number of molecular encounters. However, in a large single crystal all molecules not rotating freely have similar orientations so that a beam of parallel light encounters much the same aspect of all molecules in its path. In some cases, depending upon the nature of the *site groups* involved, a direction of approach can be selected so that no component of the electric vector will appear in one of the suitable irreducible representations of sites that are occupied. Then, only two of the components of transitory electric moment and only three of the elements of transitory polarizability will be energized. For some *site groups* it is possible in addition to select a plane of polarization for the incident light so as to exclude its components at the same time from another irreducible representation. Then, only one component of the transitory electric moment and one element of the transitory polarizability will be energized. The correspondingly sharpened selection rules and the directions of approach and planes of polarization for which they operate can be deduced easily from inspection of the external form of the crystal (provided that it is not pseudomorphous) and knowledge of the *site groups* that are in use. The irreducible representations of a *site group* that can be penetrated by a vector representing the radiation field will be the ones containing components of the transitory electric moment. The orientations of these components relative to the elements of symmetry of the *site group* can be established by inspecting the table of group characters. However, the elements of symmetry contained in the *site group* must be identical with those contained in the *crystallographic point group* and hence they can be located relative to the faces of the crystal by inspecting its external form. To predict the effect produced in the Raman spectrum is likewise easy. Each element of polarizability is associated with two, not necessarily distinct components of the electric vector of the radiation field. When two irreducible representations, not necessarily distinct but each containing a component of the electric vector, are combined in a direct product[1] the resulting irreducible representation will contain the associated element of polarizability. If either of the components is absent for a particular orientation of the crystal then the associated element of polarizability will be inoperable. The manipulation of group characters required for this analysis is exactly the same one used to predict selection rules for combinations and overtones and would be undertaken in any event. The totally symmetric irreducible representation

of a *site group* will often contain the three diagonal elements of the polarizability tensor. Then this representation will contribute to the spectrum for all orientations of the single crystal. This persistence notwithstanding it is evident that relative intensities observed in spectra of single crystals will be highly sensitive to orientation. The validity of this conclusion is well established in fact.[3,4,9,10] The entire subject has received elaborate theoretical treatment.[3,11] It is interesting to note that a crystal containing freely rotating ions should not show the expected effects of orientation. This suggests a valuable tool for study of some second-order phase transitions.

FREQUENCY ASSIGNMENTS

Finally it will be remarked that the most fruitful approach, when feasible, to the identification of vibration frequencies for a symmetrical molecule will start with the spectra of the vapor, proceed to the spectra of the solid, and conclude with the spectra of the liquid. In favorable cases a complete assignment of frequencies can be made in this way without having any resort to data for isotopic molecules.

APPENDIX

Availabilities and Symmetries of Sites in the 230 Space Groups[5]

The standard symbol for the space group will be found below in boldface type. Following it are a series of symbols describing the various sites. The description for a site consists of the standard point group symbol preceded by the number of distinct sets of this kind and followed in parentheses by the number of equivalent sites per set. The numbers are appended only when they differ from unity. Thus, the entry $\mathbf{C}_4^1$: $2C_4$, $C_2(2)$ signifies that the space group $\mathbf{C}_4^1$ contains 2 distinct sets of sites having point symmetry C_4 with one site per set and 1 set of sites having point symmetry C_2 with two equivalent sites per set. If the symbol for a space group is absent this means that it contains no sites.

$\mathbf{C}_i^1$: $8C_i$; $\mathbf{C}_s^1$: $2C_s$; $\mathbf{C}_s^3$: $C_s(2)$; $\mathbf{C}_2^1$: $4C_2$; $\mathbf{C}_2^3$: $2C_2(2)$; $\mathbf{C}_{2h}^1$: $8C_{2h}$, $4C_2(2)$, $2C_s(2)$; $\mathbf{C}_{2h}^2$: $4C_i(2)$, $C_s(2)$; $\mathbf{C}_{2h}^3$: $4C_{2h}(2)$, $2C_i(4)$, $2C_2(4)$, $C_s(4)$; $\mathbf{C}_{2h}^4$: $4C_i(2)$, $2C_2(2)$; $\mathbf{C}_{2h}^5$: $4C_i(2)$; $\mathbf{C}_{2h}^6$: $4C_i(4)$, $C_2(4)$; $\mathbf{C}_{2v}^1$: $4C_{2v}$, $4C_s(2)$; $\mathbf{C}_{2v}^2$: $2C_s(2)$; $\mathbf{C}_{2v}^3$: $4C_2(2)$; $\mathbf{C}_{2v}^4$: $2C_2(2)$, $C_s(2)$; $\mathbf{C}_{2v}^6$: $2C_2(2)$; $\mathbf{C}_{2v}^7$: $C_s(2)$; $\mathbf{C}_{2v}^8$: $2C_2(2)$; $\mathbf{C}_{2v}^{10}$: $2C_2(2)$; $\mathbf{C}_{2v}^{11}$: $2C_{2v}(2)$, $C_2(4)$, $2C_s(4)$; $\mathbf{C}_{2v}^{12}$: $C_s(4)$; $\mathbf{C}_{2v}^{13}$: $3C_2(4)$; $\mathbf{C}_{2v}^{14}$: $2C_{2v}(2)$, $3C_s(4)$; $\mathbf{C}_{2v}^{15}$: $2C_2(4)$, $C_s(4)$; $\mathbf{C}_{2v}^{16}$: $C_2(4)$, $C_s(4)$; $\mathbf{C}_{2v}^{17}$: $C_2(4)$; $\mathbf{C}_{2v}^{18}$: $C_{2v}(4)$, $C_2(8)$, $2C_s(8)$; $\mathbf{C}_{2v}^{19}$: $C_2(8)$; $\mathbf{C}_{2v}^{20}$: $2C_{2v}(2)$, $2C_s(4)$; $\mathbf{C}_{2v}^{21}$: $2C_2(4)$; $\mathbf{C}_{2v}^{22}$: $C_2(4)$, $C_s(4)$; $\mathbf{V}^1$: $8V$, $12C_2(2)$; $\mathbf{V}^2$: $4C_2(2)$; $\mathbf{V}^3$: $2C_2(2)$; $\mathbf{V}^5$: $2C_2(4)$; $\mathbf{V}^6$: $4V(2)$, $7C_2(4)$; $\mathbf{V}^7$: $4V(4)$, $6C_2(8)$; $\mathbf{V}^8$: $4V(2)$, $6C_2(4)$; $\mathbf{V}^9$: $3C_2(4)$; $\mathbf{V}_h^1$: $8V_h$, $12C_{2v}(2)$, $6C_s(4)$; $\mathbf{V}_h^2$: $4V(2)$, $2C_i(4)$, $6C_2(4)$; $\mathbf{V}_h^3$: $4C_{2h}(2)$, $4V(2)$, $8C_2(4)$, $C_s(4)$; $\mathbf{V}_h^4$: $4V(2)$, $2C_i(4)$, $6C_2(4)$; $\mathbf{V}_h^5$: $4C_{2h}(2)$, $2C_{2v}(2)$, $2C_2(4)$, $3C_s(4)$; $\mathbf{V}_h^6$: $2C_i(4)$, $2C_2(4)$; $\mathbf{V}_h^7$: $4C_{2h}(2)$, $3C_2(4)$, $C_s(4)$; $\mathbf{V}_h^8$: $2C_i(4)$, $3C_2(4)$; $\mathbf{V}_h^9$: $4C_{2h}(2)$, $2C_2(4)$, $2C_s(4)$; $\mathbf{V}_h^{10}$: $2C_i(4)$, $2C_2(4)$; $\mathbf{V}_h^{11}$: $2C_i(4)$, $C_2(4)$, $C_s(4)$; $\mathbf{V}_h^{12}$: $4C_{2h}(2)$, $2C_2(4)$, $C_s(4)$; $\mathbf{V}_h^{13}$: $2C_{2v}(2)$, $2C_i(4)$, $2C_s(4)$; $\mathbf{V}_h^{14}$: $2C_i(4)$, $C_2(4)$; $\mathbf{V}_h^{15}$: $2C_i(4)$; $\mathbf{V}_h^{16}$: $2C_i(4)$, $C_s(4)$; $\mathbf{V}_h^{17}$: $2C_{2h}(4)$, $C_{2v}(4)$, $C_i(8)$, $C_2(8)$, $2C_s(8)$; $\mathbf{V}_h^{18}$: $2C_{2h}(4)$, $C_i(8)$, $2C_2(8)$, $C_s(8)$; $\mathbf{V}_h^{19}$: $4V_h(2)$, $2C_{2h}(4)$, $6C_{2v}(4)$, $C_2(8)$, $4C_s(8)$; $\mathbf{V}_h^{20}$: $2V(4)$, $4C_{2h}(4)$, $5C_2(8)$, $C_s(8)$; $\mathbf{V}_h^{21}$: $2V(4)$, $4C_{2h}(4)$, $C_{2v}(4)$, $5C_2(8)$, $2C_s(8)$; $\mathbf{V}_h^{22}$: $2V(4)$, $2C_i(8)$, $4C_2(8)$; $\mathbf{V}_h^{23}$: $2V_h(4)$, $3C_{2h}(8)$, $V(8)$, $3C_{2v}(8)$, $3C_2(16)$, $3C_s(16)$; $\mathbf{V}_h^{24}$: $2V(8)$, $2C_i(16)$, $3C_2(16)$; $\mathbf{V}_h^{25}$: $4V_h(2)$, $6C_{2v}(4)$, $C_i(8)$, $3C_s(8)$; $\mathbf{V}_h^{26}$: $2V(4)$, $2C_{2h}(4)$, $C_i(8)$, $4C_2(8)$, $C_s(8)$; $\mathbf{V}_h^{27}$: $2C_i(8)$, $3C_2(8)$; $\mathbf{V}_h^{28}$: $4C_{2h}(4)$, $C_{2v}(4)$, $2C_2(8)$, $2C_s(8)$; $\mathbf{S}_4^1$: $4S_4$, $3C_2(2)$; $\mathbf{S}_4^2$: $4S_4(2)$, $2C_2(4)$; $\mathbf{V}_d^1$: $4V_d$, $2V(2)$, $2C_{2v}(2)$, $5C_2(4)$, $C_s(4)$; $\mathbf{V}_d^2$: $4V(2)$, $2S_4(2)$, $7C_2(4)$; $\mathbf{V}_d^3$: $2S_4(2)$, $C_{2v}(2)$, $C_2(4)$, $C_s(4)$; $\mathbf{V}_d^4$: $2S_4(2)$, $2C_2(4)$; $\mathbf{V}_d^5$: $4V_d(2)$, $3C_{2v}(4)$, $2C_2(8)$, $2C_s(8)$; $\mathbf{V}_d^6$: $2V(4)$, $2S_4(4)$, $5C_2(8)$; $\mathbf{V}_d^7$: $2S_4(4)$, $2V(4)$, $4C_2(8)$; $\mathbf{V}_d^8$: $2S_4(4)$, $2V(4)$, $4C_2(8)$; $\mathbf{V}_d^9$: $4V_d(4)$, $2C_{2v}(8)$, $2C_2(16)$, $C_s(16)$; $\mathbf{V}_d^{10}$: $2S_4(8)$, $2V(8)$, $4C_2(16)$; $\mathbf{V}_d^{11}$: $2V_d(2)$, $V(4)$, $S_4(4)$, $C_{2v}(4)$, $3C_2(8)$, $C_s(8)$; $\mathbf{V}_d^{12}$: $2S_4(4)$, $2C_2(8)$; $\mathbf{C}_4^1$: $2C_4$, $C_2(2)$; $\mathbf{C}_4^3$: $3C_2(2)$; $\mathbf{C}_4^5$: $C_4(2)$, $C_2(4)$; $\mathbf{C}_4^6$: $C_2(4)$; $\mathbf{C}_{4h}^1$: $4C_{4h}$, $2C_{2h}(2)$, $2C_4(2)$, $C_2(4)$, $2C_s(4)$; $\mathbf{C}_{4h}^2$: $4C_{2h}(2)$, $2S_4(2)$, $3C_2(4)$, $C_s(4)$; $\mathbf{C}_{4h}^3$: $2S_4(2)$, $C_4(2)$, $2C_i(4)$, $C_2(4)$; $\mathbf{C}_{4h}^4$: $2S_4(2)$, $2C_i(4)$, $2C_2(4)$; $\mathbf{C}_{4h}^5$: $2C_{4h}(2)$, $C_{2h}(4)$, $S_4(4)$, $C_4(4)$, $C_i(8)$, $C_2(8)$, $C_s(8)$; $\mathbf{C}_{4h}^6$: $2S_4(4)$, $2C_i(8)$, $C_2(8)$; $\mathbf{C}_{4v}^1$: $2C_{4v}$, $C_{2v}(2)$, $3C_s(4)$; $\mathbf{C}_{4v}^2$: $C_4(2)$, $C_{2v}(2)$, $C_s(4)$; $\mathbf{C}_{4v}^3$: $2C_{2v}(2)$, $C_2(4)$, $C_s(4)$; $\mathbf{C}_{4v}^4$: $C_{2v}(2)$, $C_2(4)$, $C_s(4)$; $\mathbf{C}_{4v}^5$: $2C_4(2)$, $C_2(4)$; $\mathbf{C}_{4v}^6$: $C_4(2)$, $C_2(4)$; $\mathbf{C}_{4v}^7$: $3C_{2v}(2)$, $2C_s(4)$; $\mathbf{C}_{4v}^8$: $2C_2(4)$; $\mathbf{C}_{4v}^9$: $C_{4v}(2)$, $C_{2v}(4)$, $2C_s(8)$; $\mathbf{C}_{4v}^{10}$: $C_4(4)$, $C_{2v}(4)$, $C_s(8)$; $\mathbf{C}_{4v}^{11}$: $C_{2v}(4)$,

[9] S. Bhagavantam, Proc. Ind. Acad. Sci. **11A**, 62 (1940).
[10] R. B. Barnes, Phys. Rev. **39**, 562 (1932).
[11] J. Cabannes, Comptes rendus **211**, 625, 750 (1940).

$C_s(8)$; $\mathbf{C}_{4v}^{12}$: $C_2(8)$; $\mathbf{D}_4^1$: $4D_4$, $2V(2)$, $2C_4(2)$, $7C_2(4)$; $\mathbf{D}_4^2$: $2V(2)$, $C_4(2)$, $3C_2(4)$; $\mathbf{D}_4^3$: $3C_2(4)$; $\mathbf{D}_4^4$: $C_2(4)$; $\mathbf{D}_4^5$: $6V(2)$, $9C_2(4)$; $\mathbf{D}_4^6$: $2V(2)$, $4C_2(4)$; $\mathbf{D}_4^7$: $3C_2(4)$; $\mathbf{D}_4^8$: $C_2(4)$; $\mathbf{D}_4^9$: $2D_4(2)$, $2V(4)$, $C_4(4)$, $5C_2(8)$; $\mathbf{D}_4^{10}$: $2V(4)$, $4C_2(8)$; $\mathbf{D}_{4h}^1$: $4D_{4h}$, $2V_h(2)$, $2C_{4v}(2)$, $7C_{2v}(4)$, $5C_s(8)$; $\mathbf{D}_{4h}^2$: $2D_4(2)$, $2C_{4h}(2)$, $V(4)$, $C_{2h}(4)$, $2C_4(4)$, $4C_2(8)$, $C_s(8)$; $\mathbf{D}_{4h}^3$: $2D_4(2)$, $2V_d(2)$, $2C_{2h}(4)$, $C_4(4)$, $C_{2v}(4)$, $4C_2(8)$, $C_s(8)$; $\mathbf{D}_{4h}^4$: $2D_4(2)$, $V(4)$, $S_4(4)$, $C_4(4)$, $C_i(8)$, $4C_2(8)$; $\mathbf{D}_{4h}^5$: $2C_{4h}(2)$, $2V_h(2)$, $C_4(4)$, $3C_{2v}(4)$, $3C_s(8)$; $\mathbf{D}_{4h}^6$: $2C_{4h}(2)$, $C_{2h}(4)$, $V(4)$, $C_4(4)$, $2C_2(8)$, $C_s(8)$; $\mathbf{D}_{4h}^7$: $2V_d(2)$, $C_{4v}(2)$, $2C_{2h}(4)$, $C_{2v}(4)$, $2C_2(8)$, $2C_s(8)$; $\mathbf{D}_{4h}^8$: $V(4)$, $S_4(4)$, $C_4(4)$, $C_i(8)$, $2C_2(8)$; $\mathbf{D}_{4h}^9$: $4V_h(2)$, $2V_d(2)$, $7C_{2v}(4)$, $C_2(8)$, $3C_s(8)$; $\mathbf{D}_{4h}^{10}$: $2V_d(2)$, $2V_h(2)$, $V(4)$, $C_{2h}(4)$, $4C_{2v}(4)$, $3C_2(8)$, $2C_s(8)$; $\mathbf{D}_{4h}^{11}$: $3V(4)$, $S_4(4)$, $C_i(8)$, $5C_2(8)$; $\mathbf{D}_{4h}^{12}$: $2V_d(2)$, $2V(4)$, $2C_{2h}(4)$, $C_{2v}(4)$, $5C_2(8)$, $C_s(8)$; $\mathbf{D}_{4h}^{13}$: $2C_{2h}(4)$, $S_4(4)$, $V(4)$, $3C_2(8)$, $C_s(8)$; $\mathbf{D}_{4h}^{14}$: $2V_h(2)$, $C_{2h}(4)$, $S_4(4)$, $3C_{2v}(4)$, $C_2(8)$, $2C_s(8)$; $\mathbf{D}_{4h}^{15}$: $2V_d(2)$, $2C_{2v}(4)$, $C_i(8)$, $C_2(8)$, $C_s(8)$; $\mathbf{D}_{4h}^{16}$: $V(4)$, $S_4(4)$, $2C_{2h}(4)$, $C_{2v}(4)$, $3C_2(8)$, $C_s(8)$; $\mathbf{D}_{4h}^{17}$: $2D_{4h}(2)$, $V_h(4)$, $V_d(4)$, $C_{4v}(4)$, $C_{2h}(8)$, $4C_{2v}(8)$, $C_2(16)$, $3C_s(16)$; $\mathbf{D}_{4h}^{18}$: $D_4(4)$, $V_d(4)$, $C_{4h}(4)$, $V_h(4)$, $C_{2h}(8)$, $C_4(8)$, $2C_{2v}(8)$, $2C_2(16)$, $2C_s(16)$; $\mathbf{D}_{4h}^{19}$: $2V_d(4)$, $2C_{2h}(8)$, $C_{2v}(8)$, $2C_2(16)$, $C_s(16)$; $\mathbf{D}_{4h}^{20}$: $V(8)$, $S_4(8)$, $C_i(16)$, $3C_2(16)$; $\mathbf{T}^1$: $2T$, $2V(3)$, $C_3(4)$, $4C_2(6)$; $\mathbf{T}^2$: $4T(4)$, $C_3(16)$, $2C_2(24)$; $\mathbf{T}^3$: $T(2)$, $V(6)$, $C_3(8)$, $2C_2(12)$; $\mathbf{T}^4$: $C_3(4)$; $\mathbf{T}^5$: $C_3(8)$, $C_2(12)$; $\mathbf{T}_h^1$: $2T_h$, $2V_h(3)$, $4C_{2v}(6)$, $C_3(8)$, $2C_s(12)$; $\mathbf{T}_h^2$: $T(2)$, $2C_{3i}(4)$, $V(6)$, $C_3(8)$, $2C_2(12)$; $\mathbf{T}_h^3$: $2T_h(4)$, $T(8)$, $C_{2h}(24)$, $C_{2v}(24)$, $C_3(32)$, $C_2(48)$, $C_s(48)$; $\mathbf{T}_h^4$: $2T(8)$, $2C_{3i}(16)$, $C_3(32)$, $C_2(48)$; $\mathbf{T}_h^5$: $T_h(2)$, $V_h(6)$, $C_{3i}(8)$, $2C_{2v}(12)$, $C_3(16)$, $C_s(24)$; $\mathbf{T}_h^6$: $2C_{3i}(4)$, $C_3(8)$; $\mathbf{T}_h^7$: $2C_{3i}(8)$, $C_3(16)$, $C_2(24)$; $\mathbf{T}_d^1$: $2T_d$, $2V_d(3)$, $C_{3v}(4)$, $2C_{2v}(6)$, $C_2(12)$, $C_s(12)$; $\mathbf{T}_d^2$: $4T_d(4)$, $C_{3v}(16)$, $2C_{2v}(24)$, $C_s(48)$; $\mathbf{T}_d^3$: $T_d(2)$, $V_d(6)$, $C_{3v}(8)$, $S_4(12)$, $C_{2v}(12)$, $C_2(24)$, $C_s(24)$; $\mathbf{T}_d^4$: $T(2)$, $V(6)$, $2S_4(6)$, $C_3(8)$, $3C_2(12)$; $\mathbf{T}_d^5$: $2T(8)$, $2S_4(24)$, $C_3(32)$, $2C_2(48)$; $\mathbf{T}_d^6$: $2S_4(12)$, $C_3(16)$, $C_2(24)$; $\mathbf{O}^1$: $2O$, $2D_4(3)$, $2C_4(6)$, $C_3(8)$, $3C_2(12)$; $\mathbf{O}^2$: $T(2)$, $2D_3(4)$, $3V(6)$, $C_3(8)$, $5C_2(12)$; $\mathbf{O}^3$: $2O(4)$, $T(8)$, $V(24)$, $C_4(24)$, $C_3(32)$, $3C_2(48)$; $\mathbf{O}^4$: $2T(8)$, $2D_3(16)$, $C_3(32)$, $2C_2(48)$; $\mathbf{O}^5$: $O(2)$, $D_4(6)$, $D_3(8)$, $V(12)$, $C_4(12)$, $C_3(16)$, $3C_2(24)$; $\mathbf{O}^6$: $2D_3(4)$, $C_3(8)$, $C_2(12)$; $\mathbf{O}^7$: $2D_3(4)$, $C_3(8)$, $C_2(12)$; $\mathbf{O}^8$: $2D_3(8)$, $2V(12)$, $C_3(16)$, $3C_2(24)$; $\mathbf{O}_h^1$: $2O_h$, $2D_{4h}(3)$, $2C_{4v}(6)$, $C_{3v}(8)$, $3C_{2v}(12)$, $3C_s(24)$; $\mathbf{O}_h^2$: $O(2)$, $D_4(6)$, $C_{3i}(8)$, $S_4(12)$, $C_4(12)$, $C_3(16)$, $2C_2(24)$; $\mathbf{O}_h^3$: $T_h(2)$, $V_h(6)$, $2V_d(6)$, $D_3(8)$, $3C_{2v}(12)$, $C_3(16)$, $C_2(24)$, $C_s(24)$; $\mathbf{O}_h^4$: $T_d(2)$, $2D_{3d}(4)$, $V_d(6)$, $C_{3v}(8)$, $V(12)$, $C_{2v}(12)$, $2C_2(24)$, $C_s(24)$; $\mathbf{O}_h^5$: $2O_h(4)$, $T_d(8)$, $V_h(24)$, $C_{4v}(24)$, $C_{3v}(32)$, $3C_{2v}(48)$, $2C_s(96)$; $\mathbf{O}_h^6$: $O(8)$, $T_h(8)$, $V_d(24)$, $C_{4h}(24)$, $C_{2v}(48)$, $C_4(48)$, $C_3(64)$, $C_2(96)$, $C_s(96)$; $\mathbf{O}_h^7$: $2T_d(8)$, $2D_{3d}(16)$, $C_{3v}(32)$, $C_{2v}(48)$, $C_s(96)$, $C_2(96)$; $\mathbf{O}_h^8$: $T(16)$, $D_3(32)$, $C_{3i}(32)$, $S_4(48)$, $C_3(64)$, $2C_2(96)$; $\mathbf{O}_h^9$: $O_h(2)$, $D_{4h}(6)$, $D_{3d}(8)$, $V_d(12)$, $C_{4v}(12)$, $C_{3v}(16)$, $2C_{2v}(24)$, $C_2(48)$, $2C_s(48)$; $\mathbf{O}_h^{10}$: $C_{3i}(16)$, $D_3(16)$, $V(24)$, $S_4(24)$, $C_3(32)$, $2C_2(48)$; $\mathbf{C}_3^1$: $3C_3$; $\mathbf{C}_3^4$: C_3; $\mathbf{C}_{3i}^1$: $2C_{3i}$, $2C_3(2)$, $2C_i(3)$; $\mathbf{C}_{3i}^2$: $2C_{3i}$, $C_3(2)$, $2C_i(3)$; $\mathbf{C}_{3v}^1$: $3C_{3v}$, $C_s(3)$; $\mathbf{C}_{3v}^2$: C_{3v}, $C_3(2)$, $C_s(3)$; $\mathbf{C}_{3v}^3$: $3C_3(2)$; $\mathbf{C}_{3v}^4$: $2C_3(2)$; $\mathbf{C}_{3v}^5$: C_{3v}, $C_s(3)$; $\mathbf{C}_{3v}^6$: $C_3(2)$; $\mathbf{D}_3^1$: $6D_3$, $3C_3(2)$, $2C_2(3)$; $\mathbf{D}_3^2$: $2D_3$, $2C_3(2)$, $2C_2(3)$; $\mathbf{D}_3^3$: $2C_2(3)$; $\mathbf{D}_3^4$: $2C_2(3)$; $\mathbf{D}_3^5$: $2C_2(3)$; $\mathbf{D}_3^6$: $2C_2(3)$; $\mathbf{D}_3^7$: $2D_3$, $C_3(2)$, $2C_2(3)$; $\mathbf{D}_{3d}^1$: $2D_{3d}$, $2D_3(2)$, $C_{3v}(2)$, $2C_{2h}(3)$, $C_3(4)$, $2C_2(6)$, $C_s(6)$; $\mathbf{D}_{3d}^2$: $3D_3(2)$, $C_{3i}(2)$, $2C_3(4)$, $C_i(6)$, $C_2(6)$; $\mathbf{D}_{3d}^3$: $2D_{3d}$, $2C_{3v}(2)$, $2C_{2h}(3)$, $2C_2(6)$, $C_s(6)$; $\mathbf{D}_{3d}^4$: $D_3(2)$, $C_{3i}(2)$, $2C_3(4)$, $C_i(6)$, $C_2(6)$; $\mathbf{D}_{3d}^5$: $2D_{3d}$, $C_{3v}(2)$, $2C_{2h}(3)$, $2C_2(6)$, $C_s(6)$; $\mathbf{D}_{3d}^6$: $D_3(2)$, $C_{3i}(2)$, $C_3(4)$, $C_i(6)$, $C_2(6)$; $\mathbf{C}_{3h}^1$: $6C_{3h}$, $3C_3(2)$, $2C_s(3)$; $\mathbf{D}_{3h}^1$: $6D_{3h}$, $3C_{3v}(2)$, $2C_{2v}(3)$, $3C_s(6)$; $\mathbf{D}_{3h}^2$: $3D_3(2)$, $3C_{3h}(2)$, $3C_3(4)$, $C_2(6)$, $C_s(6)$; $\mathbf{D}_{3h}^3$: $2D_{3h}$, $2C_{3h}(2)$, $C_{3v}(2)$, $2C_{2v}(3)$, $C_3(4)$, $3C_s(6)$; $\mathbf{D}_{3h}^4$: $D_3(2)$, $3C_{3h}(2)$, $2C_3(4)$, $C_2(6)$, $C_s(6)$; $\mathbf{C}_6^1$: C_6, $C_3(2)$, $C_2(3)$; $\mathbf{C}_6^4$: $2C_2(3)$; $\mathbf{C}_6^5$: $2C_2(3)$; $\mathbf{C}_6^6$: $2C_3(2)$; $\mathbf{C}_{6v}^1$: C_{6v}, $C_{3v}(2)$, $C_{2v}(3)$, $2C_s(6)$; $\mathbf{C}_{6v}^2$: $C_6(2)$, $C_3(4)$, $C_2(6)$; $\mathbf{C}_{6v}^3$: $C_{3v}(2)$, $C_3(4)$, $C_s(6)$; $\mathbf{C}_{6v}^4$: $2C_{3v}(2)$, $C_s(6)$; $\mathbf{C}_{6h}^1$: $2C_{6h}$, $2C_{3h}(2)$, $C_6(2)$, $2C_{2h}(3)$, $C_3(4)$, $C_2(6)$, $2C_s(6)$; $\mathbf{C}_{6h}^2$: $3C_{3h}(2)$, $C_{3i}(2)$, $2C_3(4)$, $C_i(6)$, $C_s(6)$; $\mathbf{D}_6^1$: $2D_6$, $2D_3(2)$, $C_6(2)$, $2V(3)$, $C_3(4)$, $5C_2(6)$; $\mathbf{D}_6^2$: $2C_2(6)$; $\mathbf{D}_6^3$: $2C_2(6)$; $\mathbf{D}_6^4$: $4V(3)$, $6C_2(6)$; $\mathbf{D}_6^5$: $4V(3)$, $6C_2(6)$; $\mathbf{D}_6^6$: $4D_3(2)$, $2C_3(4)$, $2C_2(6)$; $\mathbf{D}_{6h}^1$: $2D_{6h}$, $2D_{3h}(2)$, $C_{6v}(2)$, $2V_h(3)$, $C_{3v}(4)$, $5C_{2v}(6)$, $4C_s(12)$; $\mathbf{D}_{6h}^2$: $D_6(2)$, $C_{6h}(2)$, $D_3(4)$, $C_{3h}(4)$, $C_6(4)$, $V(6)$, $C_{2h}(6)$, $C_3(8)$, $3C_2(12)$, $C_s(12)$; $\mathbf{D}_{6h}^3$: $D_{3h}(2)$, $D_{3d}(2)$, $C_{3h}(4)$, $D_3(4)$, $C_{3v}(4)$, $C_{2h}(6)$, $C_{2v}(6)$, $C_3(8)$, $C_2(12)$, $2C_s(12)$; $\mathbf{D}_{6h}^4$: $D_{3d}(2)$, $3D_{3h}(2)$, $2C_{3v}(4)$, $C_{2h}(6)$, $C_{2v}(6)$, $C_2(12)$, $2C_s(12)$.

Kinetics of OH Radicals as Determined by Their Absorption Spectrum

VI. Attempt to Trace OH Radicals in the Thermal Hydrogen-Oxygen Reaction[1]

O. OLDENBERG, J. E. MORRIS, C. T. MORROW, E. G. SCHNEIDER,* AND H. S. SOMMERS, JR.*
Research Laboratory of Physics, Harvard University, Cambridge, Massachusetts

(Received August 28, 1945)

The steady thermal reaction of hydrogen and oxygen at a pressure of 60 cm and a temperature in the region of 550° C was searched by absorption spectrum technique for free OH radicals. None were detected, although the apparatus would have been sensitive to an OH radical pressure of 4×10^{-4} mm. This negative result indicates that the OH radicals have a very short lifetime in the reacting mixture.

I. PROBLEM

THE existence and life history of free hydroxyl radicals has been investigated, as described in preceding papers,[2] by observing their absorption spectrum. In particular, this method was applied to free OH generated in low pressure water vapor by an electric discharge. The present paper describes an attempt to trace free OH in the thermal hydrogen-oxygen reaction. The various theories of this reaction agree in assuming the formation of free OH as an intermediary step. If we were able to test the concentration of free OH as a function of the time, interesting conclusions could be drawn regarding the mechanism of the reaction. The negative result reported below gives an upper limit for the free OH present under the most favorable conditions that can be prepared with a reasonable effort.

II. EXPERIMENT

(a) The Thermal Reaction

The *reaction vessel*, which was designed to have the greatest possible path length for the light used in the measurement of the absorption spectra, consisted of a Pyrex tube, of length 134 cm, and inner diameter 4.8 cm. Heavy windows of fused quartz were sealed with glyptal onto both ends. The two gases were admitted successively. If the gases were admitted through an inlet attached to one end of the long cylindrical reaction vessel, the mixing would possibly not be quite thorough. In order to secure a uniform mixture the gases were admitted through two inlets properly located.

The reaction vessel was heated by an *electric oven* 11 cm shorter than the vessel. To protect the seals the protruding ends of the vessel were cooled with water running through lead pipes. The temperature was between 540 and 559°C. Great care was taken to keep the temperature uniform along the vessel. This was necessary since the rate of the reaction strongly depends on the temperature,[3] so that any local high temperature would cause an explosion. The temperature was kept uniform within ±2°C from the average along a section of 80 cm length with the help of auxiliary heating coils wound on the same core with the main coil. The oven was thermostated by the arrangement described by Bancroft.[4] The temperature was measured with a platinum/platinum-rhodium thermocouple tested for homogeneity of the wires. To guard against danger from explosions the oven containing the reaction vessel was surrounded by copper gauze screens. *Electrolytic hydrogen and oxygen* were used, each being purified by passage through tubes containing P_2O_5, platinized asbestos, and again P_2O_5.

For most of the experiments, the surface of the reaction vessel was conditioned by successive reactions, separated by short periods of pumping. Previous work[3] had shown that this procedure leads to reproducible reaction rates.

* At present at the Radiation Laboratory, Massachusetts Institute of Technology, Cambridge, Massachusetts.

[1] The experiments reported were performed during the years 1938–41. The results obtained by the first group of experiments were reported in Phys. Rev. **58**, 1121 (1940).

[2] For references see O. Oldenberg and F. F. Rieke, J. Chem. Phys. **7**, 485 (1939).

[3] O. Oldenberg and H. S. Sommers, Jr., J. Chem. Phys. **9**, 432 (1941).

[4] D. Bancroft, Rev. Sci. Inst. **13**, 24, 114 (1942).

(b) Optical Arrangement

The optical arrangement has been described in preceding papers.[5] In order to make the test by the absorption spectrum as sensitive as possible, a 21-foot concave grating was used in the second order. The length of the spectral lines was reduced and so the astigmatism, which is caused by the concave grating, was largely removed by a cylindrical quartz lens placed in front of the plate. For a continuous background the spectrum from the positive carbon of an arc burning in dry nitrogen was used. This seems to be the most intense background available around 3000A. For some exposures the continuous spectrum from a discharge through dry hydrogen was applied. With the apparatus available, this was not quite as intense as the spectrum from the carbon, but it was more uniform with time.

In order to take advantage of the full resolving power of the grating, Eastman Process Plates or Spectroscopic Plates III-O were used. The times of exposure were between one and one-half and three minutes.

In order to increase the sensitivity of the test for OH and so give the negative result reported below greater significance, in the final group of experiments the light was twice reflected and so passed three times through the reaction vessel. This increased the effective length of the absorbing gas to 240 cm.

(c) Procedure

The hydrogen was admitted to the reaction vessel first, and the oxygen second, to prevent a second-limit explosion during the mixing of the gases. This was particularly important in the experiments in which the hydrogen represented two thirds of the mixture. Immediately after the admission of both gases, the reaction had its maximum rate; that is, the induction period was negligible provided that the vessel had been prepared by preceding runs.[3] The rate was measured by the usual method of observing the pressure as a function of time. In most experiments the total initial pressure of the mixture was 60 cm. No pressures higher than 65.4 cm were used, because of the danger of a third-limit explosion.

The absorption spectrum was photographed while the reaction progressed at a high rate. In some cases several exposures were made during one reaction, but in most cases only one exposure.

III. RESULT

No trace of the absorption spectrum of OH could be observed. The conditions were so varied that in every attempt a high rate was obtained (see preceding section). The highest rate obtainable was 4.0 cm/min. In two cases it happened that the absorption spectra were taken at rates of the reaction so high that the steady reactions ended in violent explosions ("third" explosion) shattering the quartz windows. Even in these most favorable cases the photographic plates showed no trace of the absorption spectrum. (One of these plates was underexposed, but could be utilized when combined with another plate so that the two emulsions were in contact.)

In three experiments equal parts of hydrogen and oxygen were used, instead of the stoichiometric mixture, with the same negative result.

A quantitative statement can be made on the basis of the recent measurements of Dwyer and Oldenberg,[6] who observed absorption spectra of OH with the same spectrograph and with a known concentration of OH. In a mixture of $\frac{2}{3}H_2O+\frac{1}{3}O_2$ at thermal equilibrium, the faintest observable trace of the absorption spectrum was found at a temperature of 768°C. From the equilibrium constants, the partial pressure of OH follows as 4.2×10^{-4} mm. (For our estimate we may disregard the fact that in our case the conditions are a little more favorable for the observation of the absorption spectrum, because, at our lower temperature [823 instead of 1041°K], the rotational energy is distributed over not quite so many levels and, furthermore, the lines are slightly narrower.) When we take into account the different lengths and temperatures of the absorbing layers, we find that in the rapid, steady thermal reaction the OH radicals, if present at all, are present in a mole fraction of less than 2×10^{-7}.

This negative result does not necessarily indicate that the free OH radical takes no part

[5] O. Oldenberg and F. F. Rieke, J. Chem. Phys. **6**, 442 (1938).

[6] R. J. Dwyer and O. Oldenberg, J. Chem. Phys. **12**, 351 (1944).

in the thermal reaction. More plausible is the alternative assumption, made by von Elbe and Lewis,[7] that, near 550°C, the rate of the reaction which consumes OH is so high that no appreciable accumulation of OH can occur.

At present, the theory of von Elbe and Lewis does not predict the concentration of OH, nor does any other theory, since the rates of the reactions *producing* and *consuming* OH are not sufficiently known. All schemes ever proposed agree in the assumption that the reaction *consuming* OH—except adsorption at the surface—is $OH+H_2 \rightarrow H_2O+H$. This reaction is exothermic by 15.7 kcal. Its heat of activation is not known. On the other hand, many different reactions *producing* OH have been proposed, as is evident in the reaction scheme of von Elbe and Lewis. The principal result of the present experiment is that at 550°C the reaction just mentioned, consuming OH, is so rapid that no noticeable accumulation of OH occurs. This agrees with the result recently published by Avramenko,[8] who, on the basis of observations in dilute hydrogen flames, concluded that the reaction mentioned is very rapid.

IV. INCIDENTAL OBSERVATIONS

(a) Search for H_2O_2

Pease[9] discovered that a considerable percentage of H_2O_2 was formed at 520–550°C in Pyrex vessels through which a 2:1 hydrogen-oxygen mixture was passing at atmospheric pressure. The yield of H_2O_2 strongly depended on the treatment of the surface. Since this yield was as high as 1 mole H_2O_2 to each 4 moles of H_2O, it seemed worth while to attempt to trace the concentration of H_2O_2 by the intensity of its absorption spectrum.

It is known that the absorption spectrum of H_2O_2 is continuous and has an intensity increasing toward short wave-lengths.[10] Therefore it is convenient to use as a background the continuous emission spectrum of the electric discharge through H_2. We observed the shortest wave-length easily photographed with a quartz spectrograph, that is, 2300A. The reaction vessel was the same as in the experiments reported above, that is, Pyrex treated by preceding reactions, hence presumably covered with H_2O. The highest rate used was 2.6 cm/min.

The result was negative. Since consecutive exposures were compared, the accuracy of the photometric method was not higher than, say, 10 percent. This would indicate a partial pressure of H_2O_2 of less than 0.6 mm. In view of the results of Pease, this low limiting value should be attributed to the surface conditions.

(b) Emission Spectra

Since in the experiments described an unusually deep layer of the reacting gases was available, it seemed worth while to investigate the *emission* spectra of the various types of the reaction.

Beginning with low pressure, at the *explosion of the second limit* ten successive explosions gave only the faintest trace of the OH bands photographed with a quartz spectrograph of high intensity.

The *steady reaction* between the second and third limits does not emit any light of appreciable intensity. This agrees with the result of W. Jono,[11] who needed (for photographing the OH bands) as many as 16,000 steady reactions at a rate only slightly below the first explosion limit.

These observations are in agreement with the proposed reaction schemes which entail free radicals and atoms, but not radicals or atoms or molecules in excited states.

When the first gas admitted has too low a pressure, *inflammation* (or explosion of the second limit) takes place at the admission of the other gas. When the admission is continued, burning takes place. The spectrum contains the OH bands with strongly abnormal rotation.[12] The rotational lines can be traced to about the same limit (quantum number 29) as in the hydrogen-oxygen flame.

[7] G. von Elbe and B. Lewis, J. Chem. Phys. **10**, 393 (1942).

[8] L. I. Avramenko, Chem. Abs. **39**, 3194 (1945); J. Phys. Chem. (U.S.S.R.) **18**, 197–206 (1944).

[9] R. N. Pease, J. Am. Chem. Soc. **52**, 5106 (1930) and **53**, 3188 (1931).

[10] H. C. Urey, L. H. Dawsey, and F. O. Rice, J. Am. Chem. Soc. **51**, 1371 (1929). In this paper the absorption coefficients a of H_2O_2 are determined. However, the value of cd is given by a figure ten times too large. We assume that this is due to a misprint, so that the figures given for the absorption coefficients a are correct.

[11] Reported by S. Horiba, Rev. Phys. Chem. Japan, **11**, 195 (1937).

[12] O. Oldenberg, Phys. Rev. **46**, 210 (1934).

THE JOURNAL OF CHEMICAL PHYSICS VOLUME 14, NUMBER 1 JANUARY, 1946

Electric Circuit Models for the Vibration Spectrum of Polyatomic Molecules

GABRIEL KRON*
General Electric Company, Schenectady, New York
(Received August 20, 1945)

Electrical circuits are developed to determine the normal frequencies and normal modes of vibration of polyatomic molecules having arbitrary configurations. The networks for each molecule are set up without equations from physical considerations alone and may be solved by an a.c. network analyzer, by numerical methods, or by digital (punch card, etc.) calculating machines. The networks also allow the establishment of the resultant secular equations of the molecule by simple inspection. The potential function considered is either a general quadratic form of the displacements, or it may correspond to the customary "valence-force" system employing stretching, bending, and twisting of the valence bonds and valence angles. A companion paper contains network analyzer tests on the CO_2, OCS, and ethyl alcohol molecules by the "valence-force" model. Both the normal frequencies and normal modes of vibration check satisfactorily with known results within the accuracy of the instruments.

PART I. GENERALIZATION POSTULATES

Mathematical Models[1]

TO account for the fundamental frequencies of the infra-red and Raman spectra, the chemist devised several types of mathematical models:

(1) The nuclei execute harmonic vibrations requiring a quadratic potential energy function.

(2) The nuclei execute anharmonic vibrations requiring cubic and quartic, etc., terms in addition to the quadratic terms in the potential function.

(3) The "central force" model assumes forces only along the lines connecting the nuclei.

(4) The "valence force" model associates with the valence bonds appropriate mechanical properties such as stretching and twisting of the bonds, bending of the angles between two bonds or between two planes containing the bonds.

(5) The general model contains a mixture of the quadratic and the valence force models.

Physical Models

Since the analytical study of the above types of models becomes increasingly complex with increasing numbers of atoms or radicals, attempts were made to introduce mechanical models.[2] To represent the valence force model, the atoms were replaced by weights, the bonds between them by springs (or beams), and the angular bending between two bonds was given by the bending of the beams themselves. Such mechanical models, however, do not lend themselves to satisfactory measurements nor do they allow the variation of the various weights and elastic coefficients by the necessary small steps.

On the other hand, electric circuit models set up on an a.c. network analyzer can be adjusted to variations by rather small steps and allow easy measurement of both the normal frequencies and the modes of vibration not only of the valence force but of any type of model as long as it is linear. In the absence of a network analyzer, the electric circuits may be solved

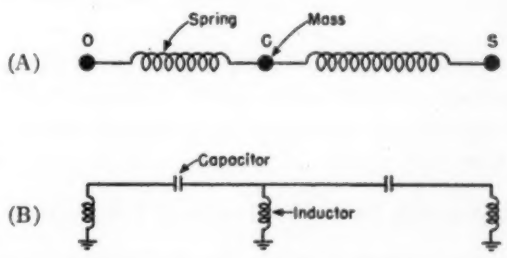

FIG. 1. Masses and springs with one degree of freedom. (A) The OCS molecule. (B) Its electrical analog.

* Consulting engineer.

[1] The writer wishes to acknowledge his indebtedness to Dr. R. M. Fuoss, Sterling Professor of Chemistry, Yale University for several discussions and for his encouragement to pursue the electric-circuit model study of complex molecules. Also he wishes to thank Drs. S. Dushman, J. P. Blewett, and R. P. Johnson, of the Research Laboratory of the General Electric Company, for their comments and encouragement.

[2] D. E. Teets and D. H. Andrews, J. Chem. Phys. **3**, 175 (1935); Murray, Deitz, and Andrews, *ibid.* **3**, 180 (1935).

numerically[3] by hand or by punch-card methods. The circuits also allow the setting up of the resultant secular equations by simple inspection.

Systems with One Degree of Freedom

It has been known for over a century that a mass is analagous to an inductance and a spring to a capacitor. Let, for instance, the OCS molecule be considered, Fig. 1. The three masses representing the three atomic nuclei lie in a straight line along the x axis and are connected by two springs that represent the bonds between the nuclei. The electrical model consists of two capacitors connected to the ground by three inductors. If all the three masses vibrate along the x direction at one of their natural frequencies, in the model oscillatory electric currents of the same frequency flow. Then

(1) The voltages across the inductors represent the displacement of the corresponding masses in the x direction.

(2) The currents in the inductors represent the forces acting on the masses.

Two important limitations of this conventional electrical model should be noted.

(*1*) *Each mass must vibrate along one direction only, namely along the x axis.*

Actually in the OCS molecule the nuclei also vibrate at right angles to the x axis, but the electrical model is unable to represent that type of motion. In more general molecules each mass may have six degrees of freedom, namely three translational motions along the x, y, and z axes and three rotational motions around them. The conventional electrical model completely fails there.

(*2*) *Each valence bond also must lie along the x axis.*

If the angle at C is different from 180 degrees, the conventional electrical model again fails. Of course, in general molecules the bonds extend in every direction.

Systems with Several Degrees of Freedom

It is the purpose of this paper to develop electrical circuits that represent the vibration properties of nuclei that have six degrees of freedom. They are connected by valence bonds that extend in space along arbitrary directions and are endowed with arbitrary properties.

A mechanical system which is rather similar to that of vibrating molecules is a spatial frame structure of beams. Equivalent circuits for such a frame structure have already been developed in another publication.[4] However, *a frame structure is not an exact analog of the chemist's molecule.* In some respects it is too general and in other respects it lacks many of the properties with which the molecules are endowed. For instance, in the molecular model there is no uniform bending along the length of a bond and any bending at the junctions takes place in a plane only. On the other hand, the chemist assumes cross-product stretching between two bonds, a concept that does not occur in a structural frame.

The equations of a simplified beam that can be stretched, twisted, and bent at the junctions will be developed here anew from fundamentals in a manner that will enable it to acquire properties that a physical beam does not possess. For that purpose it will be necessary to decompose each beam into several composite beams, each of the latter possessing only one particular property such as a stretching or an angular bending, etc. Each bond will then be a summation of several of such properties and each molecule will be a summation of several of such beams.

Three Principles to Establish Models for Physical Systems

The mathematical model of a physical system is a set of symbols arranged in the form of equations, while the physical model considered here is a set of stationary electrical coils (resistors, inductors, and capacitors) arranged in a configuration that spatially is analogous to the original system. For simple systems these models are also simple, but for complex configurations, such as a polyatomic molecule, both types of models soon become unmanageable and one gets lost in a maze of mathematical symbols or electrical coils.

However, in going from simpler to more com-

[3] Gabriel Kron, "Numerical Solution of Ordinary and Partial Differential Equations by Means of Equivalent Circuits," J. App. Phys. **16**, 172–186 (March, 1945).

[4] Gabriel Kron, "Tensorial Analysis and Equivalent Circuits of Elastic Structures," J. Frank. Inst. **238**, 399–442 (December, 1944).

plex physical systems, it is possible to follow certain guiding principles that bound the course of reasoning in a narrow channel and establish along the flow guideposts to direct a straight-line progress. These principles must run a parallel course for either type of model and must have a one-to-one correspondence. They have already proved indispensable in establishing models for complex engineering systems representable either by sets of algebraic or by sets of partial differential equations.

To establish a *mathematical* model for a complex physical system it has been postulated that[5]

"The set of equations of a complex system composed of several units, each with n degrees of freedom, are the same as the set of equations of a simple system composed of units, each with one (or a small number of) degrees of freedom except that each scalar symbol in the latter set is replaced by an appropriate tensor."

A tensor is a scalar, one-rowed matrix, rectangular or cubic matrix, in general an n-dimensional matrix, which obeys certain definite laws of transformation. A tensor is considered as the mathematical equivalent of a physical entity with n degrees of freedom (such as a bond between two nuclei) and as such it is represented (for purposes of manipulation) by a single mathematical symbol.

The parallel principle for establishing an electrical (physical) model is postulated as follows:

"The equivalent circuit of a complex system composed of units with n degrees of freedom is the same as the equivalent circuit of a simple system composed of units with one (or a few) degrees of freedom, except that each coil in the latter model is replaced by an appropriate n-wire transmission system."

The n-wire transmission line contains in general as many coils as the corresponding tensor contains components. (See Fig. 4.) The transmission line is the electrical equivalent of a physical entity with n degrees of freedom and as such it is represented (for purposes of manipulation) by a single electrical symbol, that of a coil.

(It is not intended to restrict the physical model to stationary coils and to stationary transmission lines, nor to restrict it to the use of electrical coils.)

[5] Gabriel Kron, "Equivalent Circuits of the Elastic Field," J. App. Mech. **A11**, 146–61 (September, 1944).

The connecting link between the two parallel postulates is a third postulate:

"Only a tensor equation (an equation in which each symbol is a tensor) is representable by a physical model. *Vice versa*, all physical systems (or rather their models) can be mathematically represented correctly only by tensor equations."

This last postulate denies the possibility of constructing a *physical* model (an equivalent circuit) for any haphazard set of mathematical equations claiming to describe the behavior of a physical system. The equations must be in a definite tensorial form to correspond term by term to a model. This postulate denies the existence of even a *mental* model (the type engineers like to use, such as "cutting" of flux lines) dictated by a set of non-tensor equations. (The non-existence of a *geometrical* model for a non-tensor equation is commonly understood.)

Since the physical system to be analyzed presently consists of elementary springs and masses whose conventional equations are already in a tensorial form, the third postulate will play only a subsidiary role in the following. (It plays a crucial role, however, in the model representation of partial differential equations along curvilinear coordinates or of moving and rotating mechanical and electromechanical systems.) The main emphasis will be on the first and second postulates to help establish comparatively simple equations and comparatively simple networks for the otherwise very complex molecular phenomena.

The Course of Procedure

These postulates suggest the following course of procedure to establish either the equations or the equivalent circuits of a complex physical system.

(1) Divide the system into its component units. The collection of units will be called the "primitive" system.

(2) Since the units themselves are rather complex, rotate and re-adjust each of the latter along its simplest possible reference frame (without destroying, of course, its essential unity).

(3) Set up the equations, or the equivalent circuits, of each of the simplified units as if all the others were absent.

(4) Re-adjust and rotate each of the simplified units into the form in which it actually occurs in the system, either by a matrix of transformation (in the mathematical model) or by an actual rotation (in the physical model). That is, re-establish the primitive system of the model.

(5) Reconnect the units (the primitive system) into the resultant system either by a matrix of transformation or by an analogous actual interconnection of the equivalent circuits.

By the use of the concept of "interconnection" in the form of a matrix of transformation, the intricate relations due to the simultaneous presence of several units are automatically taken care of without further thought.

In really complex systems, as in organic molecules, the subdivisions may continue through several successive steps, introducing thereby "multiply compound" tensors, that is, tensors in which each component itself is a compound tensor (whose components are again tensors) and "multiply compound" networks, that is, networks in which each coil itself stands for a whole network each coil in which again represents, say, an n-wire transmission line.

Units to be Assumed

Since it is customary to assume often a mixture of the several types of models possible, the following six types of units of a molecule will be studied here individually.[6]

(1) Mass of a nucleus. Occurs in all models. (See Fig. 2.)

(2) Stretching of a bond between two nuclei. Occurs in both central and valence force models and it also represents the square term in a quadratic form (Fig. 3).

(3) Cross-product between two bonds. Occurs in the quadratic potential model (Fig. 5).

(4) Bending of the angle between two valence bonds in the absence of torsion. Occurs in the valence bond models (Fig. 7).

(5) Torsion of a bond.

(6) Bending of the angle between two valence bonds in the presence of torsion (Fig. 9).

There are several other units possible which are not treated here. For instance,

(7) Cross-product between two angles.

(8) Bending of the angle between a bond and a plane containing several bonds.

(9) Bending of the angle between two planes.

When no torsion is present, each component of a unit has three degrees of freedom, namely, translations along the x, y, and z axes. In the presence of torsion, three additional degrees of freedom appear, namely rotations around the x, y, and z axes, denoted here by p, q, and r.

Determination of Normal Frequencies

While the examples in the present paper express the equations and the electric model along Cartesian coordinates, the same general procedure applies when other types of coordinates are used, such as "internal" or "symmetry" coordinates. In a more convenient reference frame the network model may split into several independent networks.

The solution of the secular equations is well known. The electrical network gives the desired information by the following steps:

(1) Insert a constant frequency generator between any one of the junction points and the ground.

(2) Assume an arbitrary frequency of oscillations ω and adjust the value of coils (representing the masses) accordingly.

(3) Measure the generator current.

As ω varies, the generator current will also vary. Now *the series of value of ω at which the generator current becomes zero represent the normal frequencies of the molecule.* Also, the corresponding absolute potentials at the junctions (assuming the ground at zero potential) represent the particular modes of vibration.

With zero generator current the electrical power stored in the network oscillates between the inductors and capacitors, requiring no extraneous source to maintain the oscillations.

It may happen that for one normal frequency several modes are possible. In such cases placing the generator to a different junction produces a different type of mode. The measured potentials supply sufficient equations to determine each of the degenerate modes.

It should be noted that the generator frequency is not varied as the frequency of the system varies. The networks are of the type

[6] G. Herzberg, *Infrared and Raman Spectra for Polyatomic Molecules* (D. Van Nostrand Company, New York, 1945).

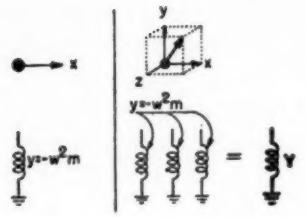

FIG. 2. Equivalent circuit of a particle. (A) One-dimensional motion. (B) Three-dimensional motion.

that require the generator frequency to remain constant and the inductors representing the masses to be adjustable.

The measured normal frequency may be improved by Rayleigh's principle in the following way:

(1) Calculate the electrical power for the measured voltage distribution in all the ground coils, assuming ω as unknown. This power is the kinetic energy.

(2) Calculate the power in the rest of the network. This power is the elastic energy.

The equality of the two energies determines a more correct ω.

PART II. THE PRIMITIVE SYSTEM

A Particle

The kinetic energy of a particle oscillating along the x axis is $T=\frac{1}{2}mx^2$. The equation of force is

$$F=md^2x/dt^2=-\omega^2mx=Yx. \tag{1}$$

Expressing force as current and displacement as voltage, the equation of the electrical analog is $I=YE$. Its admittance is represented by a grounded inductor, Fig. 2(A).

When the particle vibrates along all three directions, its equation is $\mathbf{F}=\mathbf{Y}\cdot\mathbf{x}$ or $\mathbf{I}=\mathbf{Y}\cdot\mathbf{E}$ where the admittance matrix is

$$\mathbf{Y}=-\omega^2\mathbf{m}=\begin{array}{c|ccc} & \mathbf{x} & \mathbf{y} & \mathbf{z} \\ \hline \mathbf{x} & -\omega^2 m & & \\ \mathbf{y} & & -\omega^2 m & \\ \mathbf{z} & & & -\omega^2 m \end{array}. \tag{2}$$

The equivalent circuit is given in Fig. 2(B). In analogy with representing a tensor (or matrix) by a bold face letter, a compound coil will be represented by a coil drawn in heavy lines.

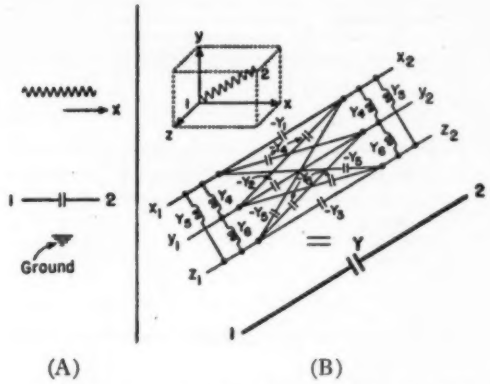

FIG. 3. Equivalent circuit of a tension spring. (A) One-dimensional motion. (B) Three-dimensional motion (Eq. (7)).

A similar matrix (along axes $\mathbf{p}$, $\mathbf{q}$, $\mathbf{r}$) may be set up to represent the moment of inertia of a particle. It is customary to neglect it, however, in molecular vibration studies.

Stretching of a Bond

A restoring force between two particles acting along the connecting line may be represented by a spring. Rotating the spring along the x axis (Fig. 3(A)), its potential energy is

$$V=\tfrac{1}{2}k(x_2-x_1)^2. \tag{3}$$

Differentiating with respect to x_1 and x_2 in succession, its equation is $\mathbf{F}=\mathbf{Y}\cdot\mathbf{x}$ or $\mathbf{I}=\mathbf{Y}\cdot\mathbf{E}$ where the admittance matrix

$$\mathbf{Y}=\begin{array}{c|cc} & \mathbf{x}_1 & \mathbf{x}_2 \\ \hline \mathbf{x}_1 & k & -k \\ \mathbf{x}_2 & -k & k \end{array}. \tag{4}$$

Its equivalent circuit is shown in Fig. 3(A). It is a three-terminal (two-junction pair) network, or a transmission line, in which the two ground coils happen to be zero because of the accidental equality of the four k's in $\mathbf{Y}$.

Let the spring be rotated to its original position whose direction cosines are l, m, and n. The matrix of transformation is

$$\mathbf{A}=\begin{array}{c|cc} & 1 & 2 \\ \hline 1 & A_1 & \\ 2 & & A_1 \end{array} \qquad \mathbf{A}_1=\mathbf{x}\begin{array}{c|ccc} & \mathbf{x}' & \mathbf{y}' & \mathbf{z}' \\ \hline & l & m & n \end{array}. \tag{5}$$

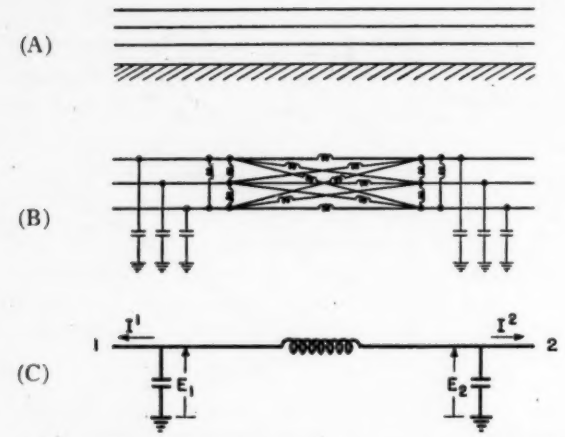

FIG. 4. Equivalent circuit of an n-wire transmission system. (A) N-wire transmission line. (B) Its equivalent circuit. (C) Compound transmission line.

The resultant equation is $\mathbf{I}'=\mathbf{Y}'\mathbf{E}'$ where

$$\mathbf{Y}'=\mathbf{A}_t\mathbf{Y}\mathbf{A}=\begin{array}{c|cc} & 1 & 2 \\ \hline 1 & \mathbf{k} & -\mathbf{k} \\ 2 & -\mathbf{k}_t & \mathbf{k} \end{array}, \tag{6}$$

$$\begin{array}{c|ccc} & \mathbf{x} & \mathbf{y} & \mathbf{z} \\ \hline \mathbf{x} & l^2 & lm & ln \\ \mathbf{y} & ml & m^2 & mn \\ \mathbf{z} & nl & nm & n^2 \end{array} \times k = \begin{array}{c|ccc} & \mathbf{x} & \mathbf{y} & \mathbf{z} \\ \hline \mathbf{x} & Y_1 & Y_4 & Y_5 \\ \mathbf{y} & Y_4 & Y_2 & Y_6 \\ \mathbf{z} & Y_5 & Y_6 & Y_3 \end{array}. \tag{7}$$

The resultant circuit is shown in Fig. 3(B). Its establishment is given in the next section.

Equivalent Circuit of an N-Wire Transmission Line

A symmetrical matrix may be looked upon, for the present purpose, to represent the impedance matrix of an n-wire transmission line, Fig. 4(B). (There are other possible interpretations.) The equivalent circuit of such a line (Fig. 4(B)) may be established from $\mathbf{Y}$ by the following steps:

(1) The mutual admittances are represented by a coil between the respective terminals. A positive "coil" is an inductor, a negative "coil" is a capacitor.

(2) The sum of each column, taken with opposite signs, is replaced by a coil between the respective terminal and the ground.

Such an n-wire transmission system is represented symbolically by the conventional transmission line diagram drawn in heavy lines (Fig. 4(C)), the "compound transmission line." In many cases considered in this paper the ground coils are absent.

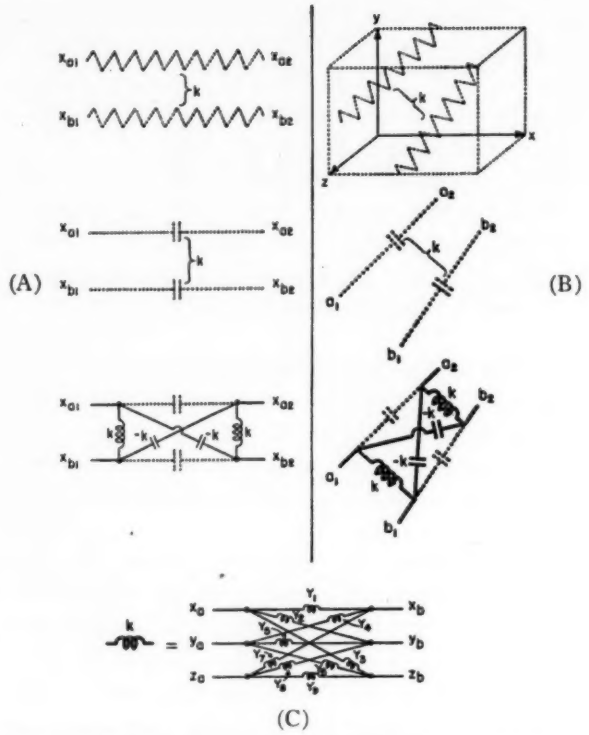

FIG. 5. Equivalent circuit of a cross-product. (A) One-dimensional motion. (B) Three-dimensional motion. (C) Equivalent circuit of a compound coil k (Eq. (9)).

The Cross-Product Terms

A cross-product term between two bonds in the potential energy, such as $\frac{1}{2}k\Delta r_{12}\Delta r_{34}$, represents a mutual spring constant between two springs (Fig. 5(A)) and is analogous to the mutual coupling between two parallel transmission lines.

Let the two springs both be rotated along the x direction, still with the mutual coupling between them. The potential energy of the latter is

$$V=\tfrac{1}{2}k(x_{a2}-x_{a1})(x_{b2}-x_{b1}). \tag{8}$$

Differentiating, the admittance matrix is

$$\mathbf{Y}=\begin{array}{c|cccc} & \mathbf{x}_{a1} & \mathbf{x}_{a2} & \mathbf{x}_{b1} & \mathbf{x}_{b2} \\ \hline \mathbf{x}_{a1} & & & k & -k \\ \mathbf{x}_{a2} & & & -k & k \\ \mathbf{x}_{b1} & k & -k & & \\ \mathbf{x}_{b2} & -k & k & & \end{array}. \tag{9}$$

The equivalent circuit of the coupling between two transmission lines consists of *four identical coils* k as shown in Fig. 5(A), two of them differing only in sign.

Let now the first spring be rotated along a line with direction cosines l_a, m_a, n_a, and the other spring along a different line with direction cosines l_b, m_b, n_b (Fig. 5(B)). The resultant matrix of transformation is

$$\mathbf{A}=\begin{array}{c|cc|cc} & a_1 & a_2 & b_1 & b_2 \\ \hline x_{a1} & A_a & & & \\ x_{a2} & & A_a & & \\ \hline x_{b1} & & & A_b & \\ x_{b2} & & & & A_b \end{array} \qquad \begin{array}{c|ccc} & x' & y' & z' \\ \hline A_a = x & l_a & m_a & n_a \end{array} \qquad \begin{array}{c|ccc} & x' & y' & z' \\ \hline A_b = x & l_b & m_b & n_b \end{array} \tag{10}$$

Multiplying Eq. (9) by Eq. (10) as $\mathbf{A}_t\mathbf{Y}\mathbf{A}$, the resultant is

$$\mathbf{Y}'=\begin{array}{c|cc|cc} & a_1 & a_2 & b_1 & b_2 \\ \hline a_1 & & & k & -k \\ a_2 & & & -k & k \\ \hline b_1 & k_t & -k_t & & \\ b_2 & -k_t & k_t & & \end{array} \tag{11}$$

$$\mathbf{k}=\begin{array}{c|ccc} & x_b & y_b & z_b \\ \hline x_a & l_al_b & l_am_b & l_an_b \\ y_a & m_al_b & m_am_b & m_an_b \\ z_a & n_al_b & n_am_b & n_an_b \end{array} \times k$$

$$=\begin{array}{c|ccc} & x_b & y_b & z_b \\ \hline x_a & Y_1 & Y_2 & Y_3 \\ y_a & Y_4 & Y_5 & Y_6 \\ z_b & Y_7 & Y_8 & Y_9 \end{array} \tag{12}$$

The transpose of $\mathbf{k}$ is denoted as $\mathbf{k}_t$.

In the electrical network the cross-product term $\mathbf{k}$ is represented by four equal "compound" coils (Fig. 5(C)) just as is the single transmission line coupling. The compound coil $\mathbf{k}$ is given in Fig. 5(C).

Bending of Valence Angles

The force resisting an angular change between two valence bonds may be replaced, in the absence of torsion in the molecule, by an angular

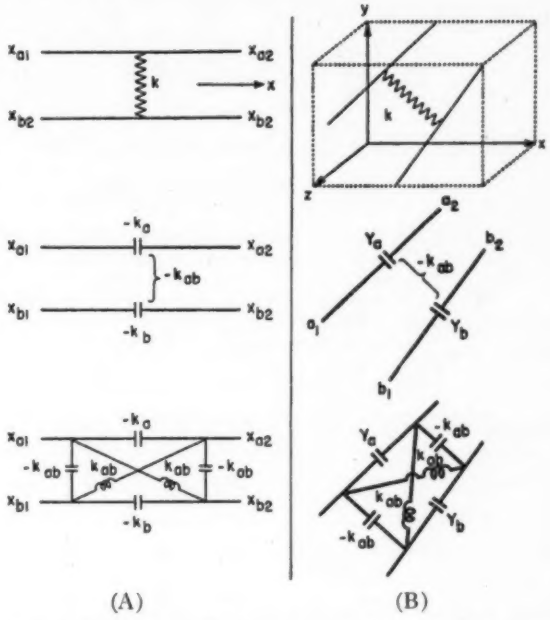

FIG. 6. Equivalent circuit of an angular spring between two *distant* bars. (A) One-dimensional motion. (B) Three-dimensional motion.

spring connecting two bars having no rigidity. Let the two bars, a and b, with the angular spring, be rotated along the x axis (Fig. 6(A)). The angle by which one of the bars is displaced is $(y_{a2}-y_{a1})/L_a$; hence the potential energy stored

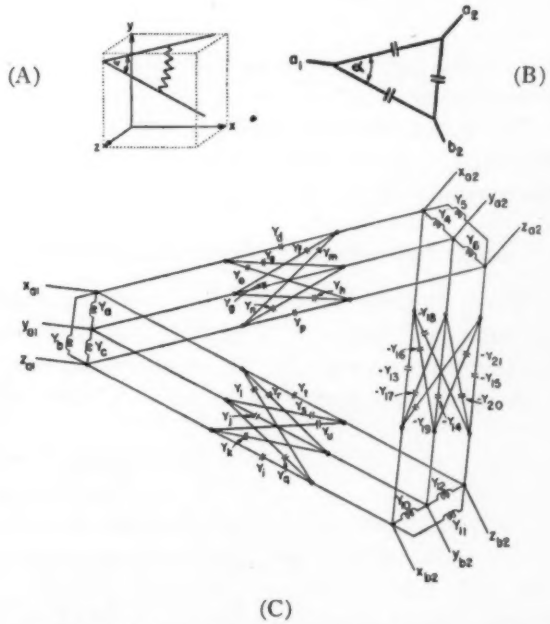

FIG. 7. Equivalent circuit of an angular spring between two *neighboring* bars. (A) Angular spring. (B) Compound network. (C) Actual network (Table I).

in the spring is

$$V=\frac{1}{2}k\left[\frac{y_{a2}-y_{a1}}{L_a}-\frac{y_{b2}-y_{b1}}{L_b}\right]^2. \tag{13}$$

Differentiating, the admittance matrix is

$$\mathbf{Y}=\begin{array}{c|cccc} & \mathbf{y}_{a1} & \mathbf{y}_{a2} & \mathbf{y}_{b1} & \mathbf{y}_{b2} \\ \hline \mathbf{y}_{a1} & k_a & -k_a & -k_{ab} & -k_{ab} \\ \mathbf{y}_{a2} & -k_a & k_a & k_{ab} & -k_{ab} \\ \mathbf{y}_{b1} & -k_{ab} & k_{ab} & k_b & -k_b \\ \mathbf{y}_{b2} & k_{ab} & -k_{ab} & -k_b & k_b \end{array}, \tag{14}$$

where $k_a=k/L_a^2$; $k_b=k/L_b^2$; and $k_{ab}=k/L_aL_b$.

The equivalent circuit of the angular spring is two-coupled transmission lines, Fig. 6(A). The coupling has a sign opposite to that in Fig. 5(A).

In place of the directions of the bars themselves, let the directions of the lines *perpendicular* to the bars and lying in their plane be considered and let their direction cosines be denoted by l_a, m_a, n_a, and l_b, m_b, n_b, respectively. The resultant transformation matrix **A** is the same as in Eq. (10) except on the left-hand side the unit vector **x** is replaced by **y**. The resultant **Y′** is by $\mathbf{A}_t\mathbf{Y}\mathbf{A}$.

$$\mathbf{Y}=\begin{array}{c|cccc} & \mathbf{a}_1 & \mathbf{a}_2 & \mathbf{b}_1 & \mathbf{b}_2 \\ \hline \mathbf{a}_1 & \mathbf{k}_a & -\mathbf{k}_a & -\mathbf{k}_{ab} & \mathbf{k}_{ab} \\ \mathbf{a}_2 & -\mathbf{k}_a & \mathbf{k}_a & \mathbf{k}_{ab} & -\mathbf{k}_{ab} \\ \mathbf{b}_1 & -\mathbf{k}_{abt} & \mathbf{k}_{abt} & \mathbf{k}_b & -\mathbf{k}_b \\ \mathbf{b}_2 & \mathbf{k}_{abt} & -\mathbf{k}_{abt} & -\mathbf{k}_b & \mathbf{k}_b \end{array}=\begin{array}{c|cc} & \mathbf{a} & \mathbf{b} \\ \hline \mathbf{a} & \mathbf{Y}_a & \mathbf{Y}_{ab} \\ \mathbf{b} & \mathbf{Y}_{ab} & \mathbf{Y}_b \end{array}, \tag{15}$$

$$\mathbf{k}_{ab}=\begin{array}{c|ccc} & \mathbf{x} & \mathbf{y} & \mathbf{z} \\ \hline \mathbf{x} & l_al_b & l_am_b & l_an_b \\ \mathbf{y} & m_al_b & m_am_b & m_an_b \\ \mathbf{z} & n_al_b & n_am_b & n_an_b \end{array}\frac{k}{L_aL_b}. \tag{16}$$

$\mathbf{k}_a$ (and $\mathbf{k}_b$) are the same as $\mathbf{k}_{ab}$ with all "b" subscripts replaced by "a" (or "a" replaced by "b").

The compound electrical network is given in Fig. 6(B). It is the same as Fig. 4(B) except that the mutual coils $\mathbf{k}_{ab}$ have opposite signs.

Angle between Two Neighboring Bonds

When the two bonds forming a valence angle are connected together (Fig. 7(A)), then one of the junctions disappears. The connection matrix connecting two junctions a_1 and b_1 into one junction is

$$\mathbf{A}=\begin{array}{c|cccc} & \mathbf{a}_1' & \mathbf{a}_2' & \mathbf{b}_2' \\ \hline \mathbf{a}_1 & 1 & & \\ \mathbf{a}_2 & & 1 & \\ \mathbf{b}_1 & 1 & & \\ \mathbf{b}_2 & & & 1 \end{array}, \tag{17}$$

$$1=\begin{array}{c|ccc} & \mathbf{x} & \mathbf{y} & \mathbf{z} \\ \hline \mathbf{x} & 1 & & \\ \mathbf{y} & & 1 & \\ \mathbf{z} & & & 1 \end{array}. \tag{18}$$

By the law of transformation $\mathbf{Y}'=\mathbf{A}_t\mathbf{Y}\mathbf{A}$, the resultant admittance matrix is

$$\mathbf{Y}''=\begin{array}{c|ccc} & \mathbf{a}_1' & \mathbf{a}_2' & \mathbf{b}_2' \\ \hline \mathbf{a}_1' & \mathbf{k}_a+\mathbf{k}_b-\mathbf{k}_{ab}-\mathbf{k}_{abt} & -\mathbf{k}_a+\mathbf{k}_{abt} & -\mathbf{k}_b+\mathbf{k}_{ab} \\ \mathbf{a}_2' & -\mathbf{k}_a+\mathbf{k}_{ab} & \mathbf{k}_a & -\mathbf{k}_{ab} \\ \mathbf{b}_2' & -\mathbf{k}_b+\mathbf{k}_{abt} & -\mathbf{k}_{abt} & \mathbf{k}_b \end{array}. \tag{19}$$

The equivalent circuit is given in Fig. 7 and in Table I. In two dimensions, $n_a=n_b=0$.

Torsion of a Bond

The treatment of the torsion of a bond is analogous to that of stretching except that the variables and unit vectors **x**, **y**, **z** are replaced by **p**, **q**, **r**. The potential energy is $V=\frac{1}{2}k(p_2-p_1)^2$. When the bond lies along x, its **Y** is given in Eq. (4) and when lying in a general direction, its **Y** is given in Eq. (6). The equivalent circuits are similar to Fig. 3.

It should be noted that the previously developed circuits cannot be interconnected with the circuit representing torsion, or rather there would be no interconnection between them. The bending of valence angles in the presence of torsion, newly treated in the next section, allows the interconnection of the **x**, **y**, **z** and **p**, **q**, **r** axes.

Bending and Torsion of Valence Angles

In the presence of torsion the single angular spring with a force constant k connecting two bars has to be replaced by two springs in series, each with a force constant $2k$, Fig. 8. Each spring now resists the angular change of a single bar so that each bar can be treated independently of the other.

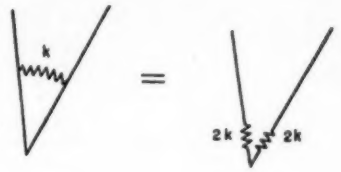

FIG. 8. Replacement of angular spring by two beams with torsion. (A) Angular spring. (B) Two beams.

It should be noted that when several angles originate on a bond, the bond is considered as composed of several bars in parallel, each bar being associated with a different angle and a different angular force constant k. (There may also be two more bars belonging to the same bond, relating to a stretching and a twisting force constant.)

Let the bond be rotated along the x axis (Fig. 9(A)). The angle by which the bar is displaced is $(y_2-y_1)/L-r_1$, where r_1 is the angular rotation of end 1 around the z axis. The potential energy in the spring is

$$V=\tfrac{1}{2}(2k)\left(\frac{y_2-y_1}{L}-r\right). \tag{20}$$

Differentiating, the admittance matrix is

$$\mathbf{Y}=\begin{array}{c|cc|c} & \mathbf{y}_1 & \mathbf{y}_2 & \mathbf{r}_1 \\ \mathbf{y}_1 & \frac{2k}{L^2} & -\frac{2k}{L^2} & \frac{2k}{L} \\ \mathbf{y}_2 & -\frac{2k}{L^2} & \frac{2k}{L^2} & -\frac{2k}{L} \\ \hline \mathbf{r}_1 & \frac{2k}{L} & -\frac{2k}{L} & 2k \end{array}. \tag{21}$$

Its equivalent circuit, Fig. 9(A), now contains ground coils.

Let the bond be rotated into its actual position and let the following directions be defined:

(1) The direction cosine of the line *perpendicular* to the bond and lying in the plane of the two bonds (the plane of the bending) be l_1, m_1, n_1.

TABLE I. Admittances of coils in Fig. 7(C).

$Y_1=k\frac{l_a^2}{L_a^2}$	$Y_7=k\frac{l_b^2}{L_b^2}$	$Y_{13}=k\frac{l_al_b}{L_aL_b}$	$Y_{19}=k\frac{l_bn_a}{L_aL_b}$
$Y_2=k\frac{m_a^2}{L_a^2}$	$Y_8=k\frac{m_b^2}{L_b^2}$	$Y_{14}=k\frac{m_am_b}{L_aL_b}$	$Y_{20}=k\frac{m_an_b}{L_aL_b}$
$Y_3=k\frac{n_a^2}{L_a^2}$	$Y_9=k\frac{n_b^2}{L_b^2}$	$Y_{15}=k\frac{n_an_b}{L_aL_b}$	$Y_{21}=k\frac{m_bn_a}{L_aL_b}$
$Y_4=k\frac{l_am_a}{L_a^2}$	$Y_{10}=k\frac{l_bm_b}{L_b^2}$	$Y_{16}=k\frac{l_am_b}{L_aL_b}$	
$Y_5=k\frac{l_an_a}{L_a^2}$	$Y_{11}=k\frac{l_bn_b}{L_b^2}$	$Y_{17}=k\frac{l_bm_a}{L_aL_b}$	
$Y_6=k\frac{m_an_a}{L_a^2}$	$Y_{12}=k\frac{m_bn_b}{L_b^2}$	$Y_{18}=k\frac{l_an_b}{L_aL_b}$	

$Y_a=Y_4+Y_{10}-Y_{16}-Y_{17}$	$Y_k=-Y_6+Y_{21}$	$Y_o=-Y_5+Y_{19}$
$Y_b=Y_5+Y_{11}-Y_{18}-Y_{19}$	$Y_i=-Y_{11}+Y_{19}$	$Y_p=-Y_3+Y_{15}$
$Y_c=Y_6+Y_{12}-Y_{18}-Y_{19}$	$Y_j=-Y_8+Y_{14}$	$Y_q=-Y_{10}+Y_{17}$
$Y_d=-Y_1+Y_{13}$	$Y_k=-Y_{12}+Y_{21}$	$Y_r=-Y_{10}+Y_{16}$
$Y_e=-Y_4+Y_{17}$	$Y_l=-Y_7+Y_{13}$	$Y_s=-Y_{12}+Y_{20}$
$Y_f=-Y_4+Y_{16}$	$Y_m=-Y_5+Y_{18}$	$Y_t=-Y_{11}+Y_{18}$
$Y_g=-Y_2+Y_{14}$	$Y_n=-Y_6+Y_{20}$	$Y_u=-Y_9+Y_{15}$

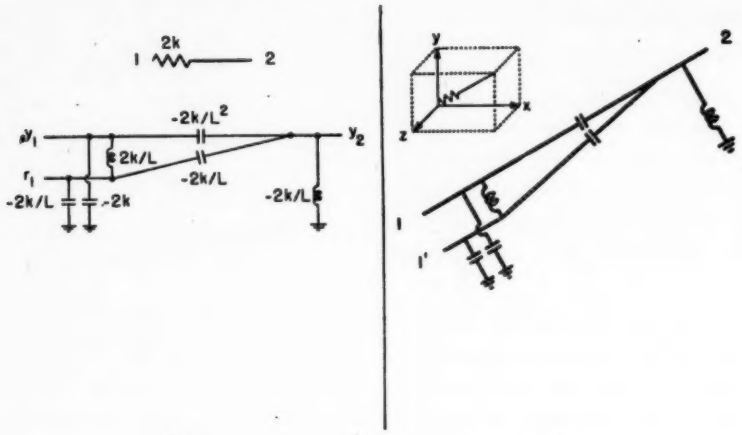

(A) (B)

FIG. 9. Beam equivalent of an angular spring in the presence of torsion. (A) One-dimensional motion. (B) Three-dimensional motion.

(2) The direction cosine of the line *perpendicular* to the plane of the two bonds be l_2, m_2, n_2. The transformation matrix is

$$\mathbf{A} = \begin{array}{c|cc|c} & 1 & 2 & 1_r \\ \hline y_1 & \mathbf{A}_1 & & \\ y_2 & & \mathbf{A}_1 & \\ \hline r_1 & & & \mathbf{A}_2 \end{array} \qquad \mathbf{A}_1 = \begin{array}{c|ccc} & x & y & z \\ \hline y & l_1 & m_1 & n_1 \end{array}$$

$$\mathbf{A}_2 = \begin{array}{c|ccc} & p_1 & q_r & r_1 \\ \hline r_1 & l_2 & m_2 & n_2 \end{array} \cdot \qquad (22)$$

The resultant $\mathbf{Y}$ is

$$\mathbf{Y} = \begin{array}{c|ccc} & 1 & 2 & 1_r \\ \hline 1 & \dfrac{2\mathbf{k}_1}{L^2} & -\dfrac{2\mathbf{k}_1}{L^2} & \dfrac{2\mathbf{k}_{12}}{L} \\ 2 & -\dfrac{2\mathbf{k}_{1t}}{L^2} & \dfrac{2\mathbf{k}_1}{L^2} & -\dfrac{2\mathbf{k}_{12}}{L} \\ \hline 1_r & \dfrac{2\mathbf{k}_{12t}}{L} & -\dfrac{2\mathbf{k}_{12t}}{L} & 2\mathbf{k}_{22} \end{array}, \qquad (23)$$

$$\mathbf{k}_{12} = \begin{array}{c|ccc} & p & q & r \\ \hline x & l_1l_2 & l_1m_2 & l_1n_2 \\ y & m_1l_2 & m_1m_2 & m_1n_2 \\ z & n_1l_2 & n_1m_2 & n_1n_2 \end{array} \cdot \qquad (24)$$

$\mathbf{k}_1$ (and $\mathbf{k}_2$) are the same as $\mathbf{k}_{12}$ with all "2" subscripts replaced by "1" (or "1" replaced by "2"). Its equivalent circuit is shown in Figs. 9 (B) and 10 and in Tables II and III.

PART III. THE RESULTANT SYSTEM

The Resultant Physical Model

Let the four-atom molecule of Fig. 11(A) be considered. Its primitive system is shown in Fig. 11(B). There exist a cross-product term between the two distant bonds f and i, and a valence angle α between two neighboring bonds. The potential energy of the system is

$$V = \tfrac{1}{2}[k_{ab}(\Delta r_{ab})^2 + k_{bc}(\Delta r_{bc})^2 + k_{ad}(\Delta r_{ad})^2 + k(\Delta r_{ad})(\Delta r_{bc}) + k_\alpha(\Delta\alpha)^2]. \qquad (25)$$

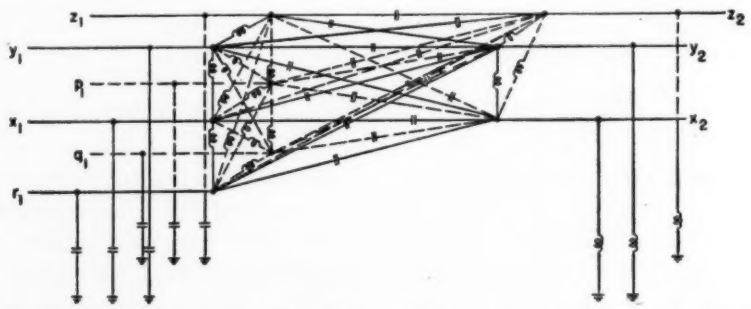

FIG. 10. Equivalent circuit of a beam. (Tables III and IV.) End 1 rigid, end 2 free to rotate.

TABLE II. Admittances of coils on Fig. 11 lying between various junctions.

$x_1 \rightarrow y_1 = Y_4$		$y_2 \rightarrow z_2 = Y_6$	$x_2 \rightarrow y_2 = Y_4$	$r_1 \rightarrow x_2 = -Y_{23}$
$z_1 = Y_5$	$y_1 \rightarrow z_1 = Y_6$		$z_2 = Y_5$	$y_2 = -Y_{24}$
$p_1 = Y_{19}$	$p_1 = Y_{25}$	$z_1 \rightarrow p_1 = Y_{26}$		$z_2 = -Y_{21}$
$q_1 = Y_{22}$	$q_1 = Y_{20}$	$q_1 = Y_{27}$	$p_1 \rightarrow q_1 = Y_{16}$	
$r_1 = Y_{23}$	$r_1 = Y_{24}$	$r_1 = Y_{21}$	$r_1 = Y_{17}$	$q_1 \rightarrow r_1 = Y_{12}$
$x_2 = -Y_1$	$x_2 = -Y_4$	$x_2 = -Y_5$	$x_2 = -Y_{19}$	$x_2 = -Y_{22}$
$y_2 = -Y_4$	$y_2 = -Y_2$	$y_2 = -Y_6$	$y_2 = -Y_{25}$	$y_2 = -Y_{20}$
$z_2 = -Y_5$	$z_2 = -Y_6$	$z_2 = -Y_3$	$z_2 = -Y_{26}$	$z_2 = -Y_{27}$

ground $\rightarrow x_1 = -(Y_{19} + Y_{22} + Y_{23})$	ground $\rightarrow x_2 = Y_{19} + Y_{22} + Y_{23}$
$y_1 = -(Y_{25} + Y_{20} + Y_{24})$	$y_2 = Y_{25} + Y_{20} + Y_{24}$
$z_1 = -(Y_{26} + Y_{27} + Y_{21})$	$z_2 = Y_{26} + Y_{27} + Y_{21}$
$p_1 = -(Y_7 + Y_{10} + Y_{11})$	
$q_1 = -(Y_{10} + Y_8 + Y_{12})$	
$r_1 = -(Y_{11} + Y_{12} + Y_9)$	

Each expression in V represents a unit in the primitive system.

The resultant electrical model, Fig. 12(B), is built up from the compound coils, Fig. 12(A), in a manner analogous to the interconnection of the units of the original system. The step from the compound coils to the actual coils consists of interconnecting all analogous **x**, **y**, **z** or **p**, **q**, **r** terminals separately as shown in Fig. 13.

The physical interpretation of the network is as follows:

(1) Relating to each *particle*

(*a*) The voltage from a terminal to ground gives the total displacement

TABLE III. Definition of admittances in Table II.

$Y_1 = 2k\frac{l_1^2}{L^2}$	$Y_7 = 2k\frac{l_2^2}{L^2}$	$Y_{13} = 2k\, l_2^2$	$Y_{19} = 2k\frac{l_1 l_2}{L}$	$Y_{25} = 2k\frac{m_1 l_2}{L}$
$Y_2 = 2k\frac{m_1^2}{L^2}$	$Y_8 = 2k\frac{m_2^2}{L^2}$	$Y_{14} = 2k\, m_2^2$	$Y_{20} = 2k\frac{m_1 m_2}{L}$	$Y_{26} = 2k\frac{n_1 l_2}{L}$
$Y_3 = 2k\frac{n_1^2}{L^2}$	$Y_9 = 2k\frac{n_2^2}{L_2}$	$Y_{15} = 2k\, n_2^2$	$Y_{21} = 2k\frac{n_1 n_2}{L}$	$Y_{27} = 2k\frac{n_1 m_2}{L}$
$Y_4 = 2k\frac{l_1 m_1}{L^2}$	$Y_{10} = 2k\frac{l_2 m_2}{L^2}$	$Y_{16} = 2k\, l_2 m_2$	$Y_{22} = 2k\frac{l_1 m_2}{L}$	
$Y_5 = 2k\frac{l_1 n_1}{L^2}$	$Y_{11} = 2k\frac{l_2 n_2}{L^2}$	$Y_{17} = 2k\, l_2 n_2$	$Y_{23} = 2k\frac{l_1 n_2}{L}$	
$Y_6 = 2k\frac{m_1 n_1}{L^2}$	$Y_{12} = 2k\frac{m_2 n_2}{L^2}$	$Y_{18} = 2k\, m_2 n_2$	$Y_{24} = 2k\frac{m_1 n_2}{L}$	

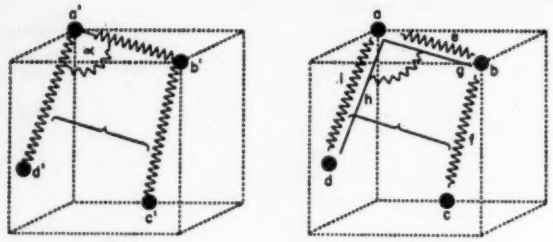

(A) (B)

FIG. 11. Assumed molecular system *XYZW*. (A) Resultant system. (B) Primitive system.

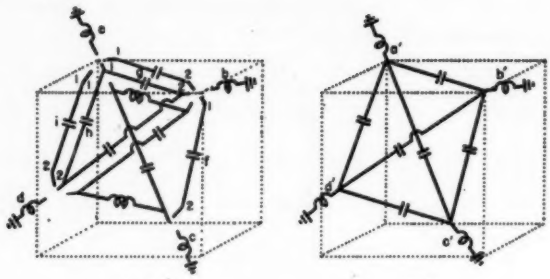

(A) (B)

FIG. 12. Electric circuit model. (A) Primitive system. (B) Resultant system.

(linear or angular) of the particle in the corresponding direction.

(*b*) The current between a terminal and a ground gives the resultant force or torque acting on the particle in the corresponding direction

(2) Relating to each *valence bond*

(*a*) The difference of potential between two terminals gives the change in the length or angular position of the bond in the corresponding direction.

(*b*) The current between two terminals gives the corresponding force in the bond.

(3) Relating to the *total system*

(*a*) The total power in the ground coils representing the masses gives the total kinetic energy of the vibrating system.

(*b*) The total power in the rest of the network gives the total potential energy stored in the vibrating system.

The Resultant Mathematical Model

The units of the mathematical model consist of the $\mathbf{Y}'$ matrices of the four masses (Eq. (2)), three stretching springs (Eq. (6)), one cross-product term (Eq. (11)), and one angular spring (Eq. (15)), all rotated in their proper spatial positions. These matrices are arranged along the diagonal line of a compound $\mathbf{Y}'$ (Eq. (26)) with thirteen rows and columns representing the equations of the primitive system $\mathbf{I}=\mathbf{YE}$, namely thirty-nine scalar equations.

The interconnected system of Fig. 12(B) has

$$
\mathbf{Y}=\begin{array}{c|ccccccccccccc}
 & \mathbf{a} & \mathbf{b} & \mathbf{c} & \mathbf{d} & \mathbf{e}_1 & \mathbf{e}_2 & \mathbf{f}_1 & \mathbf{f}_2 & \mathbf{g}_1 & \mathbf{g}_2 & \mathbf{h}_2 & \mathbf{i}_1 & \mathbf{i}_2 \\
\mathbf{a} & -\omega^2\mathbf{m}_a & & & & & & & & & & & & \\
\mathbf{b} & & -\omega^2\mathbf{m}_b & & & & & & & & & & & \\
\mathbf{c} & & & -\omega^2\mathbf{m}_c & & & & & & & & & & \\
\mathbf{d} & & & & -\omega^2\mathbf{m}_d & & & & & & & & & \\
\mathbf{e}_1 & & & & & \mathbf{Y}_e & -\mathbf{Y}_e & & & & & & & \\
\mathbf{e}_2 & & & & & -\mathbf{Y}_{et} & \mathbf{Y}_e & & & & & & & \\
\mathbf{f}_1 & & & & & & & \mathbf{Y}_f & -\mathbf{Y}_f & & & & \mathbf{Y}_{fi} & -\mathbf{Y}_{fi} \\
\mathbf{f}_2 & & & & & & & -\mathbf{Y}_f & \mathbf{Y}_f & & & & -\mathbf{Y}_{fi} & \mathbf{Y}_{fi} \\
\mathbf{g}_1 & & & & & & & & & \mathbf{Y}_{g1} & \mathbf{Y}_{g4} & \mathbf{Y}_{g5} & & \\
\mathbf{g}_2 & & & & & & & & & \mathbf{Y}_{g4t} & \mathbf{Y}_{g2} & \mathbf{Y}_{g6} & & \\
\mathbf{h}_2 & & & & & & & & & \mathbf{Y}_{g5t} & \mathbf{Y}_{g6t} & \mathbf{Y}_{g3} & & \\
\mathbf{i}_1 & & & & & & & \mathbf{Y}_{fit} & -\mathbf{Y}_{fit} & & & & \mathbf{Y}_i & -\mathbf{Y}_i \\
\mathbf{i}_2 & & & & & & & -\mathbf{Y}_{fit} & \mathbf{Y}_{fit} & & & & -\mathbf{Y}_i & \mathbf{Y}_i
\end{array}, \tag{26}
$$

only five junctions, hence four-junction pairs. If each of the new junction pairs is selected so as to include the ground, the relation between the voltages (displacements) of the primitive and the resultant system is the matrix of transformation **A**, Eq. (27).

$$\mathbf{A}' = \begin{array}{c|cccc} & a' & b' & c' & d' \\ \hline a & I & & & \\ b & & I & & \\ c & & & I & \\ d & & & & I \\ e_1 & I & & & \\ e_2 & & I & & \\ f_1 & & I & & \\ f_2 & & & I & \\ g_1 & I & & & \\ g_2 & & I & & \\ h_2 & & & & I \\ i_1 & I & & & \\ i_2 & & & & I \end{array}, \qquad (27)$$

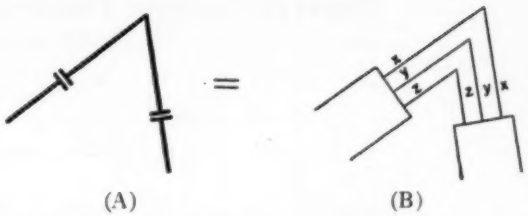

(A) (B)

FIG. 13 Interconnection of coils. (A) Interconnection of compounds coils. (B) Interconnection of actual coils.

where **I** is the unit matrix of Eq. (18). The admittance matrix of the resultant system is by $\mathbf{A}_t'\mathbf{Y}'\mathbf{A}'$.

The equations $\mathbf{I}''=\mathbf{Y}''\mathbf{E}''$ represent the twelve secular equations of the molecule.

Relations between the Two Models

The secular equations $\mathbf{I}=\mathbf{YE}$ may be established by a simple inspection of the electric circuit model of Fig. 12(B). In particular, $\mathbf{Y}''$ is established as follows.

(1) The mutual admittance terms are the coils connecting corresponding terminals.

(2) The main diagonal terms are the sum of the admittances entering each junction, taken with opposite sign.

$$\mathbf{Y}'' = \begin{array}{c|cccc} & a & b & c & d \\ \hline a & Y_e+Y_{g1}+Y_i-\omega^2 m_a & Y_{fit}-Y_e+Y_{g4} & -Y_{fit} & Y_{g5}-Y_i \\ b & Y_{fi}-Y_{et}+Y_{g4t} & Y_e+Y_f+Y_{g2}-\omega^2 m_b & -Y_f & -Y_{fi}+Y_{g6} \\ c & -Y_{fi} & -Y_{ft} & Y_f-\omega^2 m_c & Y_{fi} \\ d & Y_{g5t}-Y_i & -Y_{fit}+Y_{g6t} & Y_{fit} & Y_{g3}+Y_i-\omega^2 m_d \end{array}. \qquad (28)$$

Vice versa, the electric circuit model may be established from the secular equation by the reverse steps of those given previously. The two methods of setting up the electrical model may serve as a check on the correctness of the network.

Network Analyzer Tests of Equivalent Circuits of Vibrating Polyatomic Molecules

G. K. CARTER* AND G. KRON**
General Electric Company, Schenectady, New York

(Received August 20, 1945)

To illustrate the use of the equivalent circuits derived in the companion paper for vibrating polyatomic molecules, this paper describes network-analyzer tests of circuits for three successively more complicated molecules. The first is the symmetrical linear CO_2 molecule; the second is the unsymmetrical linear OCS molecule; and the third is the unsymmetrical nonlinear CH_3CH_2OH molecule. In each case, starting from given constants of the molecular structure, the normal frequencies and modes are measured by means of the equivalent circuit. It is shown that for these cases the analyzer measurements agree satisfactorily with the known normal-frequency characteristics.

NETWORK ANALYZER

THE alternating-current network analyzer[1] consists of a set of adjustable resistance, inductance, and capacitance units, each connected to a pair of flexible cords and plugs. Connections between units to form any desired network are made by inserting the plugs in adjacent jacks in a jack panel. As many units as desired can be connected to a common point. Alternating-current electric power is supplied by a motor-generator set to individual generator units so that several different voltages, independently adjustable, can be inserted into different parts of the network. A centrally located set of measuring instruments can be connected to any unit or circuit by means of a set of key switches.

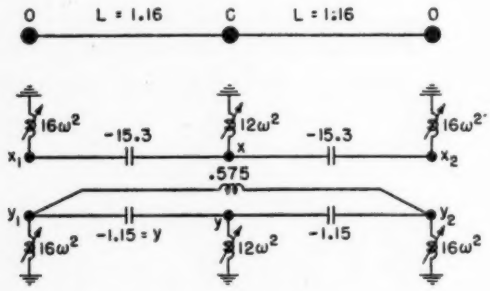

FIG. 1. Equivalent circuit of the CO_2 molecule.

Procedure

The equivalent circuits for the CO_2, OCS, and CH_3CH_2OH molecules are shown in Figs. 1–3, respectively. These circuits were obtained by methods described in the companion paper,[2] using the molecular constants listed in Table I; the

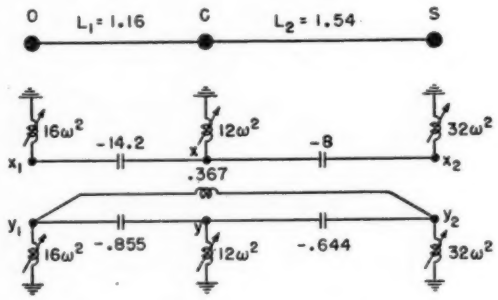

FIG. 2. Equivalent circuit of the OCS molecule.

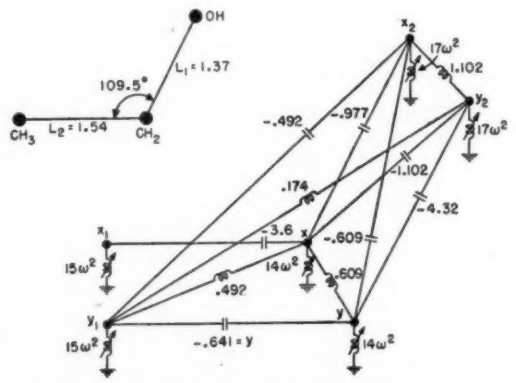

Fig. 3. Equivalent circuit of the ehtyl-alcohol molecule.

* Analytical Division, Central Station Engineering Divisions, General Electric Company, Schenectady, New York.

** Consulting Engineer, General Electric Company, Schenectady, New York.

[1] H. P. Kuehni and R. G. Lorraine, "A New A-C Network Analyzer," Trans. A.I.E.E. **57**, 67 (1938).

[2] G. Kron, "Electric Circuit Models for the Vibration Spectrum of Polyatomic Molecules," J. Chem. Phys. **14**, 19 (1945).

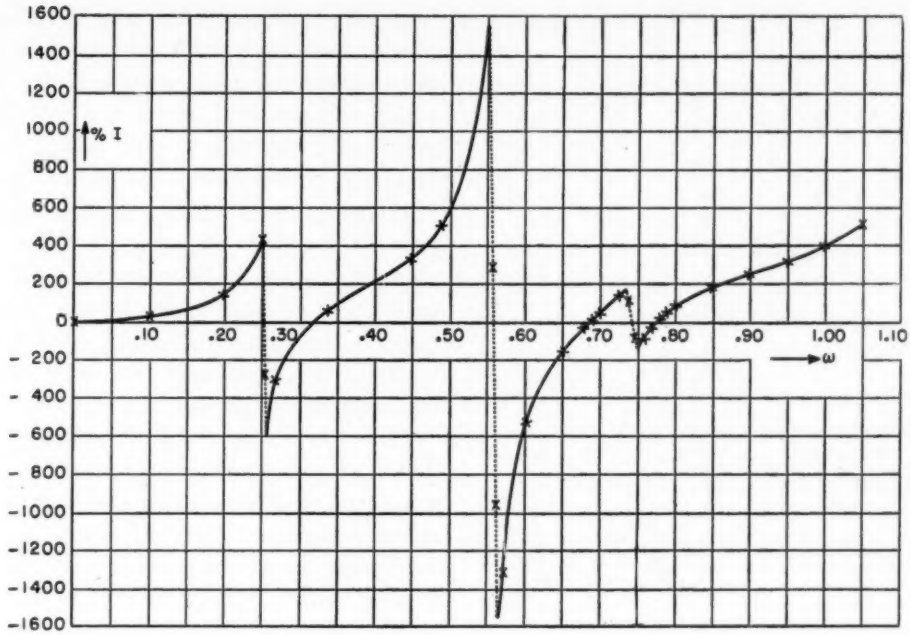

FIG. 4. Variation of generator current with frequency.

constants are based on previous data,[3,4] with the angular spring constants of the former reference corrected by a factor of one-fourth.

The process of locating the normal frequencies from these circuits is similar to that already described in connection with the study of the Schrödinger equation.[5] The circuits specify both positive and negative admittances; since negative-resistance units are difficult to work with, positive and negative reactive admittances are used, with a.c. excitation. The circuit is excited by applying a generator at any junction point, and the forced-vibration frequency is varied by varying the admittances of the units expressed in terms of ω. For any given ω, the generator current represents the applied force required to force vibration at that frequency; so that when this current is plotted as a function of ω, as in Fig. 4, the points at which the resulting curve passes through zero should correspond to frequencies at which no external force is required to sustain the

TABLE I. Molecular constants.

CO_2	$L=1.16$	$k=15.3$	$m_c=12$
		$k_\alpha=0.772$	$m_o=16$
OCS	$L_{oc}=1.16$	$k_{oc}=14.2$	$m_c=12$
	$L_{cs}=1.54$	$k_{cs}=8$	$m_o=16$
		$k_\alpha=0.655$	$m_s=32$
CH_3CH_2OH	$L_1=1.37$	$k_1=4.1$	$m_{CH_3}=15$
	$L_2=1.54$	$k_2=3.6$	$m_{CH_2}=14$
	$\alpha=109.5°$	$k_\alpha=1.102$	$m_{OH}=17$

The stretching force-constants k are expressed in 10^5 dyne/cm, the bending force-constants k_α in 10^{-11} dyne-cm/radian; m is the atomic weight (O=16); and the wave-length $\nu=1303\omega$.

TABLE II. Measured and calculated normal frequencies.

		ν_1	ν_2	ν_3
CO_2	Test	1273	670	2447
	theory	1274	668	2440
OCS	Test	860	526	2072
	theory	859	527	2079
CH_3CH_2OH	Test	897	1009	421
	theory	910	1020	430

[3] W. G. Penney and G. B. B. M. Sutherland, "On the Relation Between the Form, Force Constants, and Vibration Frequencies of Triatomic Systems," Proc. Roy. Soc. **156**, 654–678 (1936).

[4] Paul C. Cross and J. H. Van Vleck, "Molecular Vibrations of Three Particle Systems with Special Applications to the Ethyl Halides and Ethyl Alcohol," J. Chem. Phys. **1**, 350 (1933).

[5] G. Kron and G. K. Carter, "A-C Network Analyzer Study of the Schrödinger Equation," Phys. Rev. **67**, 44–49 (1945).

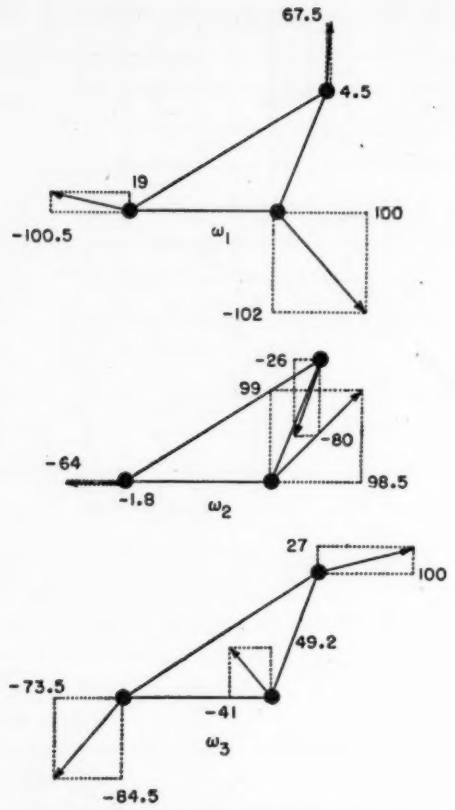

FIG. 5. Measured normal modes of vibration of the ethyl-alcohol.

vibration, that is, to the natural frequencies of the circuit and of the molecule which it represents. Ideally, the curve shown should be a continuously increasing function with increasing ω, passing through a series of infinite discontinuities; these discontinuities represent frequencies for which the point of excitation is a nodal point; practically, of course, the current supplied is incapable of increasing without limit, and instead it changes very rapidly from positive through zero to negative before once more taking the upward course. These extra zero points are generally obvious; and in any case the true natural frequencies can and should be checked by using the exciting generator at more than one junction of the network.

For the three molecules being considered, Table II shows how the natural frequencies measured on the network analyzer compare with those calculated from the constants in Table I (omitting the obvious case of zero frequency). It is seen that the check is very good; in fact, the discrepancies generally are less than might have been expected from uncorrected readings with the equipment used.

Not only the natural frequencies, but also the natural modes, can be read from the circuits by means of the analyzer. The latter are given simply by the voltages of the several junction points at the natural frequencies. Figure 5 shows, for example, the natural modes of the CH_3CH_2OH molecule as measured in this way; these are similar to the corresponding modes shown in reference 4.

THE JOURNAL OF CHEMICAL PHYSICS VOLUME 14, NUMBER 1 JANUARY, 1946

The Asymmetric Rotor

III. Punched-Card Methods of Constructing Band Spectra

GILBERT W. KING, *Arthur D. Little, Inc., Cambridge, Massachusetts,*
PAUL C. CROSS, *Brown University, Providence, Rhode Island,*

AND

GEORGE B. THOMAS, *Massachusetts Institute of Technology, Cambridge, Massachusetts*

(Received October 10, 1945)

The stochastic method of analysis of band spectra of asymmetric rotors involves the calculation of line strengths and positions for successive estimates of six molecular constants, until the calculated intensities at all wave-lengths agree satisfactorily with the observed. This paper shows that these extensive calculations, as based on tables previously published, are well adapted to standard punched-card equipment. In addition to the above calculations, it is possible to construct the appearance of the rotational structure for various values of slit width. The procedure is carried through for H_2S with some approximate constants. Very satisfactory representations of observed spectra are obtained for completely resolved spectra, as in the photographic region; for slit width 1 and 2 cm^{-1}, as in the near infra-red; for slit width 10 cm^{-1}, as in poorly resolved infra-red spectra.

I. INTRODUCTION

BAND spectra still remain an important source of information about molecular structure and of precise values of the constants for calculating the thermodynamic properties of simple substances. The analysis of bands of polyatomic molecules is very difficult when the three moments of inertia are different, that is when the molecule is an asymmetric rotor. Figure 1 shows typical infra-red bands, in this case of H_2S.[1] Although these bands are not completely resolved into lines, one feels that there is enough information given by the position and intensities of the peaks to find out the dimensions of the molecule. However, only a very few of such bands have been analyzed. The difficulty arises partly because the positions of the peaks in the case of the asymmetric rotor are very irregular. It seems that the only approach to interpretation of these bands, whether more or less resolved than the ones shown, is a stochastic one. One assumes the dimensions of the molecule in the upper and lower states, calculates the position and intensity of the lines, and compares with the observed. This has been done successfully for only a few completely resolved bands of asymmetric rotors, namely, a number of bands of H_2O and one band of H_2S, and even in these cases the comparison of intensities has been based on symmetric-rotor approximations.

The position of a line in a band is given by

$$\nu_{J'',\tau''};\,{}_{J',\tau'}=\nu_0+E'(a',b',c')_{J',\tau'}-E''(a'',b'',c'')_{J'',\tau''}, \quad (1)$$

where ν_0 is the band center, $E(a,b,c)_{J,\tau}$ being the rotational energy of the state defined by J,τ; double primes indicate the lower state, single primes the upper state. In the case of the asymmetric rotor the rotational energies can be determined only by solving polynomials of various high degrees. In a previous paper[2] we believe we have simplified this part of the problem a great deal by tabulating a quantity $E(\kappa)$ in terms of which the rotational energy, a function of the three reciprocal moments $a\geqslant b\geqslant c$, can be expressed as

$$E(a,b,c)_{J,\tau}=\tfrac{1}{2}(a-c)E(\kappa)_{J,\tau}+\tfrac{1}{2}(a+c)J(J+1), \quad (2)$$

where $\kappa=(2b-a-c)/(a-c)$ is a parameter of asymmetry varying from -1 to $+1$, and $E(\kappa)_{J,\tau}$, called reduced energy levels, have been com-

[1] H. H. Nielsen and E. F. Barker, Phys. Rev. **37**, 727 (1931). A reproduction of the completely resolved band of H_2S at 10,100A was given by P. C. Cross, J. Chem. Phys. **5**, 370 (1937).

[2] G. W. King, R. M. Hainer, and P. C. Cross, J. Chem. Phys. **11**, 27–42 (1943), hereafter referred to as I.

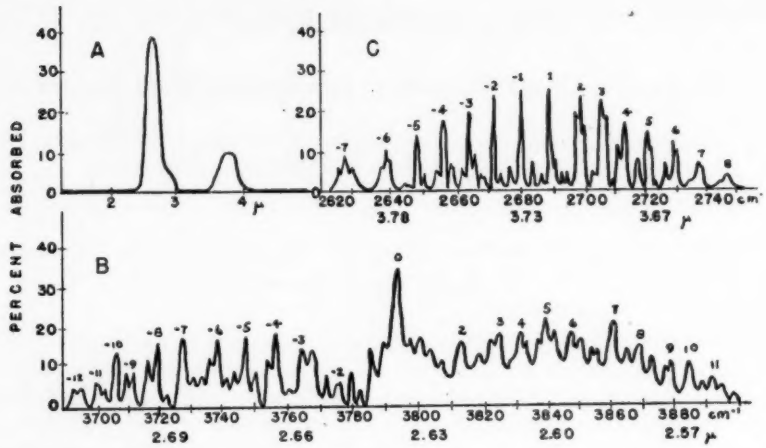

FIG. 1. Absorption bands in hydrogen sulfide. *A*, Prism curve with low dispersion. *B*, Fine structure in the band at 2.6μ. *C*, Fine structure in the band at 3.7μ. (Copied from reference 1.)

puted[3] up to $J=12$ by solving continued fractions for all possible values of κ in intervals of 0.1. Thus the energy levels for any molecule can be computed by (2) from the table of $E(\kappa)$ by simple multiplication and addition.

The intensity of a line in an absorption band as obtained[4] from II—(1) is

$$I_{J'',\tau''}{}^{;}{}_{J',\tau'} = \text{const}\ \nu(1-e^{-\nu/kT})g_{J'',\tau''} \times \exp -E''(a'', b'', c'')_{J'',\tau''}/kT \sum_{F=X,Y,Z} \sum_{M''} \sum_{M'} |\Phi_{Fg}|^2_{J'',\tau'',M''}{}^{;}{}_{J',\tau',M'}, \quad (3)$$

where ν is the line position (1) in wave numbers, k being the Boltzmann factor in cm^{-1} deg^{-1}, and $g_{J'',\tau''}$ is the nuclear-spin weight factor. The constant factor is given explicitly by II—(1) and II—(2). It includes the partition function and the absolute magnitude of the permanent and induced electric moment. The last term is the square of a matrix element of the direction cosine between the radiation field and molecular axes. The subscript g refers to the direction of the permanent and induced components of the electric moment in fixed molecular coordinates. The triple sum is the strength of a line whose components are unresolved in an isotropic radiation field with no external field. In II we have computed the values of the line strengths for five values of $\kappa(\pm 1, \pm 0.5, 0)$, which adequately cover the whole range of asymmetry possible.

Equations (1) and (3) are to be evaluated for all important lines of the spectrum. Even with the tables of energy levels and line strengths, the construction of a spectrum, which is composed even in the simplest cases of several hundred lines, is a considerable undertaking. The computational labor can be reduced by making use of certain calculating machines.

II. ACCOUNTING-MACHINE METHODS

It is the purpose of this paper to illustrate the use of business accounting machines in carrying out certain types of quantum-mechanical calculations, in this case the construction of spectra by the evaluation of the above equations for line position and line intensity. Punched-card machines are probably the most suitable for this kind of work, for although they are only capable of adding, subtracting, and multiplying, they are well suited to the quantum-mechanical operations such as symmetry classifications, sorting according to parity or changes in quantum numbers, etc.

In the International Business Machines all the quantities used in the calculations are supplied on cards, the numbers or identification letters appearing as holes punched in certain locations. The machines read the information by brushes which make electrical contacts through the holes as the card runs through the machine.

[3] Values of $E(\kappa)$, $\kappa=-1.0$ (0.1) 0.0, for $J=11$ and 12 will be published shortly.

[4] P. C. Cross, R. M. Hainer, and G. W. King, J. Chem. Phys. **12**, 210 (1944), hereafter referred to as II.

Several types of machines are available whose principal operations are briefly described below with special reference to the construction of band spectra.[5]

The ultimate object of this work is to represent a spectrum by a set of cards, each card corresponding to a line and bearing the line position, line intensity, the quantum numbers of the two states, and the symmetry classification. These cards can be prepared and handled by the following machines.

Key Punch—The original data can be punched onto cards by hand from printed tables. Since this step is subject to errors of the operator, the amount of material punched by hand should be kept to a minimum. It is necessary that the information on the cards be thoroughly checked. Various machine methods of testing the accuracy are described below.

Sorter—Fundamentally this machine separates a set of cards into ten groups depending on the value of a digit in any one column. It can be used to arrange the cards representing transitions in order of increasing wave number or to pick out the lines of intensity above any chosen value. It is also possible to classify the lines, for instance, into sub-branches, by sorting on the changes in quantum numbers.

In addition to the field in which digits are punched there are X and Y zones which can be used in combination with the digits to indicate letters, or used alone to indicate sign, parity, etc., or for control purposes. Thus lines can be sorted into symmetry classes determined by the parity of certain quantum numbers.

Collator—This machine is used to combine two sets of cards so that a card of the "primary" set defined say by a certain quantum number precedes all the cards in the "secondary" set with the same quantum number.

Reproducer—When two sets have been collated, the combined set can be put through this machine so that information is reproduced from the leading card (from the primary set) into all the cards with the same quantum numbers of the secondary set. This operation is called "gang punching."

Multiplier—This is the machine on which addition, subtraction, and multiplication can be done. The two numbers which are to be combined must appear on the same card, the answer being punched elsewhere on the card. Combined operations, such as $A \times B + C$, can be done simultaneously in this machine, the addition being called "cross-footing."

Group multiplying is the operation of multiplying all cards put through the machine by the same quantity which is inserted in the machine by a leading specially punched card. It is then not necessary to use up any columns of the detail card for the multiplier.

It is desirable in scientific work to have the Multiplier modified to take into account different signs of the terms in an equation such as (1); otherwise, the cards have to be sorted according to the signs and handled separately.

Summary Tabulator—At any stage in the operations the cards can be put through a Tabulator wired so that any or all of the information can be printed. Thus, the final results can be listed in any convenient form.

In addition, the Tabulator can sum the quantities on any part of the card and print either the grand total or subsidiary totals, the printing of which can be controlled by changes in identification columns, e.g., when a quantum number changes or when the tens digits change. Summation can also be controlled by X zone punches.

Operation

In conclusion, it should be pointed out that all the steps in the calculations can be set up in a standardized form, and the actual preparation and handling of the cards is done by specially trained operators at some computing center. All the spectroscopist has to do is to supply the necessary eight constants, namely, three reciprocal moments of inertia for both the upper and lower states, the absolute temperature, and the band center.

Punched-Card Table of Reduced Energy Levels

It was not convenient to obtain the reduced energy levels $E(\kappa)$ by punched-card methods

[5] A description of punched-card machines and of their application to astronomial calculations can be found in W. J. Eckert, *Punched-Card Methods in Scientific Computation* (Thomas J. Watson Astronomical Computing Bureau, Columbia University, New York, 1940).

since these were calculated by continued fractions, and punched-card machines are not adapted to frequent division. The table of reduced energy levels (I—Appendix) was set up on punched cards on the Key Punch. One card was made for each level for each value of κ (running from -1 to 0 in intervals of 0.1), bearing the values of J, K_{-1}, K_1, and $E(\kappa)$.

The τ-values of the levels were then obtained by finding the difference $\tau = K_{-1} - K_1$ on the Multiplier. The cards were sorted according to the parity of the K's and the resulting four symmetry species identified by punching the characters *ee*, *eo*, *oe*, *oo* (I—Sec. IV). Similarly by sorting on the last digit of τ and X punching the odd numbers, the parity of τ was indicated on the cards for use in applying weight factors. The parity of γ was obtained from that of $J+\tau$ for use in grouping into sub-branches.

The major source of error in punched-card operations is the copying of tabulated material onto punched cards, which is done by an operator. The punched cards representing the table had to be carefully checked. This was done very easily as follows: the cards were sorted on J and the four symmetry classifications and then put through a tabulator which printed the sums of each set with the same J and symmetry. These numbers are the traces of the sub-matrices whose values are known.[6]

Calculation of Term Values

To obtain the actual energy levels of any molecule, the required information is copied from the master set described above. In general it is necessary to interpolate to find $E(\kappa)$ for intermediate values of κ. This can be done by machine methods since interpolation involves only multiplication and addition. It is sometimes more convenient, however, not to interpolate, but to carry through the calculation for line position ν for several values of κ, and interpolate the line position. In many cases it will be found that the variation of ν over the interval of 0.1 in κ is either negligible or of the order of the centrifugal-distortion correction. This method emphasizes the sensitivity of certain lines to the asymmetry parameter (which in XY_2 type triatomic molecules is a function of the valence angle only, not of the interatomic distances). The positions of these lines can be used to determine κ accurately.

The original table of reduced energy levels (I—Appendix) covered only the range of negative κ. Values for positive κ are obtained by means of the symmetry relation (I—12):

$$E(\kappa)_{J,K_{-1},K_1;\tau} = -E(-\kappa)_{J,K_1,K_{-1};-\tau}. \quad (4)$$

The inversion of K_{-1} and K_1 and change of signs of τ can be done automatically on reproducing from the master set by interchanging appropriate wires.

The value of $\frac{1}{2}(a+c)J(J+1)$ is punched onto the appropriate cards by collating and gang punching, a process to be described in more detail in another connection. The pack of cards is put through the Multiplier, in which the factor $\frac{1}{2}(a-c)$ is introduced as a group multiplier. The cards run through the machine so that the product $\frac{1}{2}(a-c)E(\kappa)$ is obtained and simultaneously added to $\frac{1}{2}(a+c)J(J+1)$, so that (2) is evaluated at once and the answer $E(a, b, c)$ punched in other columns of the card.

This whole operation is repeated for the chosen constants of the upper state.

Punched-Card Table of Line Strengths

Another master set of cards has been made, one card for each possible transition between rotational levels, $J<13$, for all three components of the electric moment, bearing the quantum numbers, J'', K''_{-1} and K''_1 of the lower state, and J', K'_{-1} and K'_1 of the upper state, together with the line strengths.

Since the line strengths were obtained by ordinary methods of calculation, they had to be key punched onto cards by a hand operation. This introduced numerous errors of identification which were fairly easily corrected by the application of sum rules (II—20 to 24). The cards were sorted by direction of moment, level identification[7] J'', K''_{-1}, K''_1 (or by J', K'_{-1}, K'_1), and the sums of the line strengths obtained on the Tabulator. These sums being small whole

[6] I—Table X.

[7] Since the double suffix KK-notation involves 4 integers ($J<13$) and the τ-notation involves 2 integers plus a sign, one sorting operation can be eliminated by the use of $J+\tau$ (running from 0 to $2J+1$) as the index of the levels with the same J.

numbers, errors could be detected by visual inspection. The use of three different sum rules finally eliminated all errors except those due to rounding off.

Punched-Card Table Representing a Band

A copy of this master set of line strengths was made for the chosen value of κ and direction of the electric moment. Interpolation may be necessary, although, as in the case of $E(\kappa)$, it is sometimes of interest to carry through the calculations for the two neighboring values of κ, in order to follow the effect of changing asymmetry on intensities in the final construction of the spectrum.

This set is now sorted[7] on J'', K''_{-1}, K''_1 in the same order as the cards for the lower energy levels. The latter set is collated with the former. In this operation an energy-level card for a given value of J'', K''_{-1}, K''_1 is placed in front of the group of cards in the transition set having the same values for J'', K''_{-1}, and K''_1. The combined set is now put through a Reproducer which gang punches information from the energy-level cards onto the transition cards, namely $E''(a'', b'', c'')$ and other information to be described below. The transition set is now sorted on the quantum numbers of the upper state,[7] J', K'_{-1}, K'_1, and collated with the set for the upper energy levels, from which $E'(a', b', c')$ is gang punched.

The next step is to gang punch[8] onto the whole set the value of the band center, ν_0. The pack of cards is then put through the Multiplier, which carries out the addition and subtraction (1) to give the line position in one operation.

Calculation of Line Intensity

In order to calculate the line intensity the Boltzmann factor has first to be determined. The set for the lower energy levels is group multiplied by $1/kT$. The cards are arranged in order of increasing E/kT on the sorter and collated with a set of cards representing the table of the exponential function, the latter being the primary set. The value of $\exp -E/kT$ is gang punched onto the energy-level cards.

The next step is to insert the appropriate weight factors $g_{J'',\tau''}$. These depend on the symmetry classification of the energy levels. For instance, in the case of H_2O the levels with τ odd have a weight of three, and the levels with τ even have a weight of one. The cards can be put through the Sorter which separates the even and odd τ's. The Boltzmann factors for the τ-odd set are multiplied by three; in the τ-even set the Boltzmann factor is multiplied by unity in order that the combined factor appears in the same field on all cards. The whole set is now sorted[7] on J'', K''_{-1}, and K''_1 for the collation with the transition set described above. The Boltzmann factor is copied from this set at the same time as the energy levels.

For pure rotational spectra the quantity $\nu(1-e^{-\nu/kT})$ appearing in (3) is important. It can be calculated on the transition set by the following operations. First the exponential is evaluated by multiplying ν of (1) by $1/kT$, collating with the exponential table, gang punching $e^{-\nu/kT}$. Since the Multiplier can carry out the operation $C-AB$ in one run, the required quantity can be evaluated with $C=A=\nu$ and $B=e^{-\nu/kT}$, all of these factors having been punched on the cards.

The line intensity can now be obtained on the transition set by putting through the Multiplier, which evaluates (3). This computation can be verified by sorting on the quantum numbers of the lower state and summing the intensities of all lines arising from each lower level. The sums should be equal to

$$(2J+1)g_{J'',\tau''} \exp -E''(a'', b'', c'')/kT. \quad (5)$$

The product (5) is carried out on the lower-energy-level cards and listed.

The final result is a set of cards bearing the quantum numbers, line positions, and line intensities for each transition, constituting all the lines of the spectrum up to[9] $J<13$. These cards

[8] At present there is no straightforward way to insert a quantity which is to be *added* to all cards directly into the machine to have the counterpart of group multiplying. If ν_0 is not known beforehand, and only trial values are inserted in (1), we have found it convenient to avoid wasting columns for ν_0 by assuming a center of 10,000 cm^{-1}. It is not necessary to punch this onto the cards, but merely to introduce unity into the fifth position of the summary counter by an impulse from the unit multiplier. The value of 10,000 rather than 0 was chosen to insure all calculated ν's are positive, whereby sorting is simplified.

[9] For molecules, such as H_2O and H_2S, where one moment of inertia is small, the Boltzmann factor causes

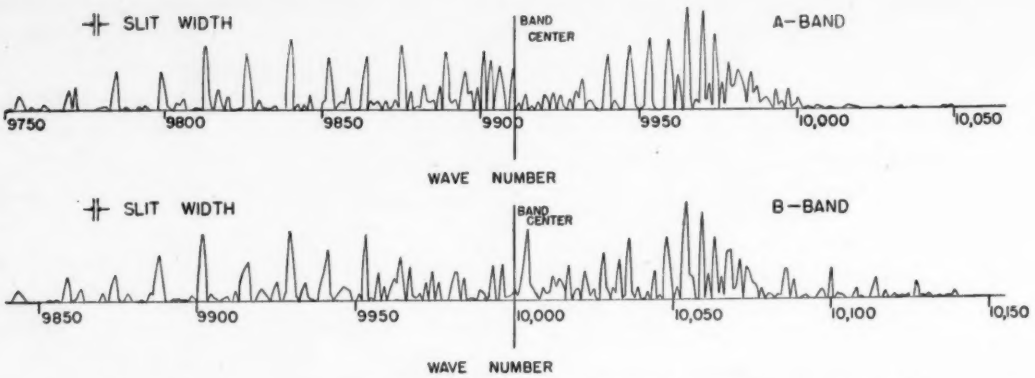

FIG. 2. The *a*-band represents the 10,100A band of H_2S (with a slight change in the intermediate inertia as described in footnote 11) as it would appear with a slit width of 1 cm^{-1} at infinite resolution. (Band center 9911 cm^{-1}.) The *b*-band respresents the appearance of a band under the same conditions arising from a transition between the same vibrational states if the moment were along the intermediate axis. (Band center arbitrarily taken as 10,000 cm^{-1}.) Note that in the asymmetric rotor there is not a very marked difference between the two types of bands when observed with a finite slit width.

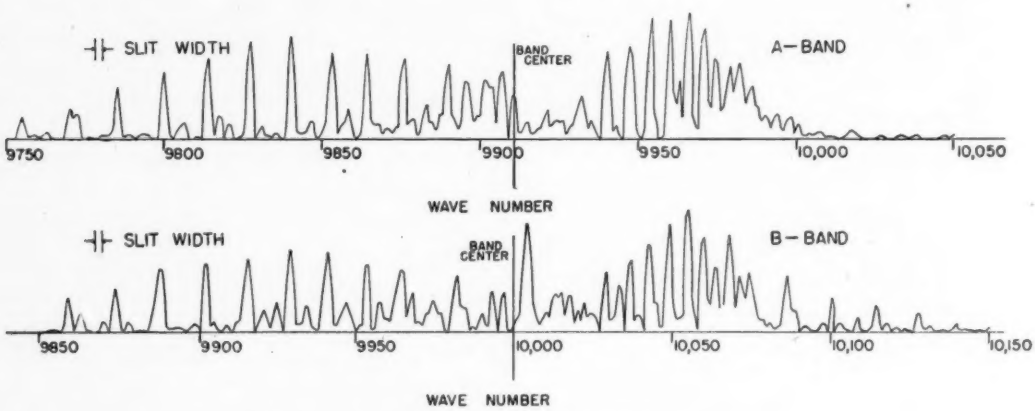

FIG. 3. Same bands as Fig. 2 with slit width 2 cm^{-1}.

can be sorted and the information listed in a variety of ways.

III. SPECTRUM ANALYSIS

Completely Resolved Spectra

By sorting on ΔJ, ΔK_{-1}, ΔK_1, and K_{-1} or K_1, the lines can be listed in branches, sub-branches, and wings (II—Appendix), by means of which the structure of a band is analyzed. Inspection of the rate of decay of intensity in the wings will indicate whether any strong lines occur above $J=12$, and the intensities of such lines can often be found by extrapolation.

all lines involving $J>12$ to be of negligible intensity. A satisfactory study of the bands of molecules with all moments large will require the extension of the tables of reduced energy levels and line strengths to higher J's. We hope to do this by means of the Correspondence Principle.

The cards can also be sorted with the lines arranged in order of increasing or decreasing wave number; or the strong lines, say with intensity greater than some predetermined value, can be listed separately. These printed lists are extremely convenient in analyzing well-resolved spectra.

Unresolved Spectra

In the analysis of incompletely resolved spectra, punched-card methods can be used to further advantage. A set of cards bearing consecutive wave numbers in the region of interest is collated with the set of transition cards arranged in order of increasing wave number. The wave-number set has X punches in various columns so that when the combined set is put through the Tabulator, successive totals can be

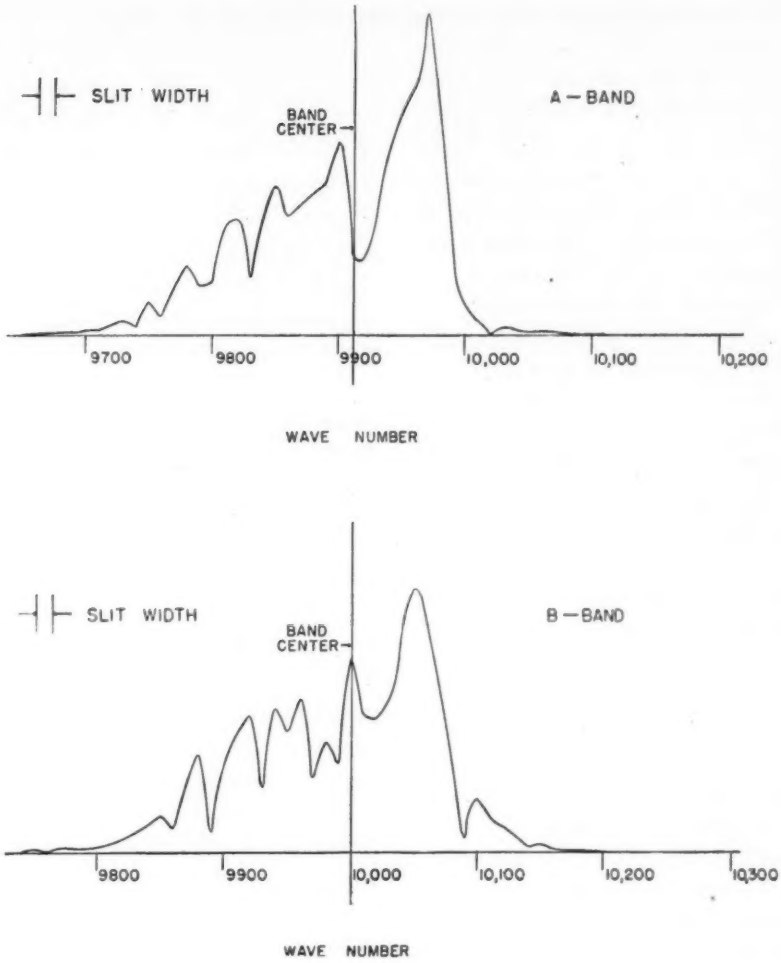

FIG. 4. Same bands as Fig. 2 with slit width 10 cm^{-1}.

listed, giving the sum of the intensities over any interval of wave numbers corresponding to a slit width. Additional X punches are available to give the intensity at intermediate positions of the "slit." A plot of the results gives the appearance of the band at the resolution of the slit width equal to the interval chosen.

IV. TYPICAL RESULTS

In order to test the punched-card procedure we have calculated the line positions and intensities $J<13$ for the 10,100A band of H_2S.[10] The constants chosen[11] were those given by Cross for the greatest and least moments, but the intermediate moments were adjusted to make κ'' and κ' exactly 0.5 and 0.4, respectively. Calculations for $\kappa'=0.5$ were done simultaneously. The plots in this paper refer to $\kappa'=0.4$ only.

A list of calculated positions and intensities, omitting all lines with intensities[12] <1.0, was

[10] P. C. Cross, Phys. Rev. **46**, 536 (1934); **47**, 7 (1935); J. Chem. Phys. **5**, 370 (1937); P. C. Cross and B. L. Crawford, Jr., *ibid.* **5**, 371 (1937); B. L. Crawford and P. C. Cross, *ibid.* **5**, 621 (1937).

[11] The values chosen for computation were

$a''=10.393$ $a'=9.910$
$(b''=8.976)$ $(b'=8.278)$ and $(b'=8.550)$
$c''=4.723$ $c'=4.470$
$\kappa''=0.5$ $\kappa'=0.4$ and $\kappa'=0.5$.

Cross's value for b'' was 9.040, giving $\kappa''=0.523$; and for b' was 8.379, giving $\kappa'=0.437$. The value of T was 298°K. The band center was taken as 9911.03 cm^{-1} for the calculations of the a-type band, and arbitrarily chosen as 10,000 cm^{-1} for the b-type.

[12] Actually, relative intensities $I_{J'',\tau'';J',\tau'}/\text{const.}\,\nu(1-e^{-\nu/kT})$ were used.

compared with the observed lines.[10] More than 90 percent of the observed lines were identified and accounted for. The exceptions were lines found in a subsidiary list of those with intensities lying between 0.5 and 1.0. A few lines whose calculated intensity is ~3 were not given in the original list of observed lines. The agreement in wave number was satisfactory considering the rigid-rotor approximation of the calculations.

The results of collating the wave-number set with progressive totals listed for successive unit wave-number intervals (slit width of 1 cm^{-1}) are plotted in Fig. 2. The curves for a resolution of 2 cm^{-1} are given in Fig. 3. The synthetic spectra obtained by this method correspond very closely in character to the experimental curves. For example, the 2.63μ band of Fig. 1 (obtained with a slit width of 1.8 cm^{-1}) compares favorably with the *b*-band of Fig. 3, although the constants chosen in the latter are those for the 10,100A band.

One immediate result of importance is that the observed band seems to have the appearance of the type where the electric moment is parallel to the intermediate axis, contrary to predictions based on symmetric-rotor formulas.

By changing the control of the Summary Tabulator, sums were obtained for an interval of ten wave numbers. The results are plotted in Fig. 4. The appearance of the bands is characteristic of the envelopes observed experimentally at this resolution.

V. CONCLUSIONS

The punched-card method of obtaining line position and intensity, and of listing the sums of the intensities within any arbitrary slit width, gives curves which correspond very closely in character to band envelopes observed experimentally at all degrees of resolution. This method remains accurate when the slit width is of the order of the average line separation, so that the detail of irregularities characteristic of the asymmetric rotor is preserved.

The method also has the advantage over other procedures that the exact values of the position and intensity of the lines of the rigid rotor are used and are not averaged by replacing sums by integrals. This is particularly advantageous in parts of the spectrum involving levels of low J.

With the procedure for drawing up spectra mechanized, dimensions of the molecules in the upper and lower states can be obtained, with an accuracy dependent on the detail of the band, by successive approximations, that is, by a process similar to that used in interpreting electron-diffraction curves.

Even when the resolution is poor, band centers can be located quite accurately. This is of value in fixing the vibrational levels of the molecules, precise values of which are of importance in calculating thermodynamic quantities from the partition function.

The interpretation of the infra-red bands in terms of characteristic vibrations of the molecule is greatly dependent on the presence of certain branches or on the shape of the envelopes. With a judicious choice of constants even the first run is sufficient to identify the direction of the electric moment with certainty and to locate the center of the band accurately.

ACKNOWLEDGMENT

The authors wish to express their appreciation of the efforts of Mrs. Hope B. Vaughan in making the preparation of the manuscript of this paper possible at this time.

Light Scattering of High Polymer Solutions*

JURG WASER, RICHARD M. BADGER, AND VERNER SCHOMAKER
The Gates and Crellin Laboratories of Chemistry, California Institute of Technology, Pasadena, California

(Received November 24, 1945)

IN principle it is possible to determine the molecular weight distribution of a high polymer, containing no excessively large molecules, from interpretation of its light scattering in solutions at various concentrations. Actually there appear to be severe limitations to this method. Not only is it evident that, considering experimental error, the resolving power is low for the detection in any part of the molecular weight distribution curve of a group of components of similar molecular weights (as contrasted to a single component), it may also happen, in consequence of the restriction of the data to a certain concentration range, that components at the ends of the distribution curve will not be detected and, moreover, that the conclusions regarding the remainder of the distribution will be distorted.

In particular it may be difficult or impossible to perform a satisfactory extrapolation to infinite dilution. In a recent letter to the Editor of this Journal[1] and in a later article[2] Zimm, Doty, and Mark have used the expansion formula

$$\frac{Hc}{\tau_2}=\frac{1}{\sum_i \frac{f_i}{\frac{1}{M_i}+\frac{2B}{RT}c+\frac{3C}{RT}c^2+\cdots}}=\frac{1}{\bar{M}}+\frac{2B}{RT}\left[1+\left\langle\left(\frac{\Delta M}{\bar{M}}\right)^2\right\rangle_{Av}\right]c$$

$$+\left\{\frac{3C}{RT}\left[1+\left\langle\left(\frac{\Delta M}{\bar{M}}\right)^2\right\rangle_{Av}\right]+\frac{4B^2\bar{M}}{R^2T^2}\left[\left(\left\langle\left(\frac{\Delta M}{\bar{M}}\right)^2\right\rangle_{Av}\right)^2-\left\langle\left(\frac{\Delta M}{\bar{M}}\right)^2\right\rangle_{Av}-\left\langle\left(\frac{\Delta M}{\bar{M}}\right)^3\right\rangle_{Av}\right]\right\}c^2+\cdots. \quad (1)$$

Here H is a constant, τ_2 the turbidity due to the solute, c the concentration of the polymer in grams per milliliter of solution, f_i the weight fraction in the polymer of the species of molecular weight M_i, and B and C are constants occurring in the expression for the osmotic pressure (see below). The weight average molecular weight is denoted by $\bar{M}$, and $\langle(\Delta M/\bar{M})^2\rangle_{Av}$ and $\langle(\Delta M/\bar{M})^3\rangle_{Av}$ are the second and third moments of the molecular weight distribution curve about the weight average molecular weight. Expansion (1) may however fail even at the low concentrations used by the above authors. For example in their letter[1] experimental points are plotted for the light scattering of a mixture of two homogeneous polystyrene fractions and compared with the parabola corresponding to the right-hand side of (1). If, however, the complete expression on the left-hand side of (1) is plotted for the mixture of the two fractions, the resulting curve is found to deviate markedly from the parabola at concentrations approaching one percent, and to be much less curved. It is therefore evident that expansion (1) may be misleading even at reasonably low concentrations.

It is to be emphasized that expansion (1) may either be satisfactory at moderate concentrations, somewhat misleading as in Zimm, Doty, and Mark's example, or wholly inadequate, depending upon the nature of the molecular weight distribution and osmotic behavior (e.g., the values of B, C, $\cdots$ in Eq. (1)) of the polymer. We now give some rather general considerations which possibly add something to our understanding of this situation.

The equations which must be handled are considerably simplified and the considerations in general are facilitated by the use of P. Debye's

* Contribution No. 1024 from the Gates and Crellin Laboratories of Chemistry.

[1] B. H. Zimm and P. M. Doty, J. Chem. Phys. **12**, 203 (1944).

[2] P. M. Doty, B. H. Zimm, and H. Mark, J. Chem. Phys. **13**, 159 (1945).

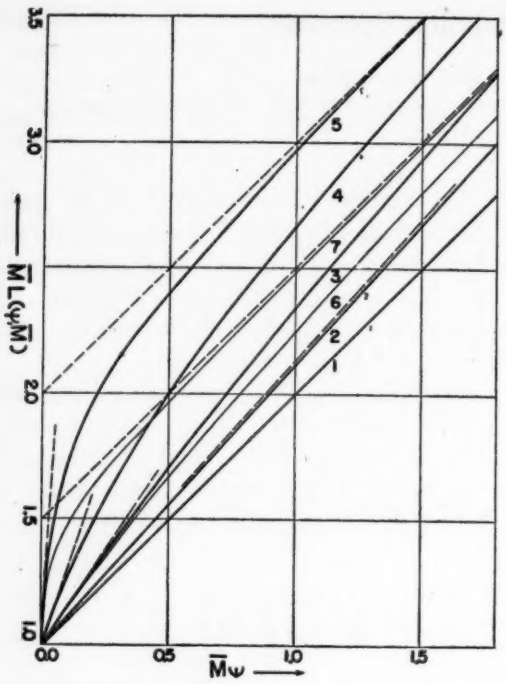

FIG. 1. Plot of $L(\psi)$ for various two-component distributions. Curve 1 represents a monodisperse system, curves 2–5 (heavily drawn) tend toward the upper asymptote, and curves 6 and 7 (lightly drawn) belong to the lower asymptote. The limiting slopes are also indicated. The parameters involved are the following:

	$\frac{\bar{M}}{\bar{M}_n}$	$\left\langle\left(\frac{\Delta M}{\bar{M}}\right)^2\right\rangle_{Av}$	$\frac{M_1}{\bar{M}}$	$\frac{M_2}{\bar{M}}$	f_1
(1)	1	0	1	0	1
(2)	2	$\frac{1}{4}$	1.14	0.11	0.86
(3)	2	$\frac{1}{2}$	1.71	.29	.50
(4)	2	2	4.56	.44	.14
(5)	2	16	32.5	.50	.016
(6)	1.5	$\frac{1}{2}$	2.0	.50	.333
(7)	1.5	16	48.3	.66	.007

suggestion[3] that Hc/τ_2 be considered as function of a quantity $\psi(c)$,

$$H\frac{c}{\tau_2}=\frac{1}{\sum_i \frac{f_i M_i}{1+\psi M_i}}=L(\psi), \tag{2}$$

where ψ is defined as follows. Let the osmotic pressure be given the representation

$$\pi=RT\left\{\sum_i \frac{f_i}{M_i}c+\varphi(c)\right\}, \tag{3}$$

in which $\varphi(c)$, whose first derivative vanishes at zero concentration, is independent of the degree of polymerization;[4] then ψ is given by $\psi(c)=(d/dc)\varphi(c)$. (In (1) $\psi=(2B/RT)c+(3C/RT)c^2+\cdots$ was used.) The form of $\psi(c)$ can be determined either by osmotic pressure studies or by measurements of the light scattering of monodisperse fractions.

The following general remarks can be made about $L(\psi)$:

(*a*) The function (3) has always a positive slope

$$\frac{\partial L}{\partial \psi}=L^2\sum_i \frac{f_i M_i^2}{(1+\psi M_i)^2} \tag{4}$$

and is never curved upward, since

$$\frac{\partial^2 L}{\partial \psi^2}=-L^3\sum_{ij}\frac{f_i M_i f_j M_j}{(1+\psi M_i)^3(1+\psi M_j)^3}(M_i-M_j)^2\leq 0. \tag{5}$$

It is evident that in general $\partial^2 L/\partial\psi^2$, and hence the deviation of $L(\psi)$ from a straight line, is greater, the greater the heterogeneity of the mixture.

(*b*) For a polydisperse system $L(\psi)$ is a curve whose initial slope is $(1+\langle(\Delta M/\bar{M})^2\rangle_{Av})^{1,2}$ and whose intercept is the weight average molecular weight. For the theoretical limit of large ψ, such that $\psi M_i \gg 1$, $L(\psi)$ approaches an asymptote of unit slope, whose intercept is the reciprocal number average molecular weight $1/\bar{M}_n$. According to this and Eq. (5) the slope of $L(\psi)$ is always greater than unity.

(*c*) For a monodisperse system $L(\psi)$ is simply a straight line of unit slope whose intercept is the reciprocal of the molecular weight.

To show some of the wide possible variations in the form of $L(\psi)$ we present theoretical plots for mixtures with various values of $\bar{M}/\bar{M}_n$ and involving solute molecules of only two different degrees of polymerization. The graphs are in terms of $\bar{M}L(\psi, M_i)$, $M_i/\bar{M}$ and $\psi\bar{M}$, since $\bar{M}L(\psi, M_i)=L(\bar{M}\psi, M_i/\bar{M})$. (Figure 1.)

It should be noted that for any solution obeying Eq. (2) (and the curves given here for bimodal distributions illustrate this) any measurement of L provides an upper limit for $\bar{M}_n$ and a lower

[3] P. Debye, General Report No. 17, August 28, 1944. War Production Board, Office of Assistant Rubber Director of Research and Development of Synthetics.

[4] For experimental evidence that this is a good approximation cf. e.g., M. L. Huggins, J. Am. Chem. Soc. 64, 1712 (1942); T. Alfrey, A. Bartovics, and H. Mark, J. Am. Chem. Soc. 65, 2319 (1943).

limit for $\bar{M}$, while any two measurements of L at different ψ establish a lower limit for $\langle(\Delta M/\bar{M})^2\rangle_{Av}$. Whether these limits lie close to the actual values of the corresponding quantities depends on the curves and the values of $\bar{M}\psi$ in question: for any range of $\bar{M}\psi$ with $\langle(\Delta M/\bar{M})^2\rangle_{Av}$ small enough compared to $\bar{M}/\bar{M}_n$ satisfactory extrapolation to $\psi=0$ (as with the aid of Eq. (1)) is feasible for determining $\langle(\Delta M/\bar{M})^2\rangle_{Av}$ and $\bar{M}$, and with $\langle(\Delta M/\bar{M})^2\rangle_{Av}/(\bar{M}/\bar{M}_n)$ great enough the estimate of $1/\bar{M}_n$ will be satisfactory, but generally the range of ψ in which significant measurements can be made may not be wide enough either to satisfy both these conditions or to make certain whether one of them is really satisfied. If extrapolation to $\psi=0$ appears to be possible it may still be unsatisfactory because of the presence of a relatively small amount of material of relatively extreme high molecular weight such that the correct curve of $L(\psi)$ bends significantly downward at values of ψ lower than that of the lowest measurement. On the other hand, in the presence of material of relatively extreme low molecular weight, the curve of $L(\psi)$ may have a maximum slope very little greater than unity and may seem to have reached an asymptote at the highest attained value of ψ when actually its asymptote lies higher.

Letters to the Editor

THIS section will accept reports of new work, provided these are terse and contain few figures, and especially few halftone cuts. The Editorial Board will not hold itself responsible for opinions expressed by the correspondents. Contributions to this section should not exceed 600 words in length and must reach the office of the Managing Editor not later than the 15th of the month preceding that of the issue in which the letter is to appear. No proof will be sent to the authors. The usual publication charge ($3.00 per page) will not be made and no reprints will be furnished free.

Theory of Multimolecular Adsorption from a Mixture of Gases

TERRELL L. HILL
Department of Chemistry, University of Rochester, Rochester, New York
October 29, 1945

THE purpose of the present note is to outline a possible way of extending the Brunauer-Emmett-Teller[1] (BET) theory of multimolecular adsorption to the case of a mixture of two gases. The problem will be discussed in more detail in a later paper, including applications and the treatment for any number of gases.

We consider the adsorption of two gases A and B at relative pressures $x_A=p_A/p_A^0$ and $x_B=p_B/p_B^0$, and at a temperature T below both critical temperatures. Let q_A, q_B, q_{AA}, q_{BB}, q_{AB}, q_{BA}, q_{AN_A}, and q_{BN_A}, be, respectively, the heats of adsorption per mole of A on the bare surface, B on the bare surface, A on a layer of pure A, B on a layer of pure B, A on a layer of pure B, B on a layer of pure A, A on a layer of composition N_A (mole fraction of A), and B on a layer of composition N_A. Let s_i represent the surface area covered by i layers of adsorbed molecules. Then, at equilibrium,

$$\begin{cases} a_A s_0 p_A = b_A s_1 N_{A1} \exp(-q_A/RT), \\ a_B s_0 p_B = b_B s_1 (1-N_{A1}) \exp(-q_B/RT), \end{cases}$$
$$\begin{cases} a_A s_{i-1} p_A = b_A s_i N_{Ai} \exp(-q_{AN_A(i-1)}/RT), \\ a_B s_{i-1} p_B = b_B s_i (1-N_{Ai}) \exp(-q_{BN_A(i-1)}/RT). \end{cases} \quad (1)$$

The above equations use average heats of adsorption and they assume that the energy of attachment of a molecule on top of the $(i-1)$th layer (to become a member of the ith layer) depends on the composition of the $(i-1)$th layer only. If we consider similar equilibria for the evaporation and condensation of A from pure A and B from pure B, we have

$$a_A s p_A^0 = b_A s \exp(-q_{AA}/RT),$$
$$a_B s p_B^0 = b_B s \exp(-q_{BB}/RT)$$

or

$$\frac{b_A}{a_A} = p_A^0 \exp(q_{AA}/RT),$$
$$\frac{b_B}{a_B} = p_B^0 \exp(q_{BB}/RT). \quad (2)$$

We make the approximation, as is done in the BET theory, that second and higher layers have the same evaporation-condensation properties as the liquid state. Thus, in the present case, it seems appropriate to assume that q_{AN_A} and q_{BN_A} can be obtained from the vapor pressure curves for a binary liquid mixture of A and B at the same temperature. As a good approximation,[2] we can write for the equations of these vapor pressure curves

$$x_A = N_A \exp[(q_{AA}-q_{AB})(1-N_A)^2/RT],$$
$$x_B = (1-N_A) \exp[(q_{BB}-q_{BA})N_A^2/RT]. \quad (3)$$

One can of course use other equations in place of Eqs. (3), or, in fact, use the experimental vapor pressure curves if available. We can get corresponding equations involving q_{AN_A} and q_{BN_A} by considering equilibria of the type used to obtain Eq. (2):

$$a_A s p_A = b_A s N_A \exp(-q_{AN_A}/RT),$$
$$a_B s p_B = b_B s (1-N_A) \exp(-q_{BN_A}/RT);$$

or, from Eq. (2),

$$x_A = N_A \exp[(q_{AA}-q_{AN_A})/RT],$$
$$x_B = (1-N_A) \exp[(q_{BB}-q_{BN_A})/RT]. \quad (4)$$

Comparing Eqs. (3) and (4), we see that

$$q_{AA}-q_{AN_A} = (q_{AA}-q_{AB})(1-N_A)^2,$$
$$q_{BB}-q_{BN_A} = (q_{BB}-q_{BA})N_A^2. \quad (5)$$

If Eqs. (2) and (5) are now substituted into Eqs. (1), one finds

$$s_i = s_{i-1}E_{i-1} = s_0 E_0 E_1 E_2 \cdots E_{i-1}, \quad i=1, 2, \cdots \quad (6)$$

$$\begin{cases} E_0 = x_A Q_A + x_B Q_B, \\ E_i = x_A Q_{AB}^{\beta(i)} + x_B Q_{BA}^{\alpha(i)}, \\ \alpha(i) = N_{Ai}^2, \quad \beta(i) = (1-N_{Ai})^2, \end{cases} \quad i=1, 2, \cdots \quad (7)$$

$$\begin{cases} N_{A1} = x_A Q_A / E_0, \\ N_{Ai} = x_A Q_{AB}^{\beta(i-1)} / E_{i-1}, \end{cases} \quad i=2, 3, \cdots \quad (8)$$

$$\begin{cases} Q_A = \exp[(q_A-q_{AA})/RT], \\ Q_B = \exp[(q_B-q_{BB})/RT], \\ Q_{AB} = \exp[(q_{AB}-q_{AA})/RT], \\ Q_{BA} = \exp[(q_{BA}-q_{BB})/RT]. \end{cases} \quad (9)$$

If v_A and v_m^A are the volume of A adsorbed and the volume of A necessary to give a complete unimolecular layer, respectively, then[3]

$$\frac{v_A}{v_m^A} = \frac{(s_1+s_2+\cdots+s_n)N_{A1}+(s_2+\cdots+s_n)N_{A2}+\cdots+s_n N_{An}}{s_0+s_1+\cdots+s_n} \quad (10)$$

$$= \frac{E_0[(1+E_1+E_1E_2+\cdots+E_1E_2\cdots E_{n-1})N_{A1}+(E_1+\cdots+E_1E_2\cdots E_{n-1})N_{A2}+\cdots+E_1\cdots E_{n-1}N_{An}}{1+E_0(1+E_1+E_1E_2+\cdots+E_1E_2\cdots E_{n-1})}. \quad (11)$$

From Eqs. (7) and (8):

$$\lim_{i\to\infty} N_{Ai} = N_A = x_A Q_{AB}^{\beta}/E, \quad (12)$$

$$\lim_{i\to\infty} E_i = E = x_A Q_{AB}^{\beta} + x_B Q_{BA}^{\alpha}. \quad (13)$$

It will be noted that v_A/v_m^A and v_B/v_m^B become infinite (condensation) when $E=1$ and $n=\infty$. Putting $E=1$ in Eqs. (12) and (13) gives Eqs. (3), as expected.

It appears that Eq. (11) may be approximated to within several percent in most cases of interest by

$$\frac{v_A}{v_m{}^A} \leqq \frac{E_0\{N_{A_1}(E^{n+1}-E^n-E+1) + N_A[(n-1)E^{n+1}-nE^n+E]\}}{(1-E)[1-E-E_0(E^n-1)]} \quad (14)$$

and, for $n=\infty$, by

$$\frac{v_A}{v_m{}^A} \leqq \frac{E_0[N_{A_1}(1-E)+N_AE]}{(1-E)(1-E+E_0)}. \quad (15)$$

The quantity $v_B/v_m{}^B$ may be obtained from Eqs. (10), (11), (14), and (15) by replacing N_A by $1-N_A$.

If $x_B=0$, these equations reduce to the usual BET equations with $N_A=1$, $E=x_A=x$ and $E_0=x_AQ_A=xc$.

In comparing theory with experiment, Q_A, Q_B, $v_m{}^A$, and $v_m{}^B$ may be found from the pure A and pure B isotherms, while the vapor pressure curves can be used to give Q_{AB} and Q_{BA}.

[1] S. Brunauer, P. H. Emmett, and E. Teller, J. Am. Chem. Soc. **60**, 309 (1938).
[2] See, for example, R. H. Fowler and E. A. Guggenheim, *Statistical Thermodynamics* (Cambridge University Press, London, 1939), p. 357.
[3] It is an approximation to use mole fractions instead of area fractions in Eqs. (10), (11), (14), and (15) unless the molar volumes of A and B are equal. This will be discussed in a later paper.

A General Theory of the Reaction Loci in Emulsion Polymerization. II*

WILLIAM D. HARKINS
Department of Chemistry, University of Chicago, Chicago, Illinois
October 18, 1945

THE earlier theory[1] has been extended to explain how two minor loci can act, either after soap micelles disappear in polymerization with soap or when no initial soap is used:

A. Loci for the initiation of polymer particle nuclei.

1. Soap micelles: When an initial soap concentration of about 3 percent is used (with 100 g monomer to 180 g water), nearly all of the polymer particle nuclei are initiated in the micelles. With more soap the polymer particles at any given yield are more numerous and smaller, and with less soap less numerous and larger. For example, an isoprene-styrene polymer at 40-percent yield gave diameters of 375A and 485A in 4-percent and 1-percent potassium myristate solutions.
2. Water: The aqueous phase, *excluding* soap micelles and polymer-monomer particles, is a secondary locus whose *relative* prominence increases as soap disappears from its micelles due to adsorption of soap molecules around the monomer-polymer (latex) particles. Finally (e.g., at a 60-percent yield) by process 4, below, too few molecules of monomer remain to make this locus effective.
3. Monomer droplets: The new evidence indicates that monomer droplets are relatively unimportant in initiating new polymer particles, since thus far no evidence has been obtained to show that a monomer droplet can do more than change into a polymer particle of much smaller size.

B. Loci for the formation of polymer.

4. Polymer-monomer particle: Almost all of the polymer is produced in this locus. (See Communication I.)
5. Monomer-emulsion droplets: The principal function of the monomer droplet is to act as a reservoir from which monomer diffuses through a seemingly thick diffusion layer into the other loci. In static experiments every emulsion monomer droplet observed changed into a very much smaller polymer droplet when suspended in a soap solution at 40° to 50°C with all of the necessary reagents present.

Water: Evidence that water (with 0.2 percent of potassium persulfate as catalyst) can act as a locus for the initiation of polymer particle nuclei is given by experiments (1) by Stearns and (2) by Corrin. (1) A flask partly filled with this aqueous phase has two side tubes, turned downward, sealed into the neck. In the bottom of one of these is isoprene, or styrene, or other monomers, and in the bottom of the other a mercaptan. The system is evacuated through the neck of the flask, which is then sealed off, after which the whole system is suspended inside the water of a thermostat held at 50°C for 18 hours. In two experiments of this type with styrene, the diameters of the polymer particles obtained by Oppenheimer were 1500 and 2000A, respectively, while the numbers were 37×10^{11} and 5.6×10^{11} per cu. cm: with isoprene the values were 2200A and 2.9×10^{11}. (2) The polymerization of styrene in water and salt solutions was investigated in the absence of the water-monomer interface. Tubes with sealed-in inner cups were employed to insure a short vapor path between the bulk styrene and water. The tubes were maintained in a 40°C bath for 42 hours. The solutions contained 0.1 percent potassium persulfate, and any salt added was potassium chloride. (Table I.)

Since at 50°C a molecule of mercaptan in the water is readily converted by the catalyst into a free radical (in (2) no mercaptan is present, so styrene itself forms the initial free radical), which can unite with a monomer molecule to give a larger free radical and again with more monomer molecules, until the growing chain is terminated, the results cited above accord with expectations. They indicate that the aqueous phase, after the disappearance of soap, can act as a locus for initiation of polymer particles.

Locus of polymerization in monomer droplets (Stearns). A drop of styrene or isoprene with 0.2 percent lauryl mercaptan was suspended in an aqueous solution of 3 percent potassium laurate, 0.3 percent potassium ferricyanide, 0.1 percent potassium persulfate, and 1 percent sodium car-

TABLE I.

% $K_2S_2O_8$	m KCl	$\mu\times10^2$ (μ = ionic strength)	Conversion (mg/cc)	Mean particle diameter in A	Number of particles per cc
0.1	0.0	1.11	2.89	1710	1.1×10^{11}
0.1	0.0025	1.36	2.99	1310	2.5×10^{11}
0.1	0.005	1.61	3.08	1370	2.3×10^{11}
0.1	0.01	2.11	2.82	2870	2.3×10^{11}
0.1	0.05	6.11	2.47	*	*
0.1	0.10	11.1	1.74	*	*

bonate at 40° or 50°C. The principal phenomenon observed was that 0.999 of the volume disappeared by diffusion of the monomer into the soap solution. However, in every one of numerous experiments the monomer droplet gradually changed into a monomer-polymer droplet.

After the drop was reduced to about a tenth its original diameter, diffusion into the soap solution ceased, since the droplet remaining consisted largely of polymer. In some cases the density was higher than that of water (plus soap), shown by its falling downward through the water. In general, the drop became deformed, becoming non-spherical as its content of polymer increased.

* The work reported in this paper was done in connection with the Government Research Program on synthetic rubber under contract with the Office of Rubber Reserve, Reconstruction Finance Corporation.
[1] W. D. Harkins, J. Chem. Phys. 13, 381 (1945).

The Density and Thermal Expansion of Liquid Phosgene

C. N. Davies
Industrial Health Research Board, Medical Research Council, London, England
December 10, 1945

1. INTRODUCTION

SOME unpublished values for the density of liquid phosgene suggested that the figures available in chemical literature might be high. The measurements described in the present paper confirmed this view; they were carried out on two samples, from the same source, which had been shown by chemical analysis to contain only traces of impurity too small to affect the density within the accuracy of the determinations.

2. EXPERIMENTAL METHOD

A bulb was blown on thick-walled Pyrex capillary tubing and the volume per cm of stem determined over the working range by using a cathetometer to measure distances of the meniscus of mercury charges of known weight from a mark on the tube. The volume up to this mark was 1.7505 ±0.0004 cm³ and the tube diameter was about 4 mm. Phosgene was distilled in and the tube sealed. The position of the phosgene meniscus was then determined at temperatures from −20°C to +60°C. The mass of phosgene was corrected for the mass in the vapor phase using the vapor pressures of Paternò and Mazzucchelli.[1] Corrections were also applied for the meniscus, and weighings were reduced to vacuum. Two series of experiments, in the order given below, were carried out independently on different samples.

Possible errors caused by the expansion of the bulb under pressure and temperature were shown to be negligible.

TABLE I.

First series Temperature	Density	Second series Temperature	Density
−9.35°C	1.444₁ g/cm³	20.05°C	1.373₀ g/cm³
−8.60	1.442₁	20.10	1.371₄
−7.75	1.439₇	27.00	1.354₇
−5.70	1.434₈	37.00	1.331₉
−3.25	1.429₀	45.45	1.309₄
−2.70	1.427₇	48.50	1.301₉
−2.00	1.426₀	19.20	1.374₅
−0.65	1.422₄	14.50	1.385₂
−0.05	1.421₄	5.00	1.407₆
15.03	1.383₉	0.00	1.418₇
16.73	1.380₃	−5.00	1.428₈
20.59	1.370₉	−10.00	1.440₆
28.01	1.353₂	−15.00	1.451₃
34.66	1.336₂	−20.00	1.463₁
40.13	1.322₉	20.00	1.371₄
45.27	1.309₃		
50.75	1.295₁		
55.50	1.283₁		
60.20	1.270₆		
17.75	1.378₂		
12.00	1.391₄		
7.55	1.402₂		
−0.20	1.420₇		
−6.10	1.434₃		
−10.40	1.445₀		
−15.50	1.457₆		

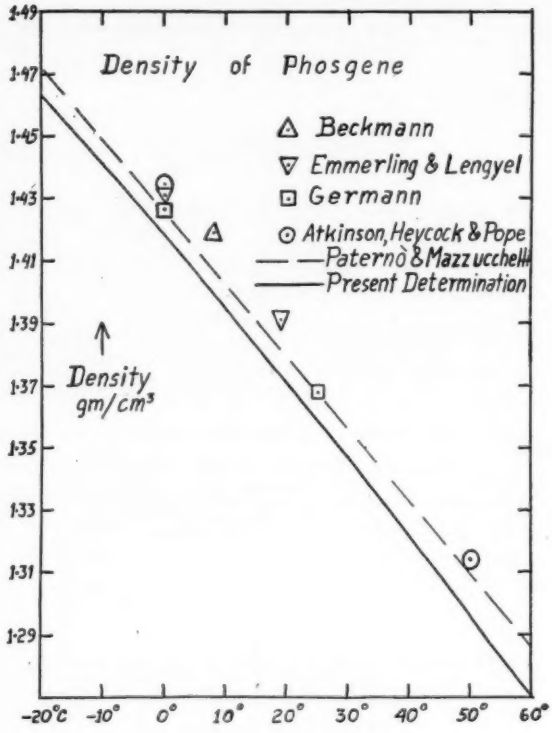

FIG. 1.

3. EXPERIMENTAL RESULTS

The results given in Table I, taking both series together, have been fitted by the method of least squares with the following regression curve:

$$\rho = 1.42014 - 0.0023120t - 0.000002872t^2$$
$$= 1.42014\,(1 - 0.001628t - 0.000002022t^2),$$

where ρ is the density in gm/cm³ at t°C.

By differentiating this equation the thermal expansion per degree centigrade was found to have the following values:

Temperature	$1/v(dv/dt)$
50°C	0.002003
30	0.001842
10	0.001696
−10	0.001563

Above 0°C the agreement between the two series and of each with the equation is better than 0.1 percent. Below

zero the scatter increases but is always less than 0.2 percent. This may be attributed to more accurate temperature control during the determinations at the higher temperatures.

4. COMPARISON WITH PREVIOUS DETERMINATIONS

Paternò and Mazzucchelli[1] give an equation based on experiments over the range −15.4°C to +59.9°C which is about 0.6 percent above the present data at 20 C and gives a slightly lower coefficient of expansion.

Atkinson, Heycock, and Pope[2] found still higher densities and exceed the latest figures by about 1.2 percent.

Germann[3] only did determinations at 0°C and 25°C and agrees closely with Paternò and Mazzucchelli.

Figures given by Emmerling and Lengyel[4] and Beckmann[5] are fairly close to Atkinson, Heycock, and Pope.

All these determinations may be compared with the present findings (see Fig. 1). It is significant that the older values are high which suggests that the presence of carbon tetrachloride might explain the discrepancies. About 6 percent would raise the density of phosgene by 1 percent and the deviation would tend to increase with rise of temperature as is observed in the case of the Italian data. It is probable that dissolved chlorine would also raise the density. The results of Atkinson, Heycock, and Pope were obtained by chemical estimation of the phosgene instead of direct weighing. It is not possible to draw any conclusions from the methods of manufacture of the phosgene since various processes have been used and no correlation with the observed densities is apparent.

5. SUMMARY

A determination of the density and thermal expansion of liquid phosgene over the range −20°C to +60°C is described. The density in this range is given by the following equation:

$$\rho = 1.42014 - 0.0023120t - 0.000002872t^2.$$

6. ACKNOWLEDGMENT

These experiments were carried out in a Ministry of Supply Research Establishment and the results are published by permission of the Director General of Scientific Research and Development.

[1] Paternò and Mazzucchelli, Gazzetta [1] **50**, 30 (1920).
[2] Atkinson, Heycock, and Pope, J. Chem. Soc. Trans. **2**, 1410 (1920).
[3] Germann, J. Phys. Chem. **29**, 138 (1925).
[4] Emmerling and Lengyel, Ann. Suppl. **7**, 106 (1870); Berichte **2**, 546 (1869).
[5] Beckmann, Zeits. f. Ann. Chem. **55**, 371 (1907).

Statistical Mechanics of Linear Association Equilibria

PAUL J. FLORY
Research Laboratory, The Goodyear Tire and Rubber Company, Akron, Ohio
November 21, 1945

In a recently published paper Tobolsky and Blatz[1] have discussed the "possible application" of the lattice model for mixtures of linear polymers with small molecules to reversible associations of liquids such as the alcohols and their solutions in non-associated solvents. It appears that they were unaware that this particular problem can be treated by previously derived relationships pertaining to heterogeneous polymer-solvent mixtures.[2] Their paper contains the unfounded and misleading statement, " . . . whereas Flory[2] was considering stable polymer molecules which did not change their size distribution when diluted, we are here concerned with the problem of reversible association. . . . " It is the writer's purpose to emphasize here the generality of the previously derived thermodynamic functions as applied to equilibria involving transformations between various polymeric species.

In applying the methods of thermodynamics, or statistical mechanics, to chemical equilibrium problems the character of the bonds, or intermolecular forces, subject to equilibration need not be specified. The treatment, previously presented, of equilibria involving polymer molecules is completely general, and although secondary valence polymers were not mentioned, it should have been clear that it is also applicable to these as well, provided that the "polymers" consist predominantly of linear sequences of structural units. This treatment led to the conclusion that the equilibrium constant for processes involving polymeric substances assumes the same form as that for the analogous reaction between monomeric species; the relationship of the equilibrium constant to the standard state free energy change is the same in the two cases. Thus, no modifications in the formulation of equilibrium constants are occasioned by the configurational randomness of the polymeric reacting species.

For the purpose of applying this principle to associative equilibria specifically, consider a solution containing N_0 associating units per unit volume, each of which is capable of entering into two "bonds" to form linear polymers. If each of these bonds forms independently of the presence or absence of other bonds attached to the adjoining units, then an equilibrium constant governing the associative process can be written

$$K = p/(1-p)^2 N_0, \tag{1}$$

where p (equivalent to the "y" of Tobolsky and Blatz) is the "degree of association," i.e., $N_0 p$ represents the concentration of association bonds at equilibrium. Also from the above assumptions and the nature of the dependence of partial molal free energies on concentrations, it follows that the molecular size distribution is given by

$$N_x = N_0(1-p)^2 p^{x-1}, \tag{2}^{3,4}$$

where N_x represents the molar concentration of x-mers; the number average degree of polymerization, according to (2), is given by

$$\bar{x}_n = 1/(1-p), \tag{3}$$

the partial molal free energy of the solvent in this system is obtained directly by substituting (3) into Eq. (17) of reference 2, giving

$$\Delta\bar{F}_1 = RT[\ln(1-v_2) + v_2 p + \mu v_2^2], \tag{4}$$

where v_2 is the volume fraction of solute including all species, and μ is a semi-empirical parameter[5,6] in which is included the heat of dilution term. Equation (4) is identical

with Tobolsky and Blatz's Eq. (5), which is merely a special case of the more general equation, namely that in which the molecular size distribution of the solute is given by (2). Similarly, if desired, partial molal free energies for any of the various solute species can be derived by appropriately substituting Eqs. (2) and (3) into Eqs. (18) and (19) of reference 2. The resulting expressions differ from Tobolsky and Blatz's (6) and (7), which latter contain the intractable quantity y' and refer to the ambiguous standard state consisting of "pure mixed" solute molecules.

Whereas Tobolsky and Blatz prefer to include the factors controlling p, the extent of association (or reaction), in the partition function, the writer has preferred to relate p separately to an equilibrium constant. The procedures are fundamentally equivalent, the writer's being generally more easily applied.

The factor $b^{n_0}+\Sigma n_x$ introduced into their intuitively derived partition function to account for mixing of molecules with holes in the lattice appears to be both unnecessary and incorrect. Tobolsky and Blatz[1] include the entropy of bond formation ($k \ln a[\Sigma(x-1)N_x]$), which had been omitted by Tobolsky[7] previously. Hence, their definition of P as the heat of association is correct, but in the previous paper[7] P must be considered to represent a standard state free energy change, as previously pointed out.[2]

In conclusion it should be emphasized that the previously derived thermodynamic relationships are general, and a new derivation of the partition function for each application to a specific problem would seem to be unnecessary.

---

[1] A. V. Tobolsky and P. J. Blatz, J. Chem. Phys. **13**, 379 (1945).
[2] P. J. Flory, J. Chem. Phys. **12**, 425 (1944).
[3] P. J. Flory, J. Am. Chem. Soc. **58**, 1877 (1936); *ibid.* **64**, 2205 (1942).
[4] K. H. Meyer and A. van der Wyk, Helv. Chim. Acta **20**, 1321 (1937), derived Eq. (2) for association processes in which the free energy change for each successive monomer added to the micell is assumed to be the same.
[5] M. L. Huggins, J. Phys. Chem. **46**, 15 (1942); Ann. N. Y. Acad. Sci. **43**, 1 (1942); *ibid.* **44**, 431 (1943); J. Am. Chem. Soc. **64**, 1712 (1942).
[6] P. J. Flory, J. Chem. Phys. **13**, 453 (1945).
[7] A. V. Tobolsky, J. Chem. Phys. **12**, 402 (1944).